Chemical Modulators of Heat Shock Protein 70 (Hsp70)

Validate this Molecular Chaperone as a Target for Tauopathy

by

Zapporah T. Young

A dissertation submitted in partial fulfillment
of the requirements for the degree of
Doctor of Philosophy
(Medicinal Chemistry)
in the University of Michigan
2016

Doctoral Committee:

Adjunct Associate Professor Jason E. Gestwicki, Co-Chair, University of California San Francisco
Professor Scott D. Larson, Co-Chair
Professor Heather A. Carlson
Professor Ronald W. Woodard

Dedication

This work is dedicated to my mother, father, sister and grandparents

Acknowledgements

I would first like to thank my advisor Jason Gestwicki. It has been a great blessing to have such a patient and encouraging teacher. The level of passion he has for science and discovery is something I admire and strive to achieve. I was excited and nervous to relocate with the lab to California in 2013, but Jason's enthusiasm and leadership was reassuring through the challenging transition. His measured guidance has contributed to my development as an independent scientist and critical thinker. Beyond my doctoral training, I am grateful for Jason's willingness to allow me to explore youth mentoring opportunities which have contributed to my growth as a scholar and a person.

I must thank my thesis committee, Dr. Scott Larsen, Dr. Heather Carlson and Dr. Ronald Woodard, for their feedback, support and patience through the long-distance Skype meetings.

I also want to thank all the members of the Gestwicki lab, past and present, for their help and guidance. Yoshi Miyata provided valuable council as the project transitioned from his hands to mine. Andrea Thompson, Leah Makley and Sharan Srinivasan taught me technical skills in cell-culture and immunoblotting. Jennifer Rauch provided aid in biochemical analysis and assay development. Xioakai Li and Hao Shao contributed their synthetic expertise to my projects, and

Victoria Assimon helped initiate the Hsp70 genetics project. Sue Ann Mok has been an amazing teacher and balancing force in the lab. Finally, I'd like to give a special thanks to Jenifer Abrams, Kojo Opoku-Nsiah and Matt Ravalin for necessary comic relief.

I am thankful to our collaborators Chad Dickey, the Dickey lab and Dr. Misol Ahn for their assistance in the tau homeostasis studies; Dr. Jonathon Weissman, Dr. Luke Gilbert and Dr. Martin Kampmann for running the CRISPRi genetic screens; and Dr. Duxin Sun and Dr. Byron Hann for pharmacokinetics experiments.

Finally, I would like to thank my friends and family. Your support, words of encouragement, and phone calls are greatly appreciated. To my parents, Alfred young and Quinton Geans-Young, thank you for allowing me to explore my love for science and chase my dreams no matter how far from home they take me. I cannot express how much your understanding and encouragement means to me. Richard, you are an amazing motivator, and I am lucky to have your support through the difficult times. Your hard work inspires me to be great. To, my sister Zarria Young, it is crazy that as I am completing the last steps in my education you are just beginning the journey in your first year of college. I hope my work can inspire you to accomplish all your goals and dreams as we continue to build upon the family legacy.

Table of Contents

List of Figures

List of Tables

List of Appendices

Abstract

Misregulation of tau, an intrinsically disordered protein, is implicated in Alzheimer's disease (AD) and more than 15 related tauopathies. These diseases are characterized by the accumulation of tau aggregates into insoluble neurofibrillary tangles (NFTs), which contribute to neurodegeneration. As discussed in Chapter 1, accelerating the clearance of tau is an emerging treatment strategy. The molecular chaperone heat shock protein 70 (Hsp70) binds tau and facilitates its degradation, making it a particularly attractive target for normalizing tau homeostasis. It was recently discovered that the rhodacyanine MKT-077 and its analogs bind Hsp70 and accelerate the degradation of pathogenic tau in multiple disease models. In Chapter 2, I was interested in using MKT-077 analogs as probes to better understand this mechanism. We found that MKT-077 analogs bind to an allosteric site on Hsp70, stabilizing the ADP-bound conformation and increasing tau binding. These molecules also disrupted protein-protein interactions between Hsp70 and its co-chaperones. These findings suggest that the affinity of Hsp70 for its substrates, like tau, is correlated with degradation. While exciting, it still was not clear which of the Hsp70 paralogs was most important for this process. There are thirteen Hsp70 genes in humans, including those expressed in the mitochondria and endoplasmic reticulum (ER). In Chapter 3, I used CRISPR/cas9 technology to

understand the targets of the MKT-077 analogs, showing that some of the compounds are selective for mitochondrial Hsp70, while others require the ER paralog. This selectivity seemed to emerge from differential subcellular partitioning of the analogs, as suggested by fluorescence microscopy. These results are important for better understanding the roles of Hsp70 in tau homeostasis, because we could then select molecules that were relatively paralog-selective and ask how well they reduce tau levels. Using this approach, I found that the ER version of Hsp70 seemed to be an excellent target for accelerating tau degradation, potentially through regulating stress response. Consistent with this finding, I found that over-expression of ER Hsp70 promotes tau clearance. As discussed in Chapter 4, these results have important implications for therapeutic treatment of tauopathies. In addition, these findings provide new insights into mechanisms of Hsp70-mediated tau homeostasis.

Chapter 1

Molecular Chaperones as Therapeutic Targets for Restoring Tau Homeostasis

1.1 Introduction

Normal tau homeostasis is achieved when there is balance in its synthesis, processing and degradation. Together, the pathways that regulate tau homeostasis ensure that the protein is at the proper levels and that its post-translational modification (PTMs) and subcellular localization are appropriately controlled. These pathways include the enzymes responsible for PTMs, those systems that regulate mRNA splicing and the molecular chaperones that control tau turnover and its binding to microtubules. In tauopathies, this delicate balance is disturbed. Tau becomes abnormally modified by PTMs, it loses affinity for microtubules and it accumulates in proteotoxic aggregates. How and why does this imbalance occur? In this chapter, we discuss how molecular chaperones and other components of the protein homeostasis (*e.g.* proteostasis) network normally govern tau quality control. We also discuss how aging might reduce the capacity of these systems and how tau mutations might further tip the balance. Finally, we discuss how small molecules are being used to probe and perturb the tau quality control systems, playing a particularly prominent role in revealing the logic of tau homeostasis. As such, there is now interest in developing these chemical probes into therapeutics, with the goal of restoring normal tau homeostasis to treat disease.

1.2 Tau's role in neurodegenerative diseases

Tau is a microtubule-associated protein that is normally soluble but has a propensity to aggregate into oligomers, paired helical filaments (PHFs) and neurofibrillary tangles (NFTs). A group of neurodegenerative diseases that are characterized by the appearance of NFTs are classified as tauopathies, including some forms of Alzheimer's disease (AD), frontotemporal dementia with parkinsonism linked to chromosome-17 (FTDP-17) and progressive supranuclear palsy (PSP). A subset of FTDP-17 cases are caused by mutations in tau, providing a direct link between tau dysfunction and disease [1]. Moreover, the levels of NFT pathology closely correlate with AD progression [2] indicating that normal wild-type tau is readily corrupted by the cellular conditions that promote disease. There is also evidence from an AD mouse model indicating that tau is required for some aspects of the observed pathologies [3]. Recent reviews further detail the links between tau and neurodegeneration [4, 5] and outline the features of the animal models [6]. Here, we will focus on how tau protein levels are maintained, how disease-associated changes in tau disrupt this balance and how this knowledge can be used to design new therapeutic strategies.

1.3 Tau structure and function

Tau is a member of a family of microtubule-associated proteins (MAPs) that directly bind tubulin and are implicated in microtubule dynamics. Tau was originally identified as an important factor for microtubule assembly or stability [7] however, more recent studies argue that this particular function is not essential or is redundant with other MAPs [8, 9]. Tau expression is mainly restricted to the nervous system, where it is abundant in neurons and at much lower levels in glial cells, such as oligodendrocytes and astrocytes [10-12]. In neurons, tau is primarily localized to the axons where it co-localizes with microtubules [13]. The tau protein is encoded by the MAPT gene and alternative splicing of exons 2, 3

and 10 generates the 6 main isoforms that are expressed in the adult brain [14]. NMR studies have shown that tau proteins are disordered in solution, only transiently sampling secondary structures [15]. Nevertheless, tau sequence characteristics can be used to define major regions within the protein including an N-terminal domain, a poly-proline region, a microtubule-binding repeat (MTBR) region, and a C-terminal segment (Figure 1.1). The MTBR region is comprised of imperfect repeat sequences (31 or 32 residues each) that, along

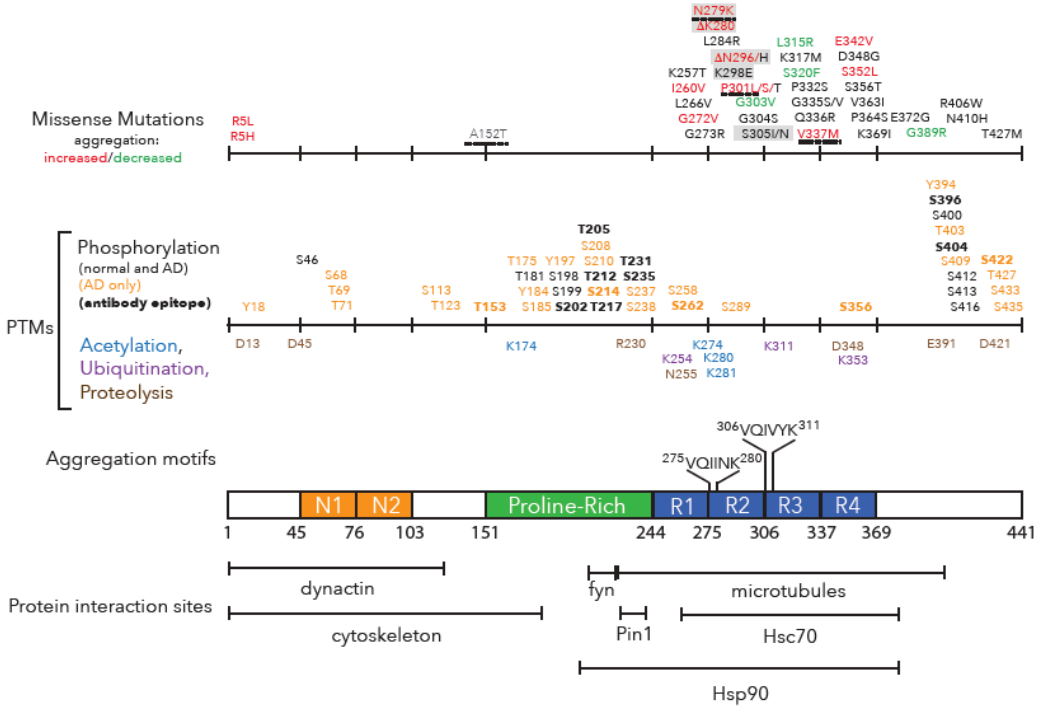

Figure 1.1 Map of the modifications and interaction sites on the tau sequence. A schematic of the longest adult isoform of tau (2N4R) is depicted. Several regions within the tau sequence are highlighted including two amino terminal inserts (N1, N2), a poly-proline region and the microtubule-binding repeat region composed of 4 imperfect repeat sequences (R1-R4). Alternative splicing of N1, N2, or R2 leads to the generation of 6 tau isoforms expressed in adults. The sequences of the two known aggregation motifs are shown, located within R2 and R3 of tau. All the known disease-associated missense mutations and the risk factor variant, A152T (grey), are mapped. Intronic mutations linked to tauopathies are not shown. Missense mutations observed to kinetically favor increased (red) or decreased (green) aggregation *in vitro* are colored. Grey boxes show mutations that alter splicing of the R2 repeat. Dashed underlines show mutations that display decreased affinity for microtubules. A selection of post-translational modifications associated with disease are mapped and color-coded as indicated in the figure. Below the tau sequence schematic, regions of tau that interact with binding-partners are charted.

with the polyproline region, mediate interactions with microtubules [16-18]. Differential splicing of exon 10 generates either 4 or 3 microtubule-binding repeats (termed 4R or 3R) and the 4R forms have tighter affinity for microtubules [19] and nucleate microtubule assembly better than 3R isoforms [20].

1.4 Normal protein-protein interactions with tau

Like many intrinsically disordered proteins (IDPs), tau interacts with multiple protein partners (for an overview see [21]) (Figure 1.1). In addition to tubulin, tau also binds actin [22], kinesin [23, 24] and dynactin [25, 26]. These interactions strongly link tau to trafficking and axonal transport. Indeed, overexpression of tau impairs both vesicle and mitochondrial transport [27-29]. Tau also binds to a number of kinases, phosphatases, proteases and acetylases that are involved in post-translational modifications (PTMs). For example, fyn kinase binds PXXP motifs in the polyproline region of tau [30] and phosphorylates its N-terminus at Tyr18 [31]. Finally, as discussed in greater detail within this chapter, molecular chaperones are also prominent protein partners of tau. For example, heat shock protein 70 (Hsp70) and heat shock protein 90 (Hsp90) both bind tau within the MTBRs [32, 33] and regulate its turnover [34]. Together, these protein-protein interactions (PPIs) between tau and its many protein partners help regulate its trafficking, its PTMs and its turnover. Thus, to understand tau homeostasis, one must understand its interactions with itself (*i.e.* aggregation) and its interactions with these partners.

1.5 Aberrant interactions of tau

One of the hallmarks of tauopathies is that tau's PPIs are altered [21], meaning that some of the interactions are favored and others are reduced. The most dramatic example of this change is the increase in tau-tau interactions, which lead to its aggregation. Two aggregation motifs within the MTBRs are required this process and several mutations in this region prevent self-assembly [35, 36].

However, this same region is also required for binding to microtubules. When tau is not in contact with microtubules, these regions acquire an abnormal, beta-sheet-rich structure that favors amyloid formation [17, 35, 37]. Further, cysteines within the MTBRs can cross-link tau monomers, which also promotes aggregation [38]. The importance of the MTBRs suggests that the loss of tau-microtubule interactions and the build up of unbound cytosolic tau may be a step towards aggregation. However, tau is surprisingly soluble *in vitro*. Accelerants, particularly poly-anionic molecules such as heparin or fatty acid micelles, are required to initiate aggregation *in vitro* [39]. It is thought that a similar aggregation trigger, such as RNA or polyglutamates [40, 41], might be similarly required *in vivo*.

Tau aggregation leads to the formation of an ensemble of aggregate structures, including oligomers and fibrils, that are found in tissue samples from AD and PSP [42, 43]. Although it isn't yet clear which tau structures are most toxic, it is likely that oligomers are especially detrimental to cells as they decrease cell viability more potently than tau fibrils [44] and antibodies against oligomers of tau are protective when administered to tauopathy animal models [45, 46]. Further, tau oligomers seem to spread in the brain and in cell culture, exhibiting prion-like characteristics [47-50]. A cell-to-cell transmission of tau aggregates fits with the characteristic spreading of pathology from an epicenter to connected brain regions observed in disease.

1.6 Tau mutations and disease-associated PTMs

Thus far, 53 pathogenic mutations within the MAPT gene encoding tau have been reported [51] (Figure 1.1). There are also reports of risk factors linked to MAPT including the A152T variant within the protein coding region [52] and the MAPT variation associated with the H1 haplotype [53]. The pathogenic mutations can be broadly characterized as missense/deletion mutations or intronic mutations. The vast majority of the mutations cluster to the MTBRs, perhaps underscoring the role played by dynamic microtubule binding and self-assembly.

The mechanism(s) of toxicity that occur due to MAPT mutations remain poorly understood. The intronic mutations and even some coding mutations promote inclusion of exon10 and lead to increased expression of 4R tau [54, 55]. *In vitro*, 4R tau binds to microtubules with a higher affinity than 3R isoforms [20, 56] but 4R tau also aggregates with faster kinetics than 3R tau [38] and 3R can inhibit 4R aggregation [57]. Thus, one could speculate that an imbalance in 3R *versus* 4R contributes to disease. Other coding mutations do not seem to alter splicing. Rather, they reduce microtubule affinity and/or increase aggregation compared to wild-type (Figure 1.1) [58-62]. It is tempting to speculate that these biochemical features are the major determinants of tauopathy. However, this possibility is unlikely because the age of onset, duration, clinical symptoms, and neuropathology differ between individuals harboring related mutants and sometimes for patients with the same mutation [63]. This data strongly suggests that other factors contribute to tau pathology. One possibility is that environmental or other genetic factors tune the response to tau mutations [64-66]. Another fascinating possibility is that specific mutations alter tau's PPI network (see Figure 1.1), perhaps releasing proteins that protect against disease and/or favoring partners that are detrimental.

Although mechanistically informative, the vast majority of tauopathies are not associated with tau variants. Rather, abnormal PTMs appear to be closely linked to NFTs and disease. Tau is potentially subject to over 100 PTMs, including phosphorylation, acetylation, proteolytic cleavage, glycosylation, ubiquitination, sumoylation, amination, nitration, oxidation, and methylation [67, 68]. Increases in tau phosphorylation have been most extensively linked to tau pathology. Tau in normal brain is phosphorylated at an average of 2-3 residues per molecule, while tau from AD brain contains 3- to 4-fold more phosphorylated residues [69]. Indeed, antibodies recognizing phospho-epitopes, such as AT8, AT180, PHF1, are commonly used to mark neuropathology in all tauopathies [70, 71]. However, a clear cause-and-effect relationship between hyperphosphorylation and disease

initiation remains to be demonstrated and tau hyperphosphorylation is associated with normal development [72] and animal hibernation [73]. Despite this, there is some evidence that hyperphosphorylated tau has weakened activity in microtubule assembly assays and that it assembles into oligomers more readily [74]. Multiple kinases have been reported to phosphorylate tau but the kinases and sites relevant to disease remain poorly defined [67]. The kinases GSK3β, fyn and Cdk5 have all been implicated in abnormal tau phosphorylation and inhibitors for these kinases are currently being developed as therapeutics [75-77]. One phosphatase, PP2A, has also been identified as the major tau dephosphatase *in vivo* and there are small molecules that enhance PP2A's activity and reduce tau phosphorylation [78-80]. Ubiquitination of tau may serve to mark abnormal or free cytosolic tau for chaperone-mediated degradation [81, 82]. Multiple ubiquitination sites have been identified through mass spec analysis of PHF-tau preparations [83-85] however, the requirement of these specific sites for the degradation of tau has not been confirmed. At least two acetylation sites on tau, at residues K280 and K274, correlate with other markers of tau neuropathology [86]. *In vitro*, multiply acetylated tau has a decreased propensity to form fibrils [87, 88], perhaps suggesting that acetylation is protective. Cleaved fragments of tau are released by proteolysis and these fragments have been observed in NFTs isolated from AD patients [89, 90]. The most well characterized cleavage site, at D421, is generally attributed to proteolytic activity of caspase 3 [91] although multiple caspases can cleave the same site i*n vitro* [92]. Cellular assays provide evidence that truncation at D421 leads to defects in microtubule binding [93], preferential degradation by autophagy [94], mitochondrial dysfunction [95], and enhanced secretion from cells [96]. Interestingly, D421 truncated tau has been detected in the CSF from AD patients and its levels inversely correlate with cognitive decline [97]. Methylation is the main modification of tau lysines observed in normal brain [98] and its levels are decreased in AD tau samples [85].

Similar to what was discussed for disease-associated mutations, one can

imagine how aberrant PTMs might weaken favorable PPIs and/or strengthen self-association. These events might even be synergistic, as evident by observations that the R406W tau mutation leads to higher rates of tau phosphorylation *in vitro* [99]. The emerging theme is that tau normally engages in a dynamic series of PPIs and PTMs. These events are important for tau's function in trafficking and its normal turnover. However, disruption of this delicate balance, either triggered by aging, mutations, trauma or other initiating event, leads to a re-modeling of the tau-associated PPIs. The net effect of this abnormal PPI state is that tau becomes aggregated and loses affinity for microtubules.

1.7 Points of intervention for treating tauopathies

The path towards the treatment of neurodegenerative tauopathies will likely involve the re-balancing of tau interactions (Figure 1.2). Perhaps the simplest form of this concept is to directly inhibit its aggregation [100]. Other initiatives have focused on small molecules that favor the normal PPIs of tau by stabilizing microtubules [101]. The idea behind this approach is that tau cannot aggregate if it is bound to microtubules because the MTBRs contain the essential aggregation motif. As mentioned above, other approaches have targeted the enzymes involved in tau PTMs, such as kinases or phosphatases. The challenges with these approaches is that it isn't clear whether the small molecules can be safely deployed in a way that normalizes tau PPIs and PTMs. However, ongoing pre-clinical programs are likely to answer this critical question.

Another promising way to treat tauopathies is to accelerate its turnover or reduce its levels. Tau$^{-/-}$ knockout mice display only subtle phenotypes [3, 102], arguing that tau may not be critical in adult animals or that it can be compensated for by other MAPs. One means of clearing tau is to target tau at the mRNA level with anti-sense oligonucleotides [103]. Another is with therapeutic antibodies [104, 105] or molecules that block tau translation [106]. As above, these approaches are being explored in pre-clinical programs. In the next sections, we focus on

another way to normalize tau homeostasis by targeting proteins that maintain its quality control.

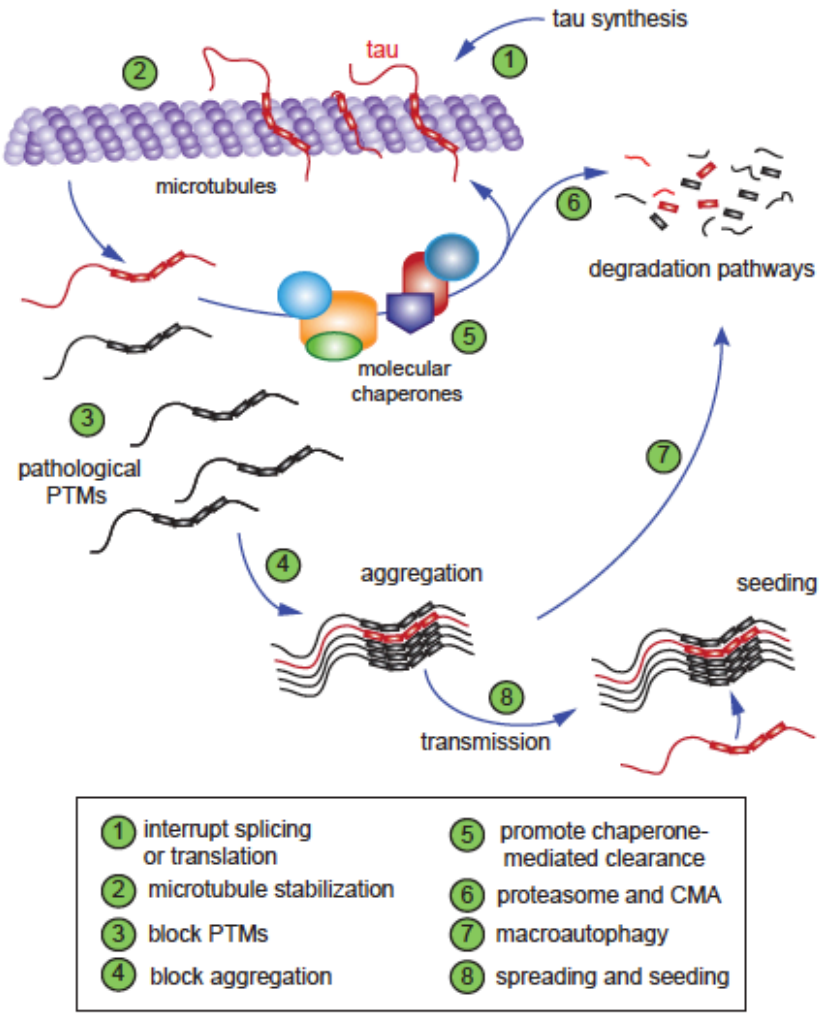

Figure 1.2 Possible mechanisms for restoring tau homeostasis. Tau homeostasis is defined as a product of its synthesis, its normal cycling on microtubules, its chaperone-mediated clearance, its aggregation and its spreading from cell-to-cell. Each of these stages of tau's life cycle is a potential site of pharmacological intervention. The goal would be to normalize tau homeostasis and re-balancing its levels.

1.8 Molecular chaperones regulate tau homeostasis

The molecular chaperone network consists of several chaperone systems, which intersect and work cooperatively to maintain protein homeostasis. Chaperones are particularly vital for maintenance of proper tau structure and function [107-

109]. For example, Hsp90 and Hsp70 assist in proper tau assembly with the microtubule [110]. In addition, Hsp90 and Hsp70 can facilitate the clearance of toxic forms of tau by acting as scaffolding proteins for degradation pathways, including both the UPS and autophagy-lysosome pathways [111-115].

1.9 The Hsp70 sub-network regulates tau stability

The 70 kDa molecular chaperone, Hsp70, has two domains: a nucleotide-binding domain (NBD) responsible for binding and hydrolyzing ATP and a substrate-binding domain (SBD) that interacts with clients (Figure 1.3), such as tau. The nucleotide-state of the NBD allosterically regulates substrate binding in the SBD [116]. Specifically, ATP binding causes the SBD to dock with the NBD, allowing clients to bind. Then, hydrolysis of ATP releases the SBD-NBD interaction, which causes a “lid” subdomain in the SBD to close on top of its clients [117]. The cycling of Hsp70 through these conformations is regulated by co-chaperones (Figure 1.3). J-proteins bind between the NBD and SBD to accelerate ATP hydrolysis [118], while nucleotide exchange factors (NEFs) bind the NBD and help release ADP [119]. Other co-chaperones for Hsp70 include the C-terminus of Hsc70 interacting protein (CHIP), which is an E3 ligase that adds ubiquitin chains to tau [81]. Overexpression of CHIP decreases tau levels [81, 82, 113], showing the dramatic effect of this system on tau homeostasis. Binding of tau to the Hsp70-CHIP complex leads to ubiquitin-mediated degradation of tau and subsequent prevention of tau aggregation [111, 120, 121]. Other co-chaperone interactions also regulate tau levels. For example, Bag-1 is a NEF for Hsp70 that, when over-expressed, increases total tau levels [122]. Knockdown of Bag-1 decreases total tau, but, counter-intuitively, increases the levels of hyper-phosphorylated tau [122]. Bag-1 also links the Hsp70 chaperone network to the UPS [123, 124], and may associate with Hsp70 client proteins to target them for degradation. Another Hsp70 NEF, Bag-2, promotes ubiquitin independent degradation of phosphorylated tau [125]. Thus, the fate of tau is partly determined by which NEF (*i.e.* Bag-1 vs. Bag-2) is associated with the Hsp70-tau complex. The J-proteins are also linked to controlling tau homeostasis. DnaJA1

is a co-chaperone that facilitates degradation of tau through the UPS [126]. Likewise, overexpression of DnaJB1 and DnaJB2 also reduce tau levels in an Hsp70 dependent manner [127]. Finally, Hsp70 isoforms can have distinct effects on tau stability [33]. Hsc70 (HSPA8), the cytosolic paralog, partitions tau onto microtubules [33, 128]. In contrast, Hsp72 (HSPA1A), the closely related and stress inducible paralog, promotes tau dissociation from microtubules and its trafficking to the proteasome [33]. This result is highly surprising, as Hsc70 and Hsp72 are nearly identical, yet subtle differences in their C-terminal domains appears to dictate diametrically opposed activities, as revealed by chimeric proteins [33].

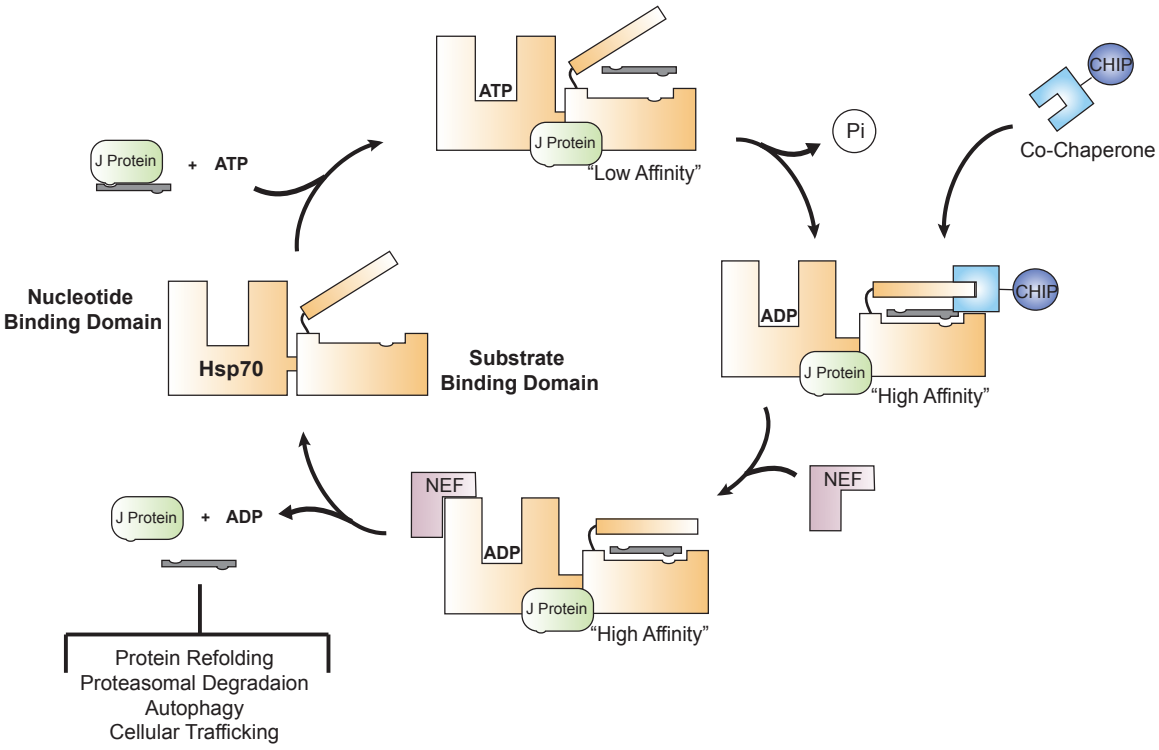

Figure 1.3 Hsp70 ATPase cycle is regulated by co-chaperones. J-proteins and NEFs facilitate ATP hydrolysis and ADP release respectively. Co-chaperones like CHIP, when bound to the C-terminus of Hsp70, lead to ubiquitination of Hsp70 substrates.

In many ways Hsp70 acts as a scaffold, which binds tau and uses co-chaperone PPIs to shuttle it to either degradation or retention pathways. Accordingly, a key interaction for tau homeostasis is its direct binding to Hsp70s. There are multiple binding sites for Hsc70 and Hsp72 on tau. Peptide microarray experiments and

mutations have shown that Hsp70s bind three sites in or near the MTBRs and an additional site in the N-terminus [129, 130]. The N-terminal tau binding site is specific for Hsp72 and may contribute to the selective pro-degradation effects of this isoform on tau [129]. NMR results confirm that Hsp70 binds two short sequences of 4R0N tau in the second and third repeat regions, specifically the aggregation motifs ^{275}VQIINK^{280} and ^{306}VQIVYK^{311} [33]. Binding of Hsp70s to these hydrophobic, repeat domains suggests that they may work to prevent tau aggregation by sequestering free tau that has been released from the microtubule. In other words, tau aggregation may be suppressed by being bound to either microtubules or Hsp70s. Indeed, Hsp70 can block tau aggregation *in vitro* [131].

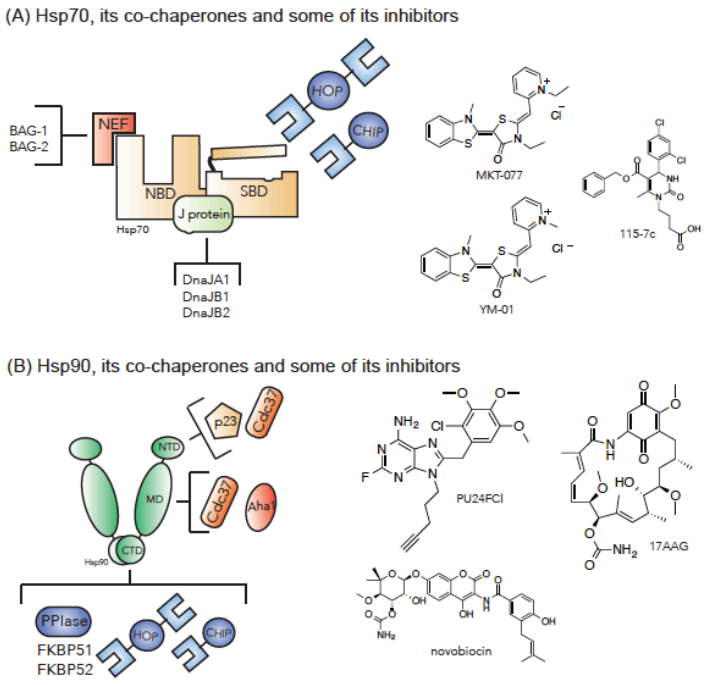

Figure 1.4 Focus on the molecular chaperones, Hsp70 and Hsp90, that are important for tau homeostasis. (A) Hsp70 and (B) Hsp90 are shown, along with a sampling of the co-chaperones and chemical inhibitors discussed in the text. Together, these systems coordinate tau quality control. Chemicals that inhibit specific aspects of chaperone function have been shown to promote tau turnover.

1.9.1 Modulators of Hsp70 and their effects on tau stability

In part, the central role of Hsp70 in tau homeostasis has been clarified and revealed through the use of small molecule agonists and antagonists. This

“chemical biology” approach is based on the idea that perturbing the function of Hsp70 and its PPIs with co-chaperones might be a powerful way to find drug targets within the Hsp70 sub-network. This concept is illustrated by recent studies using the rhodacyanine MKT-077 and its analogs (Figure 1.4A). These compounds bind the NBD of Hsp70 [132] and allosterically decouple NEF interactions [133, 134]. Treatment with these molecules reduces the levels of phosphorylated tau in multiple cellular models of tauopathy [127, 135]. Treatment with one analog, YM-01, also reduces tau levels in brain slices from rTg4510 tau transgenic mice and restores normal long-term potentiation (LTP) [127]. The same molecule has no effect on wild type tau from normal mice and, in cell models, YM-01 has preferential activity against hyper-phosphorylated tau. However, if the microtubule network is chemically disrupted, YM-01 is now able to effectively reduce even wild type tau. Together, these results suggest that Hsp70 only acts on tau that is dissociated from microtubules, consistent with the known binding site of the chaperone. This is an important distinction because eventual clinical use of an Hsp70 agonist might depend on the safe and selective activity on only abnormal, and not functional, tau. In Chapter 2, I describe my efforts to describe the molecular mechanisms by which YM-01 and its analogs promote clearance of tau through Hsp70 and in Chapter 4, I further explore the paralogs of Hsp70 that are responsible for the compound’s activity.

Beyond these compounds, other modulators of the Hsp70 multi-protein system have been described [136, 137]. Of note, the flavonoid-based natural product myricetin reduces tau levels through inhibition of Hsp70 interactions with J-proteins [136, 138]. In contrast, the dihydropyrimidines SW-02 and 115-7c activated Hsp70 ATPase turnover, which resulted in an increase in total tau levels *in vivo* [136, 137]. Interestingly, additional neurodegenerative markers such as alpha-synuclein and TDP-43 were not sensitive to treatment with Hsp70 modulators, indicating that chemical manipulation of Hsp70 can selectively target tau without necessarily interrupting homeostasis of other proteins [136].

1.9.2 Hsp90 and its co-chaperones regulate tau stability

Hsp90 is another molecular chaperone that tightly controls tau fate [139]. Hsp90 is a homodimer with each protomer consisting of three domains: an N-terminal ATP-binding domain (NTD), a middle domain (MD) for binding client proteins and a C-terminal domain (CTD), which stabilizes Hsp90 dimer formation (Figure 1.4.B). Like Hsp70, Hsp90 has an ATPase cycle that is regulated by co-chaperones, which direct conformational changes between open and closed states of Hsp90 [140]. The co-chaperone Aha1 binds the MD of Hsp90 and increases ATP hydrolysis through stabilization of the closed ATP-bound state of Hsp90 [140, 141]. The NTD binding co-chaperone p23 also stabilizes the closed state of Hsp90 and traps substrate clients while accelerating ATP hydrolysis [142]. In the closed ATP state, Hsp90 has a high affinity for its substrates. These trapped client proteins can then be modified by Hsp90 co-chaperones to initiate refolding or degradation, and upon ATP hydrolysis, substrates are released from the MD. For example, Hsp90 and CHIP coordinate to ubiquitinate phosphorylated tau, like the Hsp70-CHIP complex, leading to its degradation by the UPS [143]. Another co-chaperone, Cdc37, inhibits Hsp90 ATPase activity through binding to the NTD and MD and delaying the formation of the closed state of Hsp90, a rate-limiting step of the ATPase cycle [144]. Hsp90 and its co-chaperones have been linked to tau proteostasis through promotion of tau degradation as well as tau "refolding" (*e.g.* re-binding to microtubules). Knockdown of Aha1, p23 or Cdc37 decreases both total and phospho-tau levels [143, 145]. Upregulation of Cdc37 preserves total tau and phospho-tau but has no effect on alpha-synuclein [146]. Cdc37 localizes kinases important for tau phosphorylation to the Hsp90-tau complex; therefore, it is not surprising that changes in expression of this co-chaperone have dramatic effects on tau retention and clearance. Similarly, the Hsp90 co-chaperone, FKBP51, stabilizes tau and promotes its aggregation by preventing CHIP-mediated ubiquitination [147]. FKBP52 is another Hsp90 co-chaperone close in structure and function to FKBP51; however, this co-chaperone preferentially binds phospho-tau and prevents it accumulation *in vivo* [148]. The differential effects of co-chaperones on Hsp90-tau complexes

emphasizes that the outcome of client interactions are dependent on which co-chaperones are bound [149]. This model further supports the idea that targeting specific chaperone PPIs may be the most tunable approach to removing distinct, abnormal pools of tau.

The Hsp90 network is linked to the Hsp70 network through the shared co-chaperone, HOP. Hsp90 and Hsp70 form well characterized complexes with HOP, which allow for the exchange of substrate clients between these protein networks [150, 151]. In the case of tau, it is reported that tau can be transferred from Hsp70 to Hsp90 before its degradation [129, 152]. The Hsp90 binding site on 4R0N tau consists of the entire MTBR which overlaps with the two Hsp70 binding sites in the 3R and 4R repeat domains, suggesting that these chaperones likely do not bind tau simultaneously [32, 129]. Interestingly, transfer of tau between Hsp70 and Hsp90 may also facilitate tau refolding, as overexpression of HOP has been shown to increase levels of both total tau and phospho-tau [145].

1.9.3 Inhibitors of Hsp90 clear tau

Inhibitors of Hsp90, such as PU24FCl, bind to the NTD and compete with nucleotide. [153]. Treatment with PU24FCl reduces hyper-phosphorylated tau and insoluble tau in cellular models [143, 154] while no effect is seen on normal tau [154], suggesting that Hsp90 and its co-chaperones preferentially act on abnormal tau. Another competitive inhibitor of Hsp90, 17-(allyllamino)-17-demethoxygeldanamycin (17AAG), also reduces P301L tau levels [154], so this effect seems to occur independent of chemotype (Figure 1.4B). Hsp90 inhibitors are being explored in numerous clinical trials for cancer [155, 156], so there is some possibility that the compounds might be suitable for eventual exploration in tauopathies. However, such an approach would likely require a more chronic dosing schedule and the safety of long-term chaperone manipulation is uncertain.

Another distinct class of Hsp90 inhibitors, including novobiocin, bind to the CTD instead of the NTD [157]. Upon binding to Hsp90, novobiocin prevents dimerization of the CTDs and stalls the Hsp90 cycle by a unique mechanism [158]. Novobiocin analogues and other CTD-binding small molecules have been developed [159] and shown to reduce tau levels in cellular models [160, 161]. It is worth making the distinction between N- and C-terminal Hsp90 inhibitors because the C-terminal inhibitors do not seem to activate a stress response [162]. It isn't yet clear how a stress response might contribute to the activity of Hsp90 inhibitors, but the pharmacological tools to ask this question are becoming available.

1.10 Other pathways for reducing tau levels

Although Hsp70 and Hsp90 may be the best-studied tau-binding partners, there are many other possible targets in the proteostasis network. The goal in any of these approaches is to reduce the accumulation of aberrant tau (*e.g.* hyper-phosphorylated, free from microtubules, *etc*). It isn't yet clear whether these strategies necessarily need to spare normal tau (*e.g.* microtubule-bound), but this remains an important consideration in any drug discovery strategy. In the next sections, we introduce some of the most likely, emerging targets, which (in most cases) have more speculative links to tau quality control.

1.10.1 Hsp27

Hsp27 is a small heat shock protein that interacts with client proteins, including tau, as part of a multi-protein oligomer [163]. Upon stress-induced phosphorylation, Hsp27 disassembles from larger oligomers into smaller complexes, which seem to be potent chaperones for IDPs [164]. Indeed, Hsp27 preferentially binds phosphorylated tau in AD brain homogenates and neuronal cell models, and this chaperone is correlated with its dephosphorylation and degradation [165]. Overexpression of Hsp27 reduces tau fibril formation and restores long-term-potentiation in a transgenic mouse model expressing mutant

P301L tau [166, 167]. However, a gap in our understanding of this system is how phosphorylation regulates Hsp27 client binding. Moreover, small molecule activators of this system have not been described. However, this goal seems worthwhile because Hsp27 levels are increased 20% in AD brains [168].

1.10.2 PPIases

Peptidyl-prolyl isomerases (PPIases) are another class of co-chaperones known to effect tau homeostasis by catalyzing the isomerization of proline residues [169]. One major protein in this class, Pin1, is highly expressed in neurons and is implicated in amyloid β pathology [170] and tauopathies like FTDP-17 and AD [171, 172]. Pin1 binds tau phosphorylated at several major phosphorylation sites and localizes with NFTs in AD brains [172, 173]. Upon binding to phospho-tau, specifically pT231, Pin1 converts cis-prolines preceding phosphorylated serine and threonine residues into trans-prolines [174]. Cis-tau accumulates and aggregates in AD brains and is unable to polymerize microtubules [174]. As a result, Pin1 conversion of cis-tau to trans-tau restores microtubule assembly [173, 175], highlighting the significant role of Pin1 in maintaining cis-trans tau homeostasis. Pin1 expression is reduced in AD brains [173]; therefore, normalizing expression of Pin1 may be one therapeutic strategy to prevent the accumulation of hyperphosphorylated tau.

1.10.3 Clusterin

Genome wide association studies have implicated the molecular chaperone, clusterin, in AD [176, 177]. This chaperone, which is highly expressed in neurons, especially in AD and PD patients, is reported to promote amyloid beta pathology and is correlated with the deposition of amyloid beta fibrils [178]. Clusterin has also been linked to tau pathology due to elevated levels of intracellular clusterin in transgenic tau mouse models [179]. While there is clinical evidence to suggest that clusterin plays a critical role in AD, the molecular biology of this protein and its effects on tau remain unknown. One possible

explanation for clusterin's role in amyloid beta and tau pathology is that, in addition to modulating apoptosis and cell signaling pathways, clusterin is also a member of the autophagy/beclin-1 interactome [180]. It will be interesting to see if chemical probes targeting clusterin can be developed to aid in understanding how this protein regulates tau pathology.

1.10.4 HDAC6

Histone deacetylase 6 (HDAC6) is another key partner for tau that directly impacts its homeostasis, especially after inhibition of the proteasome [181]. HDAC6 plays an important role in autophagic clearance of tau, and HDAC6 inhibitors lead to increased tau acetylation and aggregation [182, 183]. However, to illustrate the delicate balance required for proper tau homeostasis, inhibition of HDAC6 actually reduced phospho-tau in some models [88, 184, 185], likely because of competition between acetylation and phosphorylation [88].

1.10.5 Autophagy and UPS targets

Chaperone-mediated autophagy (CMA) and the ubiquitin-proteasome system (UPS) are the major clearance pathways for removing tau [112, 115, 186]. Consistent with this idea, activation of autophagy by rapamycin reduces tau phosphorylation and tau tangle formation in cellular models of tauopathy as well as P301S tau transgenic mice [186, 187]. Rapamycin treatment also reduces phosphorylation of tau by the kinase GSK3β (glycogen synthase kinase 3 beta), highlighting the possibility that combinations of autophagy activators with kinase inhibitors may be effective at reducing the levels of hyperphosphorylated tau [187]. To accelerate clearance through the UPS, one enticing idea is to activate the proteasome with UPS14 inhibitors [188]. USP14 is a deubiquitinating enzyme that dampens turnover of proteasome substrates. Therefore, inhibitors of USP14 might be expected to re-balance tau homeostasis. In both the autophagy and UPS cases, specific targets would be expected to counter-act the age-dependent loss of clearance capacity, perhaps normalizing tau levels.

1.11 The future of tau reduction therapies

Tauopathies result from the failure of neurons to maintain proper tau homeostasis. Therefore, one approach to therapy may be to modulate targets that control the flux of tau (see Figure 1.2). As mentioned above, this goal might be achieved by blocking tau transcription or translation, preventing its aggregation or by accelerating its clearance using antibodies. An alternative approach is to target the host factors that normally regulate tau homeostasis to accelerate turnover of abnormal tau. However, the path forward for tau-based therapies remains at the pre-clinical stage. In our opinion, antibodies that bind to tau, especially phospho-tau and oligomeric tau, seem to offer the most immediate paths to clinical testing of the tau reduction hypothesis [189-191]. However, to overcome limitations associated with the cost and delivery of antibodies to the CNS, second-generation approaches might be focused on small molecule tau aggregation inhibitors and activators of chaperone-mediated tau turnover [192-194]. The major concern with these approaches will be safety because it is unclear whether any of them will be able to selectively reduce abnormal tau without causing proteostatic collapse.

One of the best-characterized ways to reduce tau levels with small molecules is through analogs of MKT-077, as described above. These molecules are known to act through Hsp70 to promote the turnover of tau and tau variants. In addition, recent efforts in the Gestwicki laboratory have generated analogs, such as YM-08, that have good blood-brain barrier permeability. While these results are promising, the mechanisms by which MKT-077 analogs activate turnover through Hsp70 are not known. In my thesis work, I explored this important question and, in Chapter 2, describe how MKT-077 analogs promote the interaction between Hsp70 and tau to stimulate turnover. In Chapter 3, I further characterize the paralogs of Hsp70 that are required for the activity of MKT-077 and its analogs. Together, these studies advance our knowledge of the role of Hsp70 in tau turnover and help validate it as a drug target for tauopathies.

Finally, a hallmark of tauopathy is the seeding and spreading of tau aggregation and pathology through the uptake of extracellular tau fibrils [195]. The mechanisms of cell-to-cell transmission remains unclear, but cell and animal models are in development [196-199], providing, for the first time, an opportunity to target proteins important in this process. Accordingly, a key part of Chapter 4 is to describe my efforts in building new tauopathy models that are specifically geared towards studying these mechanisms. We predict that a better understanding of the mechanisms of spreading will reveal unexpected, new drug targets. These targets hold the currently unfulfilled promise of better selectivity and safety.

Notes

This chapter is based on a chapter in a book titled “Prion Diseases” which is in press at Cold Harbor Spring Laboratory Press. Zapporah Young, Sue Ann Mok and Jason Gestwicki contributed intellectually to this work.

1.12 References

[1] Ghetti B, Wszolek ZK, Boeve BF, Spina S, Goedert M. Frontotemporal Dementia and Parkinsonism
Linked to Chromosome 17. In: Dickson DW, Weller RO, ed.^eds., Neurodegeneration: The Molecular Pathology of Dementia and Movement Disorders, 2011.

[2] Braak H, Braak E. Neuropathological stageing of Alzheimer-related changes. Acta Neuropathol, 1991; 82: 239-59.

[3] Roberson ED, Scearce-Levie K, Palop JJ, Yan F, Cheng IH, Wu T, Gerstein H, Yu GQ, Mucke L. Reducing endogenous tau ameliorates amyloid beta-induced deficits in an Alzheimer's disease mouse model. Science, 2007; 316: 750-4.

[4] Frost B, Hemberg M, Lewis J, Feany MB. Tau promotes neurodegeneration through global chromatin relaxation. Nat Neurosci, 2014; 17: 357-66.

[5] Spillantini MG, Goedert M. Tau pathology and neurodegeneration. Lancet Neurol, 2013; 12: 609-22.

[6] Noble W, Hanger DP, Gallo JM. Transgenic mouse models of tauopathy in drug discovery. CNS Neurol Disord Drug Targets, 2010; 9: 403-28.
[7] Weingarten MD, Lockwood AH, Hwo SY, Kirschner MW. A protein factor essential for microtubule assembly. Proc Natl Acad Sci U S A, 1975; 72: 1858-62.
[8] Fanara P, Husted KH, Selle K, Wong PY, Banerjee J, Brandt R, Hellerstein MK. Changes in microtubule turnover accompany synaptic plasticity and memory formation in response to contextual fear conditioning in mice. Neuroscience, 2010; 168: 167-78.
[9] Qiang L, Yu W, Andreadis A, Luo M, Baas PW. Tau protects microtubules in the axon from severing by katanin. J Neurosci, 2006; 26: 3120-9.
[10] LoPresti P, Szuchet S, Papasozomenos SC, Zinkowski RP, Binder LI. Functional implications for the microtubule-associated protein tau: localization in oligodendrocytes. Proc Natl Acad Sci U S A, 1995; 92: 10369-73.
[11] Shin RW, Iwaki T, Kitamoto T, Tateishi J. Hydrated autoclave pretreatment enhances tau immunoreactivity in formalin-fixed normal and Alzheimer's disease brain tissues. Lab Invest, 1991; 64: 693-702.
[12] Trojanowski JQ, Schuck T, Schmidt ML, Lee VM. Distribution of tau proteins in the normal human central and peripheral nervous system. J Histochem Cytochem, 1989; 37: 209-15.
[13] Binder LI, Frankfurter A, Rebhun LI. The distribution of tau in the mammalian central nervous system. J Cell Biol, 1985; 101: 1371-8.
[14] Goedert M, Spillantini MG, Jakes R, Rutherford D, Crowther RA. Multiple isoforms of human microtubule-associated protein tau: sequences and localization in neurofibrillary tangles of Alzheimer's disease. Neuron, 1989; 3: 519-26.
[15] Mukrasch MD, Bibow S, Korukottu J, Jeganathan S, Biernat J, Griesinger C, Mandelkow E, Zweckstetter M. Structural polymorphism of 441-residue tau at single residue resolution. PLoS Biol, 2009; 7: e34.
[16] Fauquant C, Redeker V, Landrieu I, Wieruszeski JM, Verdegem D, Laprevote O, Lippens G, Gigant B, Knossow M. Systematic identification of tubulin-interacting fragments of the microtubule-associated protein Tau leads to a highly efficient promoter of microtubule assembly. J Biol Chem, 2011; 286: 33358-68.
[17] Mukrasch MD, Biernat J, von Bergen M, Griesinger C, Mandelkow E, Zweckstetter M. Sites of tau important for aggregation populate {beta}-structure and bind to microtubules and polyanions. J Biol Chem, 2005; 280: 24978-86.
[18] Sillen A, Barbier P, Landrieu I, Lefebvre S, Wieruszeski JM, Leroy A, Peyrot V, Lippens G. NMR investigation of the interaction between the neuronal protein tau and the microtubules. Biochemistry, 2007; 46: 3055-64.
[19] Goode BL, Chau M, Denis PE, Feinstein SC. Structural and functional differences between 3-repeat and 4-repeat tau isoforms. Implications for

normal tau function and the onset of neurodegenetative disease. J Biol Chem, 2000; 275: 38182-9.
[20] Goedert M, Jakes R. Expression of separate isoforms of human tau protein: correlation with the tau pattern in brain and effects on tubulin polymerization. EMBO J, 1990; 9: 4225-30.
[21] Mandelkow EM, Mandelkow E. Biochemistry and cell biology of tau protein in neurofibrillary degeneration. Cold Spring Harb Perspect Med, 2012; 2: a006247.
[22] Moraga DM, Nunez P, Garrido J, Maccioni RB. A tau fragment containing a repetitive sequence induces bundling of actin filaments. J Neurochem, 1993; 61: 979-86.
[23] Jancsik V, Filliol D, Rendon A. Tau proteins bind to kinesin and modulate its activation by microtubules. Neurobiology (Bp), 1996; 4: 417-29.
[24] Seitz A, Kojima H, Oiwa K, Mandelkow EM, Song YH, Mandelkow E. Single-molecule investigation of the interference between kinesin, tau and MAP2c. EMBO J, 2002; 21: 4896-905.
[25] Patterson KR, Ward SM, Combs B, Voss K, Kanaan NM, Morfini G, Brady ST, Gamblin TC, Binder LI. Heat shock protein 70 prevents both tau aggregation and the inhibitory effects of preexisting tau aggregates on fast axonal transport. Biochemistry, 2011; 50: 10300-10.
[26] Magnani E, Fan J, Gasparini L, Golding M, Williams M, Schiavo G, Goedert M, Amos LA, Spillantini MG. Interaction of tau protein with the dynactin complex. EMBO J, 2007; 26: 4546-54.
[27] Ebneth A, Godemann R, Stamer K, Illenberger S, Trinczek B, Mandelkow E. Overexpression of tau protein inhibits kinesin-dependent trafficking of vesicles, mitochondria, and endoplasmic reticulum: implications for Alzheimer's disease. J Cell Biol, 1998; 143: 777-94.
[28] Ittner LM, Fath T, Ke YD, Bi M, van Eersel J, Li KM, Gunning P, Gotz J. Parkinsonism and impaired axonal transport in a mouse model of frontotemporal dementia. Proc Natl Acad Sci U S A, 2008; 105: 15997-6002.
[29] Stamer K, Vogel R, Thies E, Mandelkow E, Mandelkow EM. Tau blocks traffic of organelles, neurofilaments, and APP vesicles in neurons and enhances oxidative stress. J Cell Biol, 2002; 156: 1051-63.
[30] Reynolds CH, Garwood CJ, Wray S, Price C, Kellie S, Perera T, Zvelebil M, Yang A, Sheppard PW, Varndell IM, Hanger DP, Anderton BH. Phosphorylation regulates tau interactions with Src homology 3 domains of phosphatidylinositol 3-kinase, phospholipase Cgamma1, Grb2, and Src family kinases. J Biol Chem, 2008; 283: 18177-86.
[31] Sharma VM, Litersky JM, Bhaskar K, Lee G. Tau impacts on growth-factor-stimulated actin remodeling. J Cell Sci, 2007; 120: 748-57.
[32] Karagoz GE, Duarte AM, Akoury E, Ippel H, Biernat J, Moran Luengo T, Radli M, Didenko T, Nordhues BA, Veprintsev DB, Dickey CA, Mandelkow E, Zweckstetter M, Boelens R, Madl T, Rudiger SG. Hsp90-Tau complex reveals molecular basis for specificity in chaperone action. Cell, 2014; 156: 963-74.

[33] Jinwal UK, Akoury E, Abisambra JF, O'Leary JC, 3rd, Thompson AD, Blair LJ, Jin Y, Bacon J, Nordhues BA, Cockman M, Zhang J, Li P, Zhang B, Borysov S, Uversky VN, Biernat J, Mandelkow E, Gestwicki JE, Zweckstetter M, Dickey CA. Imbalance of Hsp70 family variants fosters tau accumulation. FASEB J, 2013; 27: 1450-9.
[34] Miyata Y, Koren J, Kiray J, Dickey Ca, Gestwicki JE. Molecular chaperones and regulation of tau quality control: strategies for drug discovery in tauopathies. Future medicinal chemistry, 2011; 3: 1523-37.
[35] von Bergen M, Barghorn S, Li L, Marx A, Biernat J, Mandelkow EM, Mandelkow E. Mutations of tau protein in frontotemporal dementia promote aggregation of paired helical filaments by enhancing local beta-structure. J Biol Chem, 2001; 276: 48165-74.
[36] von Bergen M, Friedhoff P, Biernat J, Heberle J, Mandelkow EM, Mandelkow E. Assembly of tau protein into Alzheimer paired helical filaments depends on a local sequence motif ((306)VQIVYK(311)) forming beta structure. Proc Natl Acad Sci U S A, 2000; 97: 5129-34.
[37] Goux WJ, Kopplin L, Nguyen AD, Leak K, Rutkofsky M, Shanmuganandam VD, Sharma D, Inouye H, Kirschner DA. The formation of straight and twisted filaments from short tau peptides. J Biol Chem, 2004; 279: 26868-75.
[38] Barghorn S, Mandelkow E. Toward a unified scheme for the aggregation of tau into Alzheimer paired helical filaments. Biochemistry, 2002; 41: 14885-96.
[39] Chirita CN, Necula M, Kuret J. Anionic micelles and vesicles induce tau fibrillization in vitro. J Biol Chem, 2003; 278: 25644-50.
[40] Friedhoff P, Schneider A, Mandelkow EM, Mandelkow E. Rapid assembly of Alzheimer-like paired helical filaments from microtubule-associated protein tau monitored by fluorescence in solution. Biochemistry, 1998; 37: 10223-30.
[41] Kampers T, Friedhoff P, Biernat J, Mandelkow EM, Mandelkow E. RNA stimulates aggregation of microtubule-associated protein tau into Alzheimer-like paired helical filaments. FEBS Lett, 1996; 399: 344-9.
[42] Gerson JE, Sengupta U, Lasagna-Reeves CA, Guerrero-Munoz MJ, Troncoso J, Kayed R. Characterization of tau oligomeric seeds in progressive supranuclear palsy. Acta Neuropathol Commun, 2014; 2: 73.
[43] Maeda S, Sahara N, Saito Y, Murayama M, Yoshiike Y, Kim H, Miyasaka T, Murayama S, Ikai A, Takashima A. Granular tau oligomers as intermediates of tau filaments. Biochemistry, 2007; 46: 3856-61.
[44] Flach K, Hilbrich I, Schiffmann A, Gartner U, Kruger M, Leonhardt M, Waschipky H, Wick L, Arendt T, Holzer M. Tau oligomers impair artificial membrane integrity and cellular viability. J Biol Chem, 2012; 287: 43223-33.
[45] Castillo-Carranza DL, Guerrero-Munoz MJ, Sengupta U, Hernandez C, Barrett AD, Dineley K, Kayed R. Tau immunotherapy modulates both pathological tau and upstream amyloid pathology in an Alzheimer's disease mouse model. J Neurosci, 2015; 35: 4857-68.

[46] Castillo-Carranza DL, Sengupta U, Guerrero-Munoz MJ, Lasagna-Reeves CA, Gerson JE, Singh G, Estes DM, Barrett AD, Dineley KT, Jackson GR, Kayed R. Passive immunization with Tau oligomer monoclonal antibody reverses tauopathy phenotypes without affecting hyperphosphorylated neurofibrillary tangles. J Neurosci, 2014; 34: 4260-72.
[47] Clavaguera F, Akatsu H, Fraser G, Crowther RA, Frank S, Hench J, Probst A, Winkler DT, Reichwald J, Staufenbiel M, Ghetti B, Goedert M, Tolnay M. Brain homogenates from human tauopathies induce tau inclusions in mouse brain. Proc Natl Acad Sci U S A, 2013; 110: 9535-40.
[48] de Calignon A, Polydoro M, Suarez-Calvet M, William C, Adamowicz DH, Kopeikina KJ, Pitstick R, Sahara N, Ashe KH, Carlson GA, Spires-Jones TL, Hyman BT. Propagation of tau pathology in a model of early Alzheimer's disease. Neuron, 2012; 73: 685-97.
[49] Lasagna-Reeves CA, Castillo-Carranza DL, Sengupta U, Guerrero-Munoz MJ, Kiritoshi T, Neugebauer V, Jackson GR, Kayed R. Alzheimer brain-derived tau oligomers propagate pathology from endogenous tau. Sci Rep, 2012; 2: 700.
[50] Liu L, Drouet V, Wu JW, Witter MP, Small SA, Clelland C, Duff K. Trans-synaptic spread of tau pathology in vivo. PLoS One, 2012; 7: e31302.
[51] Ghetti B, Oblak AL, Boeve BF, Johnson KA, Dickerson BC, Goedert M. Invited review: Frontotemporal dementia caused by microtubule-associated protein tau gene (MAPT) mutations: a chameleon for neuropathology and neuroimaging. Neuropathol Appl Neurobiol, 2015; 41: 24-46.
[52] Coppola G, Chinnathambi S, Lee JJ, Dombroski BA, Baker MC, Soto-Ortolaza AI, Lee SE, Klein E, Huang AY, Sears R, Lane JR, Karydas AM, Kenet RO, Biernat J, Wang LS, Cotman CW, Decarli CS, Levey AI, Ringman JM, Mendez MF, Chui HC, Le Ber I, Brice A, Lupton MK, Preza E, Lovestone S, Powell J, Graff-Radford N, Petersen RC, Boeve BF, Lippa CF, Bigio EH, Mackenzie I, Finger E, Kertesz A, Caselli RJ, Gearing M, Juncos JL, Ghetti B, Spina S, Bordelon YM, Tourtellotte WW, Frosch MP, Vonsattel JP, Zarow C, Beach TG, Albin RL, Lieberman AP, Lee VM, Trojanowski JQ, Van Deerlin VM, Bird TD, Galasko DR, Masliah E, White CL, Troncoso JC, Hannequin D, Boxer AL, Geschwind MD, Kumar S, Mandelkow EM, Wszolek ZK, Uitti RJ, Dickson DW, Haines JL, Mayeux R, Pericak-Vance MA, Farrer LA, Alzheimer's Disease Genetics C, Ross OA, Rademakers R, Schellenberg GD, Miller BL, Mandelkow E, Geschwind DH. Evidence for a role of the rare p.A152T variant in MAPT in increasing the risk for FTD-spectrum and Alzheimer's diseases. Hum Mol Genet, 2012; 21: 3500-12.
[53] Baker M, Litvan I, Houlden H, Adamson J, Dickson D, Perez-Tur J, Hardy J, Lynch T, Bigio E, Hutton M. Association of an extended haplotype in the tau gene with progressive supranuclear palsy. Hum Mol Genet, 1999; 8: 711-5.
[54] Niblock M, Gallo JM. Tau alternative splicing in familial and sporadic tauopathies. Biochem Soc Trans, 2012; 40: 677-80.

[55] Qian W, Liu F. Regulation of alternative splicing of tau exon 10. Neurosci Bull, 2014; 30: 367-77.
[56] Panda D, Samuel JC, Massie M, Feinstein SC, Wilson L. Differential regulation of microtubule dynamics by three- and four-repeat tau: implications for the onset of neurodegenerative disease. Proc Natl Acad Sci U S A, 2003; 100: 9548-53.
[57] Adams SJ, DeTure MA, McBride M, Dickson DW, Petrucelli L. Three repeat isoforms of tau inhibit assembly of four repeat tau filaments. PLoS One, 2010; 5: e10810.
[58] Barghorn S, Zheng-Fischhofer Q, Ackmann M, Biernat J, von Bergen M, Mandelkow EM, Mandelkow E. Structure, microtubule interactions, and paired helical filament aggregation by tau mutants of frontotemporal dementias. Biochemistry, 2000; 39: 11714-21.
[59] Beharry C, Cohen LS, Di J, Ibrahim K, Briffa-Mirabella S, Alonso Adel C. Tau-induced neurodegeneration: mechanisms and targets. Neurosci Bull, 2014; 30: 346-58.
[60] Chang E, Kim S, Yin H, Nagaraja HN, Kuret J. Pathogenic missense MAPT mutations differentially modulate tau aggregation propensity at nucleation and extension steps. J Neurochem, 2008; 107: 1113-23.
[61] Combs B, Gamblin TC. FTDP-17 tau mutations induce distinct effects on aggregation and microtubule interactions. Biochemistry, 2012; 51: 8597-607.
[62] Hong M, Zhukareva V, Vogelsberg-Ragaglia V, Wszolek Z, Reed L, Miller BI, Geschwind DH, Bird TD, McKeel D, Goate A, Morris JC, Wilhelmsen KC, Schellenberg GD, Trojanowski JQ, Lee VM. Mutation-specific functional impairments in distinct tau isoforms of hereditary FTDP-17. Science, 1998; 282: 1914-7.
[63] Ghetti B, Wszolek ZK, Boeve BF, Spina S, Goedert M. Frontotemporal Dementia and Parkinsonism Linked to Chromosome 17. In: Dickson DW, Weller RO, ed.^eds., Neurodegeneration: The Molecular Pathology of Dementia and Movement Disorders, 2011.
[64] Bugiani O, Murrell JR, Giaccone G, Hasegawa M, Ghigo G, Tabaton M, Morbin M, Primavera A, Carella F, Solaro C, Grisoli M, Savoiardo M, Spillantini MG, Tagliavini F, Goedert M, Ghetti B. Frontotemporal dementia and corticobasal degeneration in a family with a P301S mutation in tau. J Neuropathol Exp Neurol, 1999; 58: 667-77.
[65] Reed LA, Wszolek ZK, Hutton M. Phenotypic correlations in FTDP-17. Neurobiol Aging, 2001; 22: 89-107.
[66] Saito Y, Geyer A, Sasaki R, Kuzuhara S, Nanba E, Miyasaka T, Suzuki K, Murayama S. Early-onset, rapidly progressive familial tauopathy with R406W mutation. Neurology, 2002; 58: 811-3.
[67] Martin L, Latypova X, Terro F. Post-translational modifications of tau protein: implications for Alzheimer's disease. Neurochem Int, 2011; 58: 458-71.
[68] Morris M, Knudsen GM, Maeda S, Trinidad JC, Ioanoviciu A, Burlingame AL, Mucke L. Tau post-translational modifications in wild-type and human

amyloid precursor protein transgenic mice. Nat Neurosci, 2015; 18: 1183-9.
[69] Kopke E, Tung YC, Shaikh S, Alonso AC, Iqbal K, Grundke-Iqbal I. Microtubule-associated protein tau. Abnormal phosphorylation of a non-paired helical filament pool in Alzheimer disease. J Biol Chem, 1993; 268: 24374-84.
[70] Augustinack JC, Schneider A, Mandelkow EM, Hyman BT. Specific tau phosphorylation sites correlate with severity of neuronal cytopathology in Alzheimer's disease. Acta Neuropathol, 2002; 103: 26-35.
[71] Mercken M, Vandermeeren M, Lubke U, Six J, Boons J, Van de Voorde A, Martin JJ, Gheuens J. Monoclonal antibodies with selective specificity for Alzheimer Tau are directed against phosphatase-sensitive epitopes. Acta Neuropathol, 1992; 84: 265-72.
[72] Kenessey A, Yen SH. The extent of phosphorylation of fetal tau is comparable to that of PHF-tau from Alzheimer paired helical filaments. Brain Res, 1993; 629: 40-6.
[73] Arendt T, Stieler J, Strijkstra AM, Hut RA, Rudiger J, Van der Zee EA, Harkany T, Holzer M, Hartig W. Reversible paired helical filament-like phosphorylation of tau is an adaptive process associated with neuronal plasticity in hibernating animals. J Neurosci, 2003; 23: 6972-81.
[74] Tepper K, Biernat J, Kumar S, Wegmann S, Timm T, Hubschmann S, Redecke L, Mandelkow EM, Muller DJ, Mandelkow E. Oligomer formation of tau protein hyperphosphorylated in cells. J Biol Chem, 2014; 289: 34389-407.
[75] Hoglinger GU, Huppertz HJ, Wagenpfeil S, Andres MV, Belloch V, Leon T, Del Ser T, Investigators TM. Tideglusib reduces progression of brain atrophy in progressive supranuclear palsy in a randomized trial. Mov Disord, 2014; 29: 479-87.
[76] Kimura T, Ishiguro K, Hisanaga S. Physiological and pathological phosphorylation of tau by Cdk5. Front Mol Neurosci, 2014; 7: 65.
[77] Nygaard HB, van Dyck CH, Strittmatter SM. Fyn kinase inhibition as a novel therapy for Alzheimer's disease. Alzheimers Res Ther, 2014; 6: 8.
[78] Kickstein E, Krauss S, Thornhill P, Rutschow D, Zeller R, Sharkey J, Williamson R, Fuchs M, Kohler A, Glossmann H, Schneider R, Sutherland C, Schweiger S. Biguanide metformin acts on tau phosphorylation via mTOR/protein phosphatase 2A (PP2A) signaling. Proc Natl Acad Sci U S A, 2010; 107: 21830-5.
[79] Liu F, Grundke-Iqbal I, Iqbal K, Gong CX. Contributions of protein phosphatases PP1, PP2A, PP2B and PP5 to the regulation of tau phosphorylation. Eur J Neurosci, 2005; 22: 1942-50.
[80] van Eersel J, Ke YD, Liu X, Delerue F, Kril JJ, Gotz J, Ittner LM. Sodium selenate mitigates tau pathology, neurodegeneration, and functional deficits in Alzheimer's disease models. Proc Natl Acad Sci U S A, 2010; 107: 13888-93.
[81] Dickey CA, Yue M, Lin WL, Dickson DW, Dunmore JH, Lee WC, Zehr C, West G, Cao S, Clark AM, Caldwell GA, Caldwell KA, Eckman C,

Patterson C, Hutton M, Petrucelli L. Deletion of the ubiquitin ligase CHIP leads to the accumulation, but not the aggregation, of both endogenous phospho- and caspase-3-cleaved tau species. J Neurosci, 2006; 26: 6985-96.

[82] Sahara N, Murayama M, Mizoroki T, Urushitani M, Imai Y, Takahashi R, Murata S, Tanaka K, Takashima A. In vivo evidence of CHIP up-regulation attenuating tau aggregation. Journal of Neurochemistry, 2005; 94: 1254-1263.

[83] Cripps D, Thomas SN, Jeng Y, Yang F, Davies P, Yang AJ. Alzheimer disease-specific conformation of hyperphosphorylated paired helical filament-Tau is polyubiquitinated through Lys-48, Lys-11, and Lys-6 ubiquitin conjugation. J Biol Chem, 2006; 281: 10825-38.

[84] Morishima-Kawashima M, Hasegawa M, Takio K, Suzuki M, Titani K, Ihara Y. Ubiquitin is conjugated with amino-terminally processed tau in paired helical filaments. Neuron, 1993; 10: 1151-60.

[85] Thomas SN, Funk KE, Wan Y, Liao Z, Davies P, Kuret J, Yang AJ. Dual modification of Alzheimer's disease PHF-tau protein by lysine methylation and ubiquitylation: a mass spectrometry approach. Acta Neuropathol, 2012; 123: 105-17.

[86] Irwin DJ, Cohen TJ, Grossman M, Arnold SE, Xie SX, Lee VM, Trojanowski JQ. Acetylated tau, a novel pathological signature in Alzheimer's disease and other tauopathies. Brain, 2012; 135: 807-18.

[87] Grinberg LT, Wang X, Wang C, Sohn PD, Theofilas P, Sidhu M, Arevalo JB, Heinsen H, Huang EJ, Rosen H, Miller BL, Gan L, Seeley WW. Argyrophilic grain disease differs from other tauopathies by lacking tau acetylation. Acta Neuropathol, 2013; 125: 581-93.

[88] Cook C, Carlomagno Y, Gendron TF, Dunmore J, Scheffel K, Stetler C, Davis M, Dickson D, Jarpe M, DeTure M, Petrucelli L. Acetylation of the KXGS motifs in tau is a critical determinant in modulation of tau aggregation and clearance. Human Molecular Genetics, 2014; 23: 104-116.

[89] Basurto-Islas G, Luna-Munoz J, Guillozet-Bongaarts AL, Binder LI, Mena R, Garcia-Sierra F. Accumulation of aspartic acid421- and glutamic acid391-cleaved tau in neurofibrillary tangles correlates with progression in Alzheimer disease. J Neuropathol Exp Neurol, 2008; 67: 470-83.

[90] Horowitz PM, Patterson KR, Guillozet-Bongaarts AL, Reynolds MR, Carroll CA, Weintraub ST, Bennett DA, Cryns VL, Berry RW, Binder LI. Early N-terminal changes and caspase-6 cleavage of tau in Alzheimer's disease. J Neurosci, 2004; 24: 7895-902.

[91] Fasulo L, Ugolini G, Visintin M, Bradbury A, Brancolini C, Verzillo V, Novak M, Cattaneo A. The neuronal microtubule-associated protein tau is a substrate for caspase-3 and an effector of apoptosis. J Neurochem, 2000; 75: 624-33.

[92] Gamblin TC, Chen F, Zambrano A, Abraha A, Lagalwar S, Guillozet AL, Lu M, Fu Y, Garcia-Sierra F, LaPointe N, Miller R, Berry RW, Binder LI, Cryns VL. Caspase cleavage of tau: linking amyloid and neurofibrillary

tangles in Alzheimer's disease. Proc Natl Acad Sci U S A, 2003; 100: 10032-7.
[93] Ding H, Matthews TA, Johnson GV. Site-specific phosphorylation and caspase cleavage differentially impact tau-microtubule interactions and tau aggregation. J Biol Chem, 2006; 281: 19107-14.
[94] Dolan PJ, Johnson GV. A caspase cleaved form of tau is preferentially degraded through the autophagy pathway. J Biol Chem, 2010; 285: 21978-87.
[95] Quintanilla RA, Matthews-Roberson TA, Dolan PJ, Johnson GV. Caspase-cleaved tau expression induces mitochondrial dysfunction in immortalized cortical neurons: implications for the pathogenesis of Alzheimer disease. J Biol Chem, 2009; 284: 18754-66.
[96] Plouffe V, Mohamed NV, Rivest-McGraw J, Bertrand J, Lauzon M, Leclerc N. Hyperphosphorylation and cleavage at D421 enhance tau secretion. PLoS One, 2012; 7: e36873.
[97] Ramcharitar J, Albrecht S, Afonso VM, Kaushal V, Bennett DA, Leblanc AC. Cerebrospinal fluid tau cleaved by caspase-6 reflects brain levels and cognition in aging and Alzheimer disease. J Neuropathol Exp Neurol, 2013; 72: 824-32.
[98] Funk KE, Thomas SN, Schafer KN, Cooper GL, Liao Z, Clark DJ, Yang AJ, Kuret J. Lysine methylation is an endogenous post-translational modification of tau protein in human brain and a modulator of aggregation propensity. Biochem J, 2014; 462: 77-88.
[99] Alonso Adel C, Mederlyova A, Novak M, Grundke-Iqbal I, Iqbal K. Promotion of hyperphosphorylation by frontotemporal dementia tau mutations. J Biol Chem, 2004; 279: 34873-81.
[100] Bulic B, Pickhardt M, Mandelkow EM, Mandelkow E. Tau protein and tau aggregation inhibitors. Neuropharmacology, 2010; 59: 276-89.
[101] Brunden KR, Yao Y, Potuzak JS, Ferrer NI, Ballatore C, James MJ, Hogan AM, Trojanowski JQ, Smith AB, 3rd, Lee VM. The characterization of microtubule-stabilizing drugs as possible therapeutic agents for Alzheimer's disease and related tauopathies. Pharmacol Res, 2011; 63: 341-51.
[102] Morris M, Hamto P, Adame A, Devidze N, Masliah E, Mucke L. Age-appropriate cognition and subtle dopamine-independent motor deficits in aged tau knockout mice. Neurobiol Aging, 2013; 34: 1523-9.
[103] DeVos SL, Goncharoff DK, Chen G, Kebodeaux CS, Yamada K, Stewart FR, Schuler DR, Maloney SE, Wozniak DF, Rigo F, Bennett CF, Cirrito JR, Holtzman DM, Miller TM. Antisense reduction of tau in adult mice protects against seizures. J Neurosci, 2013; 33: 12887-97.
[104] Sigurdsson EM. Immunotherapy targeting pathological tau protein in Alzheimer's disease and related tauopathies. Journal of Alzheimer's disease : JAD, 2008; 15: 157-68.
[105] Chai X, Wu S, Murray TK, Kinley R, Cella CV, Sims H, Buckner N, Hanmer J, Davies P, O'Neill MJ, Hutton ML, Citron M. Passive immunization with anti-Tau antibodies in two transgenic models: reduction

of Tau pathology and delay of disease progression. J Biol Chem, 2011; 286: 34457-67.
[106] Lee VMY, Brunden KR, Hutton M, Trojanowski JQ. Developing Therapeutic Approaches to Tau, Selected Kinases, and Related Neuronal Protein Targets. Cold Spring Harbor Perspectives in Medicine:, 2011; 1: a006437.
[107] Patury S, Miyata Y, Gestwicki JE. Pharmacological Targeting of the Hsp70 Chaperone. Current topics in medicinal chemistry, 2009; 9: 1337-51.
[108] Gestwicki JE, Garza D. Protein quality control in neurodegenerative disease. Progress in molecular biology and translational science, 2012; 107: 327-53.
[109] Pratt WB, Gestwicki JE, Osawa Y, Lieberman AP. Targeting Hsp90/Hsp70-Based Protein Quality Control for Treatment of Adult Onset Neurodegenerative Diseases. Annual Review of Pharmacology and Toxicology, 2015; 55: 353-371.
[110] Dou F, Netzer WJ, Tanemura K, Li F, Hartl FU, Takashima A, Gouras GK, Greengard P, Xu H. Chaperones increase association of tau protein with microtubules. Proc Natl Acad Sci U S A, 2003; 100: 721-6.
[111] Petrucelli L, Dickson D, Kehoe K, Taylor J, Snyder H, Grover A, De Lucia M, McGowan E, Lewis J, Prihar G, Kim J, Dillmann WH, Browne SE, Hall A, Voellmy R, Tsuboi Y, Dawson TM, Wolozin B, Hardy J, Hutton M. CHIP and Hsp70 regulate tau ubiquitination, degradation and aggregation. Human molecular genetics, 2004; 13: 703-14.
[112] Wang Y, Martinez-Vicente M, Kruger U, Kaushik S, Wong E, Mandelkow EM, Cuervo AM, Mandelkow E. Tau fragmentation, aggregation and clearance: the dual role of lysosomal processing. Hum Mol Genet, 2009; 18: 4153-70.
[113] Dickey CA, Koren J, Zhang YJ, Xu YF, Jinwal UK, Birnbaum MJ, Monks B, Sun M, Cheng AQ, Pattersonl C, Bailey RM, Dunmore J, Soresh S, Leon C, Morgan D, Petrucelli L. Akt and CHIP coregulate tau degradation through coordinated interactions. Proceedings of the National Academy of Sciences of the United States of America, 2008; 105: 3622-3627.
[114] Kruger U, Wang Y, Kumar S, Mandelkow EM. Autophagic degradation of tau in primary neurons and its enhancement by trehalose. Neurobiol Aging, 2012; 33: 2291-305.
[115] Wong ESP, Tan JMM, Soong W-E, Hussein K, Nukina N, Dawson VL, Dawson TM, Cuervo AM, Lim K-L. Autophagy-mediated clearance of aggresomes is not a universal phenomenon. Human Molecular Genetics, 2008; 17: 2570-2582.
[116] Zhuravleva A, Gierasch LM. Allosteric signal transmission in the nucleotide-binding domain of 70-kDa heat shock protein (Hsp70) molecular chaperones. Proceedings of the National Academy of Sciences of the United States of America, 2011; 108: 6987-92.
[117] Zhuravleva A, Clerico EM, Gierasch LM. An interdomain energetic tug-of-war creates the allosterically active state in Hsp70 molecular chaperones. Cell, 2012; 151: 1296-307.

[118] Ahmad A, Bhattacharya A, McDonald RA, Cordes M, Ellington B, Bertelsen EB, Zuiderweg ERP. Heat shock protein 70 kDa chaperone/DnaJ cochaperone complex employs an unusual dynamic interface. Proceedings of the National Academy of Sciences, 2011; 108: 18966-18971.
[119] Brehmer D, Rüdiger S, Gässler CS, Klostermeier D, Packschies L, Reinstein J, Mayer MP, Bukau B. Tuning of chaperone activity of Hsp70 proteins by modulation of nucleotide exchange. Nature structural biology, 2001; 8: 427-32.
[120] Shimura H, Schwartz D, Gygi SP, Kosik KS. CHIP-Hsc70 complex ubiquitinates phosphorylated tau and enhances cell survival. The Journal of biological chemistry, 2004; 279: 4869-76.
[121] Laiq-Jan Saidia MP, Kevin R. Kaya, Laura Sancheza, Eva-Maria Mandelkow,, Spires-Jones BTHaTL. Carboxy Terminus Heat Shock Protein 70 Interacting Protein Reduces Tau-Associated Degenerative Changes. J Alzheimers Dis, 2015; 44: 937-47.
[122] Elliott E, Tsvetkov P, Ginzburg I. BAG-1 associates with Hsc70.Tau complex and regulates the proteasomal degradation of Tau protein. The Journal of biological chemistry, 2007; 282: 37276-84.
[123] Lüders J, Demand J, Höhfeld J. The ubiquitin-related BAG-1 provides a link between the molecular chaperones Hsc70/Hsp70 and the proteasome. The Journal of biological chemistry, 2000; 275: 4613-7.
[124] Demand J, Alberti S, Patterson C, Hohfeld J. Cooperation of a ubiquitin domain protein and an E3 ubiquitin ligase during chaperone/proteasome coupling. Curr Biol, 2001; 11: 1569-77.
[125] Carrettiero DC, Hernandez I, Neveu P, Papagiannakopoulos T, Kosik KS. The cochaperone BAG2 sweeps paired helical filament- insoluble tau from the microtubule. J Neurosci, 2009; 29: 2151-61.
[126] Abisambra JF, Jinwal UK, Suntharalingam A, Arulselvam K, Brady S, Cockman M, Jin Y, Zhang B, Dickey CA. DnaJA1 antagonizes constitutive Hsp70-mediated stabilization of tau. Journal of molecular biology, 2012; 421: 653-61.
[127] Abisambra J, Jinwal UK, Miyata Y, Rogers J, Blair L, Li X, Seguin SP, Wang L, Jin Y, Bacon J, Brady S, Cockman M, Guidi C, Zhang J, Koren J, Young ZT, Atkins CA, Zhang B, Lawson LY, Weeber EJ, Brodsky JL, Gestwicki JE, Dickey CA. Allosteric Heat Shock Protein 70 Inhibitors Rapidly Rescue Synaptic Plasticity Deficits by Reducing Aberrant Tau. Biological psychiatry, 2013; 74: 367-374.
[128] Fontaine SN, Martin MD, Akoury E, Assimon VA, Borysov S, Nordhues BA, Sabbagh JJ, Cockman M, Gestwicki JE, Zweckstetter M, Dickey CA. The active Hsc70/tau complex can be exploited to enhance tau turnover without damaging microtubule dynamics. Hum Mol Genet, 2015; 24: 3971-81.
[129] Thompson AD, Scaglione KM, Prensner J, Gillies AT, Chinnaiyan A, Paulson HL, Jinwal UK, Dickey CA, Gestwicki JE. Analysis of the tau-

associated proteome reveals that exchange of Hsp70 for Hsp90 is involved in tau degradation. ACS chemical biology, 2012; 7: 1677-86.
[130] Sarkar M, Kuret J, Lee G. Two motifs within the tau microtubule-binding domain mediate its association with the hsc70 molecular chaperone. Journal of neuroscience research, 2008; 86: 2763-73.
[131] Voss K, Combs B, Patterson K, Binder LI, Gamblin TC. Hsp70 alters tau function and aggregation in an isoform specific manner. Biochemistry, 2012; 51: 888-98.
[132] Rousaki A, Miyata Y, Jinwal UK, Dickey Ca, Gestwicki JE, Zuiderweg ERP. Allosteric drugs: the interaction of antitumor compound MKT-077 with human Hsp70 chaperones. Journal of molecular biology, 2011; 411: 614-32.
[133] Li X, Colvin T, Rauch JN, Acosta-Alvear D, Kampmann M, Dunyak B, Hann B, Aftab BT, Murnane M, Cho M, Walter P, Weissman JS, Sherman MY, Gestwicki JE. Validation of the Hsp70–Bag3 Protein–Protein Interaction as a Potential Therapeutic Target in Cancer. Molecular Cancer Therapeutics, 2015; 14: 642-648.
[134] Colvin TA, Gabai VL, Gong J, Calderwood SK, Li H, Gummuluru S, Matchuk ON, Smirnova SG, Orlova NV, Zamulaeva IA, Garcia-Marcos M, Li X, Young ZT, Rauch JN, Gestwicki JE, Takayama S, Sherman MY. Hsp70–Bag3 Interactions Regulate Cancer-Related Signaling Networks. Cancer Research, 2014; 74: 4731-4740.
[135] Miyata Y, Li X, Lee H-F, Jinwal U, Srinivasan SR, Seguin SP, Young ZT, Brodsky JL, Dickey CA, Sun D, Gestwicki JE. Synthesis and Initial Evaluation of YM-08, a Blood-Brain Barrier Permeable Derivative of the Heat Shock Protein 70 (Hsp70) Inhibitor MKT-077, Which Reduces Tau Levels. ACS chemical neuroscience, 2013; 4: 930-939.
[136] Jinwal UK, Miyata Y, Koren J, Jones JR, Trotter JH, Chang L, O'Leary J, Morgan D, Lee DC, Shults CL, Rousaki A, Weeber EJ, Zuiderweg ERP, Gestwicki JE, Dickey Ca. Chemical manipulation of hsp70 ATPase activity regulates tau stability. The Journal of neuroscience : the official journal of the Society for Neuroscience, 2009; 29: 12079-88.
[137] Chang L, Bertelsen EB, Wisén S, Larsen EM, Zuiderweg ERP, Gestwicki JE. High-throughput screen for small molecules that modulate the ATPase activity of the molecular chaperone DnaK. Analytical biochemistry, 2008; 372: 167-76.
[138] Chang L, Miyata Y, Ung PMU, Bertelsen EB, McQuade TJ, Carlson Ha, Zuiderweg ERP, Gestwicki JE. Chemical screens against a reconstituted multiprotein complex: myricetin blocks DnaJ regulation of DnaK through an allosteric mechanism. Chemistry & biology, 2011; 18: 210-21.
[139] Salminen A, Ojala J, Kaarniranta K, Hiltunen M, Soininen H. Hsp90 regulates tau pathology through co-chaperone complexes in Alzheimer's disease. Prog Neurobiol, 2011; 93: 99-110.
[140] Hessling M, Richter K, Buchner J. Dissection of the ATP-induced conformational cycle of the molecular chaperone Hsp90. Nat Struct Mol Biol, 2009; 16: 287-293.

[141] Retzlaff M, Hagn F, Mitschke L, Hessling M, Gugel F, Kessler H, Richter K, Buchner J. Asymmetric activation of the hsp90 dimer by its cochaperone aha1. Mol Cell, 2010; 37: 344-54.
[142] McLaughlin SH, Sobott F, Yao Z-p, Zhang W, Nielsen PR, Grossmann JG, Laue ED, Robinson CV, Jackson SE. The Co-chaperone p23 Arrests the Hsp90 ATPase Cycle to Trap Client Proteins. Journal of Molecular Biology, 2006; 356: 746-758.
[143] Dickey CA, Kamal A, Lundgren K, Klosak N, Bailey RM, Dunmore J, Ash P, Shoraka S, Zlatkovic J, Eckman CB, Patterson C, Dickson DW, Jr NSN, Hutton M, Burrows F, Petrucelli L. The high-affinity HSP90-CHIP complex recognizes and selectively degrades phosphorylated tau client proteins. The Journal of clinical investigation, 2007; 117.
[144] Eckl JM, Rutz DA, Haslbeck V, Zierer BK, Reinstein J, Richter K. Cdc37 (cell division cycle 37) restricts Hsp90 (heat shock protein 90) motility by interaction with N-terminal and middle domain binding sites. J Biol Chem, 2013; 288: 16032-42.
[145] Jinwal UK, Koren J, Dickey CA. Reconstructing the Hsp90/Tau Machine. Current enzyme inhibition, 2013; 9: 41-45.
[146] Jinwal UK, Trotter JH, Abisambra JF, Koren J, Lawson LY, Vestal GD, O'Leary JC, Johnson AG, Jin Y, Jones JR, Li Q, Weeber EJ, Dickey CA. The Hsp90 Kinase Co-chaperone Cdc37 Regulates Tau Stability and Phosphorylation Dynamics. Journal of Biological Chemistry, 2011; 286: 16976-16983.
[147] Jinwal UK, Koren J, Borysov SI, Schmid AB, Abisambra JF, Blair LJ, Johnson AG, Jones JR, Shults CL, O'Leary JC, Jin Y, Buchner J, Cox MB, Dickey CA. The Hsp90 Cochaperone, FKBP51, Increases Tau Stability and Polymerizes Microtubules. The Journal of Neuroscience, 2010; 30: 591-599.
[148] Chambraud B, Sardin E, Giustiniani J, Dounane O, Schumacher M, Goedert M, Baulieu E-E. A role for FKBP52 in Tau protein function. Proceedings of the National Academy of Sciences, 2010; 107: 2658-2663.
[149] Rohl A, Rohrberg J, Buchner J. The chaperone Hsp90: changing partners for demanding clients. Trends Biochem Sci, 2013; 38: 253-62.
[150] Alvira S, Cuellar J, Rohl A, Yamamoto S, Itoh H, Alfonso C, Rivas G, Buchner J, Valpuesta JM. Structural characterization of the substrate transfer mechanism in Hsp70/Hsp90 folding machinery mediated by Hop. Nat Commun, 2014; 5: 5484.
[151] Rohl A, Wengler D, Madl T, Lagleder S, Tippel F, Herrmann M, Hendrix J, Richter K, Hack G, Schmid AB, Kessler H, Lamb DC, Buchner J. Hsp90 regulates the dynamics of its cochaperone Sti1 and the transfer of Hsp70 between modules. Nat Commun, 2015; 6.
[152] Fontaine SN, Rauch JN, Nordhues BA, Assimon VA, Stothert AR, Jinwal UK, Sabbagh JJ, Chang L, Stevens SM, Jr., Zuiderweg ER, Gestwicki JE, Dickey CA. Isoform-selective Genetic Inhibition of Constitutive Cytosolic Hsp70 Activity Promotes Client Tau Degradation Using an Altered Co-chaperone Complement. J Biol Chem, 2015; 290: 13115-27.

[153] Vilenchik M, Solit D, Basso A, Huezo H, Lucas B, He H, Rosen N, Spampinato C, Modrich P, Chiosis G. Targeting Wide-Range Oncogenic Transformation via PU24FCl, a Specific Inhibitor of Tumor Hsp90. Chemistry & Biology, 2004; 11: 787-797.
[154] Luo W, Dou F, Rodina A, Chip S, Kim J, Zhao Q, Moulick K, Aguirre J, Wu N, Greengard P, Chiosis G. Roles of heat-shock protein 90 in maintaining and facilitating the neurodegenerative phenotype in tauopathies. Proceedings of the National Academy of Sciences, 2007; 104: 9511-9516.
[155] Do K, Speranza G, Chang L-C, Polley E, Bishop R, Zhu W, Trepel J, Lee S, Lee M-J, Kinders R, Phillips L, Collins J, Lyons J, Jeong W, Antony R, Chen A, Neckers L, Doroshow J, Kummar S. Phase I study of the heat shock protein 90 (Hsp90) inhibitor onalespib (AT13387) administered on a daily for 2 consecutive days per week dosing schedule in patients with advanced solid tumors. Investigational New Drugs, 2015; 33: 921-930.
[156] Kummar S, Gutierrez ME, Gardner ER, Chen X, Figg WD, Zajac-Kaye M, Chen M, Steinberg SM, Muir CA, Yancey MA, Horneffer YR, Juwara L, Melillo G, Ivy SP, Merino M, Neckers L, Steeg PS, Conley BA, Giaccone G, Doroshow JH, Murgo AJ. Phase I trial of 17-dimethylaminoethylamino-17-demethoxygeldanamycin (17-DMAG), a heat shock protein inhibitor, administered twice weekly in patients with advanced malignancies. European Journal of Cancer, 2010; 46: 340-347.
[157] Marcu MG, Schulte TW, Neckers L. Novobiocin and related coumarins and depletion of heat shock protein 90-dependent signaling proteins. J Natl Cancer Inst, 2000; 92: 242-8.
[158] Matts RL, Dixit A, Peterson LB, Sun L, Voruganti S, Kalyanaraman P, Hartson SD, Verkhivker GM, Blagg BSJ. Elucidation of the Hsp90 C-Terminal Inhibitor Binding Site. ACS Chemical Biology, 2011; 6: 800-807.
[159] Moroni E, Zhao H, Blagg BS, Colombo G. Exploiting conformational dynamics in drug discovery: design of C-terminal inhibitors of Hsp90 with improved activities. J Chem Inf Model, 2014; 54: 195-208.
[160] Khalid S, Paul S. Identifying a C-terminal ATP binding sites-based novel Hsp90-Inhibitor in silico: a plausible therapeutic approach in Alzheimer's disease. Med Hypotheses, 2014; 83: 39-46.
[161] Ansar S, Burlison JA, Hadden MK, Yu XM, Desino KE, Bean J, Neckers L, Audus KL, Michaelis ML, Blagg BS. A non-toxic Hsp90 inhibitor protects neurons from Abeta-induced toxicity. Bioorg Med Chem Lett, 2007; 17: 1984-90.
[162] Wang Y, McAlpine SR. C-terminal heat shock protein 90 modulators produce desirable oncogenic properties.
[163] Jakob U, Gaestel M, Engel K, Buchner J. Small heat shock proteins are molecular chaperones. J Biol Chem, 1993; 268: 1517-20.
[164] Jovcevski B, Kelly Megan A, Rote Anthea P, Berg T, Gastall Heidi Y, Benesch Justin LP, Aquilina JA, Ecroyd H. Phosphomimics Destabilize Hsp27 Oligomeric Assemblies and Enhance Chaperone Activity. Chemistry & Biology, 2015; 22: 186-195.

[165] Shimura H, Miura-Shimura Y, Kosik KS. Binding of Tau to Heat Shock Protein 27 Leads to Decreased Concentration of Hyperphosphorylated Tau and Enhanced Cell Survival. Journal of Biological Chemistry, 2004; 279: 17957-17962.
[166] Abisambra JF, Jinwal UK, Jones JR, Blair LJ, Koren J, 3rd, Dickey CA. Exploiting the diversity of the heat-shock protein family for primary and secondary tauopathy therapeutics. Curr Neuropharmacol, 2011; 9: 623-31.
[167] Abisambra JF, Blair LJ, Hill SE, Jones JR, Kraft C, Rogers J, Koren J, Jinwal UK, Lawson L, Johnson AG, Wilcock D, O'Leary JC, Jansen-West K, Muschol M, Golde TE, Weeber EJ, Banko J, Dickey CA. Phosphorylation Dynamics Regulate Hsp27-Mediated Rescue of Neuronal Plasticity Deficits in Tau Transgenic Mice. The Journal of Neuroscience, 2010; 30: 15374-15382.
[168] Bjorkdahl C, Sjogren MJ, Zhou X, Concha H, Avila J, Winblad B, Pei JJ. Small heat shock proteins Hsp27 or alphaB-crystallin and the protein components of neurofibrillary tangles: tau and neurofilaments. J Neurosci Res, 2008; 86: 1343-52.
[169] Blair LJ, Baker JD, Sabbagh JJ, Dickey CA. The emerging role of peptidyl-prolyl isomerase chaperones in tau oligomerization, amyloid processing, and Alzheimer's disease. J Neurochem, 2015; 133: 1-13.
[170] Pastorino L, Sun A, Lu P-J, Zhou XZ, Balastik M, Finn G, Wulf G, Lim J, Li S-H, Li X, Xia W, Nicholson LK, Lu KP. The prolyl isomerase Pin1 regulates amyloid precursor protein processing and amyloid-[beta] production. Nature, 2006; 440: 528-534.
[171] Yotsumoto K, Saito T, Asada A, Oikawa T, Kimura T, Uchida C, Ishiguro K, Uchida T, Hasegawa M, Hisanaga S-i. Effect of Pin1 or Microtubule Binding on Dephosphorylation of FTDP-17 Mutant Tau. Journal of Biological Chemistry, 2009; 284: 16840-16847.
[172] Kimura T, Tsutsumi K, Taoka M, Saito T, Masuda-Suzukake M, Ishiguro K, Plattner F, Uchida T, Isobe T, Hasegawa M, Hisanaga S-i. Isomerase Pin1 Stimulates Dephosphorylation of Tau Protein at Cyclin-dependent Kinase (Cdk5)-dependent Alzheimer Phosphorylation Sites. Journal of Biological Chemistry, 2013; 288: 7968-7977.
[173] Lu P-J, Wulf G, Zhou XZ, Davies P, Lu KP. The prolyl isomerase Pin1 restores the function of Alzheimer-associated phosphorylated tau protein. Nature, 1999; 399: 784-788.
[174] Nakamura K, Greenwood A, Binder L, Bigio Eileen H, Denial S, Nicholson L, Zhou Xiao Z, Lu Kun P. Proline Isomer-Specific Antibodies Reveal the Early Pathogenic Tau Conformation in Alzheimer's Disease. Cell, 2012; 149: 232-244.
[175] Liou YC, Sun A, Ryo A, Zhou XZ, Yu ZX, Huang HK, Uchida T, Bronson R, Bing G, Li X, Hunter T, Lu KP. Role of the prolyl isomerase Pin1 in protecting against age-dependent neurodegeneration. Nature, 2003; 424: 556-61.

[176] Lambert J-C, Heath S, Even G, Campion D, Sleegers K, Hiltunen M, Combarros O, Zelenika D, Bullido MJ, Tavernier B, Letenneur L, Bettens K, Berr C, Pasquier F, Fievet N, Barberger-Gateau P, Engelborghs S, De Deyn P, Mateo I, Franck A, Helisalmi S, Porcellini E, Hanon O, de Pancorbo MM, Lendon C, Dufouil C, Jaillard C, Leveillard T, Alvarez V, Bosco P, Mancuso M, Panza F, Nacmias B, Bossu P, Piccardi P, Annoni G, Seripa D, Galimberti D, Hannequin D, Licastro F, Soininen H, Ritchie K, Blanche H, Dartigues J-F, Tzourio C, Gut I, Van Broeckhoven C, Alperovitch A, Lathrop M, Amouyel P. Genome-wide association study identifies variants at CLU and CR1 associated with Alzheimer's disease. Nat Genet, 2009; 41: 1094-1099.

[177] Harold D, Abraham R, Hollingworth P, Sims R, Gerrish A, Hamshere ML, Pahwa JS, Moskvina V, Dowzell K, Williams A, Jones N, Thomas C, Stretton A, Morgan AR, Lovestone S, Powell J, Proitsi P, Lupton MK, Brayne C, Rubinsztein DC, Gill M, Lawlor B, Lynch A, Morgan K, Brown KS, Passmore PA, Craig D, McGuinness B, Todd S, Holmes C, Mann D, Smith AD, Love S, Kehoe PG, Hardy J, Mead S, Fox N, Rossor M, Collinge J, Maier W, Jessen F, Schurmann B, Heun R, van den Bussche H, Heuser I, Kornhuber J, Wiltfang J, Dichgans M, Frolich L, Hampel H, Hull M, Rujescu D, Goate AM, Kauwe JSK, Cruchaga C, Nowotny P, Morris JC, Mayo K, Sleegers K, Bettens K, Engelborghs S, De Deyn PP, Van Broeckhoven C, Livingston G, Bass NJ, Gurling H, McQuillin A, Gwilliam R, Deloukas P, Al-Chalabi A, Shaw CE, Tsolaki M, Singleton AB, Guerreiro R, Muhleisen TW, Nothen MM, Moebus S, Jockel K-H, Klopp N, Wichmann HE, Carrasquillo MM, Pankratz VS, Younkin SG, Holmans PA, O'Donovan M, Owen MJ, Williams J. Genome-wide association study identifies variants at CLU and PICALM associated with Alzheimer's disease. Nat Genet, 2009; 41: 1088-1093.

[178] Desikan RS, Thompson WK, Holland D, et al. THe role of clusterin in amyloid-β–associated neurodegeneration. JAMA Neurology, 2014; 71: 180-187.

[179] Zhou Y, Hayashi I, Wong J, Tugusheva K, Renger JJ, Zerbinatti C. Intracellular Clusterin Interacts with Brain Isoforms of the Bridging Integrator 1 and with the Microtubule-Associated Protein Tau in Alzheimer's Disease. PLoS ONE, 2014; 9: e103187.

[180] Salminen A, Kaarniranta K, Kauppinen A, Ojala J, Haapasalo A, Soininen H, Hiltunen M. Impaired autophagy and APP processing in Alzheimer's disease: The potential role of Beclin 1 interactome. Progress in Neurobiology, 2013; 106–107: 33-54.

[181] Ding H, Dolan PJ, Johnson GV. Histone deacetylase 6 interacts with the microtubule-associated protein tau. J Neurochem, 2008; 106: 2119-30.

[182] Noack M, Leyk J, Richter-Landsberg C. HDAC6 inhibition results in tau acetylation and modulates tau phosphorylation and degradation in oligodendrocytes. Glia, 2014; 62: 535-47.

[183] Leyk J, Goldbaum O, Noack M, Richter-Landsberg C. Inhibition of HDAC6 modifies tau inclusion body formation and impairs autophagic clearance. J Mol Neurosci, 2015; 55: 1031-46.
[184] Cook C, Stankowski J, Carlomagno Y, Stetler C, Petrucelli L. Acetylation: a new key to unlock tau's role in neurodegeneration. Alzheimer's Research & Therapy, 2014; 6: 29.
[185] Cook C, Gendron TF, Scheffel K, Carlomagno Y, Dunmore J, DeTure M, Petrucelli L. Loss of HDAC6, a novel CHIP substrate, alleviates abnormal tau accumulation. Hum Mol Genet, 2012; 21: 2936-45.
[186] Ozcelik S, Fraser G, Castets P, Schaeffer V, Skachokova Z, Breu K, Clavaguera F, Sinnreich M, Kappos L, Goedert M, Tolnay M, Winkler DT. Rapamycin Attenuates the Progression of Tau Pathology in P301S Tau Transgenic Mice. PLoS ONE, 2013; 8: e62459.
[187] Jiang T, Yu J-T, Zhu X-C, Zhang Q-Q, Cao L, Wang H-F, Tan M-S, Gao Q, Qin H, Zhang Y-D, Tan L. Temsirolimus attenuates tauopathy in vitro and in vivo by targeting tau hyperphosphorylation and autophagic clearance. Neuropharmacology, 2014; 85: 121-130.
[188] Lee B-H, Lee MJ, Park S, Oh D-C, Elsasser S, Chen P-C, Gartner C, Dimova N, Hanna J, Gygi SP, Wilson SM, King RW, Finley D. Enhancement of proteasome activity by a small-molecule inhibitor of USP14. Nature, 2010; 467: 179-84.
[189] Ittner A, Bertz J, Suh LS, Stevens CH, Götz J, Ittner LM. Tau-targeting passive immunization modulates aspects of pathology in tau transgenic mice. Journal of Neurochemistry, 2015; 132: 135-145.
[190] Funk KE, Mirbaha H, Jiang H, Holtzman DM, Diamond MI. Distinct Therapeutic Mechanisms of Tau Antibodies: Promoting Microglial Clearance Versus Blocking Neuronal Uptake. J Biol Chem, 2015; 290: 21652-62.
[191] Selenica ML, Davtyan H, Housley SB, Blair LJ, Gillies A, Nordhues BA, Zhang B, Liu J, Gestwicki JE, Lee DC, Gordon MN, Morgan D, Dickey CA. Epitope analysis following active immunization with tau proteins reveals immunogens implicated in tau pathogenesis. J Neuroinflammation, 2014; 11: 152.
[192] Blair LJ, Zhang B, Dickey CA. Potential synergy between tau aggregation inhibitors and tau chaperone modulators. Alzheimers Res Ther, 2013; 5: 41.
[193] Calcul L, Zhang B, Jinwal UK, Dickey CA, Baker BJ. Natural products as a rich source of tau-targeting drugs for Alzheimer's disease. Future Med Chem, 2012; 4: 1751-61.
[194] Paranjape SR, Riley AP, Somoza AD, Oakley CE, Wang CC, Prisinzano TE, Oakley BR, Gamblin TC. Azaphilones inhibit tau aggregation and dissolve tau aggregates in vitro. ACS Chem Neurosci, 2015; 6: 751-60.
[195] Frost B, Diamond MI. The expanding realm of prion phenomena in neurodegenerative disease. Prion, 2009; 3: 74-7.
[196] Yanamandra K, Kfoury N, Jiang H, Mahan TE, Ma S, Maloney SE, Wozniak DF, Diamond MI, Holtzman DM. Anti-tau antibodies that block

tau aggregate seeding in vitro markedly decrease pathology and improve cognition in vivo. Neuron, 2013; 80: 402-14.
[197] Frost B, Jacks RL, Diamond MI. Propagation of tau misfolding from the outside to the inside of a cell. The Journal of biological chemistry, 2009; 284: 12845-52.
[198] Holmes BB, Furman JL, Mahan TE, Yamasaki TR, Mirbaha H, Eades WC, Belaygorod L, Cairns NJ, Holtzman DM, Diamond MI. Proteopathic tau seeding predicts tauopathy in vivo. Proc Natl Acad Sci U S A, 2014; 111: E4376-85.
[199] Kfoury N, Holmes BB, Jiang H, Holtzman DM, Diamond MI. Trans-cellular propagation of Tau aggregation by fibrillar species. The Journal of biological chemistry, 2012; 287: 19440-51.

Chapter 2

Stabilizing the Hsp70-Tau Complex Normalizes Proteostasis in a Model of Tauopathy

2.1 Introduction

As discussed in Chapter 1, Hsp70 is a chaperone that normally scans the proteome and “decides” whether proteins should be retained or degraded by linking them to either the folding or turnover pathways. This activity is critical to normal protein homeostasis (or proteostasis), yet it appears to fail in many protein-misfolding diseases. As discussed in Chapter 1, it is especially important to understand the molecular mechanisms by which Hsp70 makes decisions for the microtubule-binding protein tau. Hsp70 is a multi-domain protein that uses ATP hydrolysis to regulate its affinity for client proteins. Here, we use a chemical biology strategy, in combination with genetics, to systematically perturb the affinity of Hsp70 for tau. This approach revealed that tight complexes between Hsp70 and tau are associated with accelerated turnover while transient interactions are linked to tau retention. Further, we found that disease-associated tau mutants, including A152T and K280Q, have an intrinsically weaker affinity for Hsp70 but that chaperone binding could be chemically restored to enhance their

degradation. Together, these results suggest that persistence of the Hsp70-client complex is one important parameter governing Hsp70-mediated quality control.

2.2 Allosteric modulation of Hsp70 regulates tau proteostasis

Hsp70/HSPA1A and Hsc70/HSPA8 are highly conserved molecular chaperones that are expressed in the cytosol of all eukaryotic cells. These factors are often referred to as "triage" chaperones because they bind to misfolded proteins and somehow choose to preserve them [1, 2] or shuttle them to the lysosome-autophagy pathway or UPS for degradation [3, 4]. Although they play a complex and important role in proteostasis, members of the Hsp70 family have a relatively simple structure, composed of a 45 kDa nucleotide binding domain (NBD) and 25 kDa substrate binding domain (SBD) [5, 6]. The NBD has a deep cleft for binding ATP, while client proteins bind in a β-sandwich region of the SBD [7]. These two domains are allosterically linked, with nucleotide turnover in the NBD controlling the affinity of SBD-client interactions [8-12]. In the ATP-bound form, clients bind Hsp70s with fast-on, fast-off kinetics, while hydrolysis to the ADP-bound form stabilizes the SBD-client interaction by slowing the off-rate [13].

As discussed in Chapter 1, co-chaperones bind to Hsp70/Hsc70 and regulate this nucleotide cycling. These co-chaperones include J-proteins, which accelerate ATP hydrolysis, and NEFs that promote the discharge of ADP [14, 15]. Together, J proteins and NEFs coordinate turnover, ultimately regulating the affinity of Hsp70s for their clients. Then, additional co-chaperone families,

including the tetratricopeptide repeat (TPR) domain proteins, bind Hsp70s and help direct the fate of the bound clients. Another important co-chaperone Hsc70 interacting protein (HIP) binds to the NBD and blocks interactions with NEFs, essentially prolonging the association of Hsp70s with their clients [16]. Together, Hsp70, Hsc70 and their co-chaperones cooperate to identify unfolded proteins and somehow enact the “decision” to either retain or degrade them. This process is central to health and proteostasis because it limits accumulation of misfolded proteins, blocks aggregation and aids in proper folding. However, the molecular mechanisms that guide the logic of quality control are not clear. How does Hsp70 “know” whether a client is competent for folding or whether it is prone to misfolding?

2.3 Tau as a model substrate for understanding chaperone triage

MAPT/tau has served as an important client for understanding chaperone-mediated quality control [17-19]. As introduced in Chapter 1, the accumulation of tau is a pathological feature of many neurodegenerative disorders, including Alzheimer’s disease (AD), frontotemporal dementia (FTD) and progressive supranuclear tauopathy (PSP). Tau is an intrinsically disordered protein [20] that normally stabilizes microtubules. Mutations, such as P301L and A152T [21-24], and/or PTMs, such as hyperphosphorylation and acetylation [25-27], disrupt this normal function by damaging the affinity of tau for microtubules and promoting its aggregation as discussed in Chapter 1. Members of the Hsp70 family are well known to play an important role in tau quality control [18, 28], serving to protect

against tauopathies. In Chapter 4, we will discuss how these mutations and PTMs alter tau proteostasis in disease relevant tau mutant cell models. Both Hsc70 and Hsc70 bind to the microtubule-binding repeats of tau [29, 30] to limits its aggregation. Further, over-expression of Hsp70 leads to a dramatic reduction in tau [18, 30] through activation of the UPS degradation pathways. This pro-degradation activity of Hsp70 was isolated to the C-terminal domain [30], a region that contains the least similarity between Hsc70 and Hsp70. Interestingly, over-expression of Hsc70, despite its overall high similarity with Hsp70, causes *retention* of tau (Appendix 2.3D) [30]. This diametrically opposed activity seems to occur through preferentially enhanced coupling between Hsp70, tau and CHIP. However, over-expression of a dominant negative form of Hsc70 also leads to enhanced turnover of tau [2], suggesting that both Hsc70 and Hsp70 are capable of directing tau to the degradation pathway. The differential effects of Hsp70 paralogs on tau stability as well as other Hsp70 substrates will be further explored in Chapter 4. The quality control decisions made by Hsc70 and Hsp70 in the tau-bound complex are further tuned by co-chaperones. For example, over-expression of DnaJA1, BAG3 or CHIP promotes tau turnover through a mechanism that requires Hsp70s [31-33]. Together, these results show a close relationship between Hsp70s, their co-chaperones and tau homeostasis, but the molecular mechanisms are not clear. In other words, the players are known but it isn’t yet clear how they coordinate their actions.

We wanted to use a chemical biology approach to better understand how Hsp70s "decide" to retain or degrade tau. Inhibitors of Hsp70's ATPase activity, such as YM-01, are known to reduce accumulation of phosphorylated tau in cell-based models [34] in a process that requires the chaperone [31]. In these findings, we saw an opportunity to use YM-01 as a chemical probe to unravel the molecular mechanisms of Hsp70-mediated quality control. To do this, we first had to synthesize an analog of YM-01, JG-48, which had spectral properties that permitted access to a wider variety of mechanistic assays. We found that JG-48, but not a closely related, control compound, JG-273, stabilized the ADP-bound state of Hsc70 and blocked the ability of NEFs to facilitate ADP and client release. The net effect of this allosteric perturbation is that the affinity of Hsp70s for tau is significantly enhanced *in vitro* and in cells. To test whether affinity for tau might be linked to the "decision" to degrade, we used a collection of chemical inhibitors, belonging to distinct chemical series, and a new series of Hsc70 point mutants to systematically enhance or decrease the affinity of chaperone for tau. The results, discussed in this chapter, significantly advance our understanding of the mechanism of Hsp70-mediated quality control and suggest a path towards the discovery of compounds that might normalize tau levels in disease.

2.4 Results

2.4.1 JG-48 reduces tau accumulation in multiple models and restores long-term potentiation.

YM-01 and its analogs are known to enhance tau turnover through interactions with Hsp70 [31, 34]. However, these compounds contain a cationic pyridinium that precludes many *in vitro* studies because they absorb at the same wavelengths that are used in common chaperone assays (*e.g.* 535 to 620 nm, see Appendix 2.1B). To provide a molecule suitable for use in these expanded platforms, we assembled JG-48 using a previously established synthetic route [35] (Appendix 2.1A). At the same time, we synthesized a control compound, JG-273, that lacks the fused phenyl group predicted to be important for binding [36]. As anticipated, JG-48 and JG-273 lacked the strong absorbance in the region of 535 to 620 nm (Appendix 2.1B), which previously hindered use of YM-01.

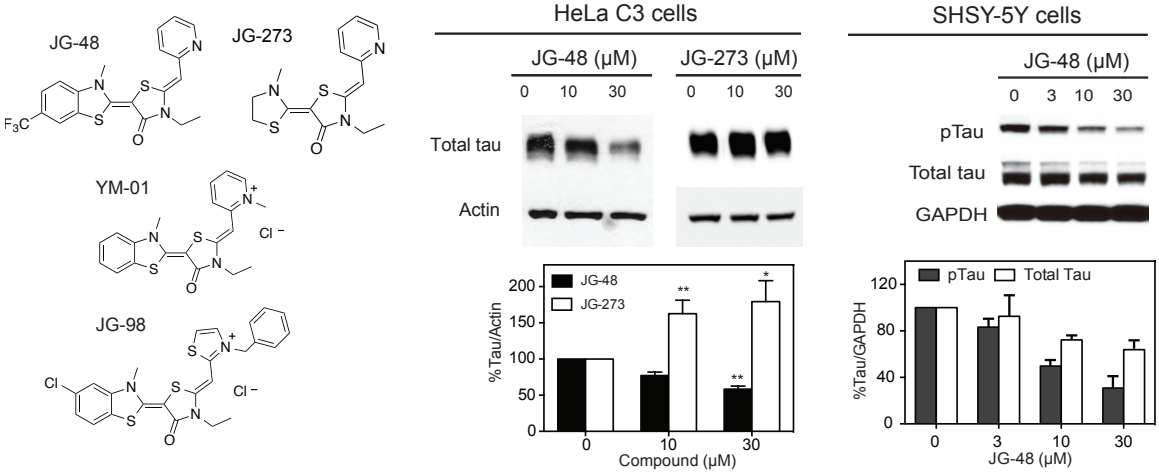

Figure 2.1 JG-48 reduces tau levels in cellular models of tauopathy. JG-48, but not JG-273, significantly reduces tau in HeLa C3 cells stably transfected with 4R0N tau. Statistical analysis was performed using a 2-way ANOVA with Dunnett's test.*p<0.001, **p<0.005. JG-48 also reduces phosphorylated, endogenous tau in SHSY-5Y neuroblastoma cells. Cells were treated for 24 hours.

The ability of JG-48 and JG-273 to reduce tau burden was then tested in HeLa C3 cells stably transfected with human 4R0N tau. These cells were treated for 24 hours, lysed and the total tau levels analyzed by Western blot. We found that JG-48, but not JG-273, reduced tau levels by ~50% at 30 μM (Figure 2.1). Then, to test if JG-48 could reduce endogenous tau, SHSY-5Y neuroblastoma cells were treated. We found that JG-48 decreased total tau levels, but it was even more effective at clearing phosphorylated tau (Figure 2.1), as indicated by an antibody that recognizes the paired helical filament (PHF) form that is present in these cells and in the brains of tauopathy patients [37].

We next tested the potency of JG-48 in brain slices from the rTg4510 transgenic mouse model of tauopathy [38]. rTg4510 mice express the tau mutant, P301L, and they present many of the symptoms associated with tauopathies, including tau tangles in the forebrain, neuron loss and memory impairment [39]. Brain slice cultures from these mice were treated for six hours with JG-48. We found that this treatment reduced total tau levels and that it was especially effective against phosphorylated tau (Figure 2.2A). A key feature of this rTg4510 model is that hippocampal brain slices show deficits in long-term potentiation (LTP) when compared to WT brain slices from non-transgenic mice [40, 41]. Therefore, we evaluated the ability of JG-48 to restore LTP in rTG4510 brain slices using a previously described theta burst stimulation method [31]. JG-48 (10 μM) significantly improved LTP in the brain slices from rTg4510 mice when compared

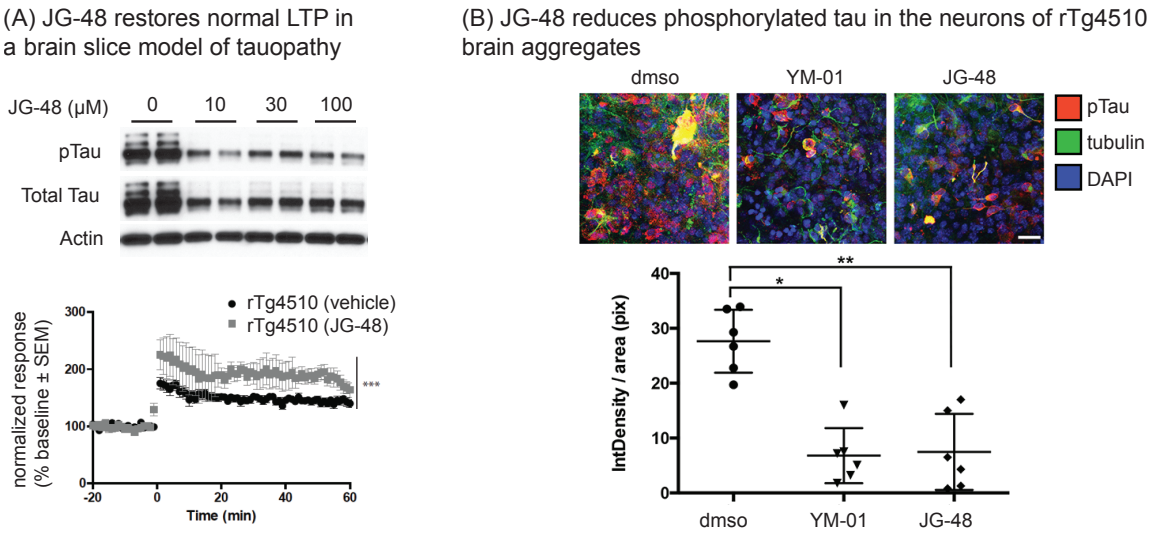

Figure 2.2 Characterization of JG-48 in transgenic tauopathy models. (A) Acute hippocampal slice cultures from 3-4 month old rTg4510 tau transgenic mice were treated with JG-48 (10 μM) for 6 hours. Electrophysiology experiments show that JG-48 restores synaptic plasticity. fEPSP traces are an average of JG-48 (n=7) or vehicle-treated (n=17). Statistical analysis was performed using a 2-way ANOVA with Bonferroni posttest. *** p<0.001. (B) Brain aggregates were infected with 10% rTg4510 brain homogenates from 15 to 25 days in culture and treated with YM-01 or JG-48 (10 μM) for 24 hrs prior to harvesting at 35 days in culture. They were stained with anti-phospho-tau (red), anti-beta tubulin (green) and DAPI (blue). 15-20 confocal images were stacked and phospho-tau intensity was measured with Image J. N=6. *p<0.0001, **p<0.0003. Bar = 25 μm.

to the vehicle control (Figure 2.2A). Importantly, no effect was seen when JG-48 was added to brain slice cultures from non-transgenic, wild type mice (Appendix 2.1C). This control is important because it shows that the compound does not artificially enhance plasticity; rather, JG-48 appeared to preferentially accelerate clearance of pathogenic tau to improve neuronal function. Finally, we created aggregate cultures from rTg4510 brains and treated them with compounds to understand whether tau was reduced in neurons. This system was used because, compared to brain slices, the aggregate model provides a more convenient platform for immunofluorescence and imaging. We found that tau levels in tubulin-positive neurons were significantly reduced by either YM-01 or JG-48 (10 μM) (Figure 2.2B). These results establish JG-48 as a chemical probe

for better understanding the mechanisms of chaperone-mediated tau quality control.

2.4.2 JG-48 binds the NBD of Hsc70 but does not inhibit ATP binding

Our overall strategy was to explore the activity of JG-48 in a battery of both *in vitro* and cellular models in an attempt to understand how Hsp70s might regulate tau homeostasis. Our first question was whether JG-48 might compete with nucleotide (ATP or ADP) for binding to the chaperone, which would provide a potential clue to its mechanism-of-action. NMR titration and docking experiments had previously shown that compounds similar to JG-48, such as MKT-077 and JG-98, bind in a deep, conserved pocket of the NBD of Hsc70 [34, 36, 42]. To confirm that JG-48 binds similarly, we repeated the HSQC titration study with ^{15}N Hsc70 NBD in the presence of ADP. In these studies, we used $Hsc70_{NBD}$, rather than $Hsp70_{NBD}$ because the peak assignments were available, but the predicted binding site is 100% conserved between these paralogs [36]. Consistent with the previous work, JG-48 caused selective chemical shift perturbations (CSPs) in residues adjacent to a deep cleft composed of hydrophobic and anionic residues (R72, D199, E175, G201, T204, F205 and T226) (Figure 2.3A). Guided by the CSPs, we performed docking simulations of JG-48 bound to $Hsc70_{NBD}$ (PDB: 3C7N). Similar to what has been found with previous analogs, the most favorable poses positioned JG-48 in a cleft between subdomains IIA and IIB (Figure 2.3A). In the docked binding mode, the benzothiazole ring system of JG-48, which is missing in JG-273, was predicted to make a number of important interactions.

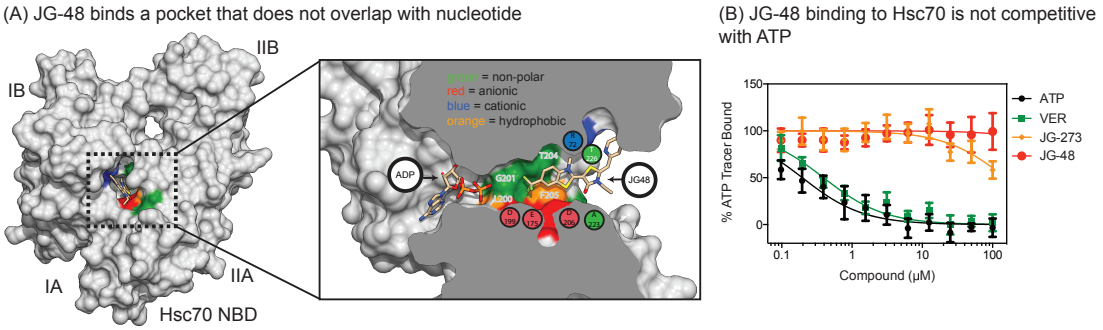

Figure 2.3 JG-48 does not compete with ATP for binding to Hsc70. (A) Docking of JG-48 to the NBD of Hsc70. Based on NMR chemical shift perturbations, the binding site of JG-48 was modeled. JG-48 is predicted to bind a deep cleft in Hsc70, which is not overlapping with the ATP/ADP-binding cleft. Hydrophobics in orange, apolar in green, anionic in red, cationic in blue. (B) Positive controls, ATP and VER-155008 (VER) compete with a fluorescent ATP tracer (ATP-FAM) for binding to the NBD of Hsc70. Results are the average of three independent experiments performed in triplicate and the error bars represent the standard deviations.

The docked pose of JG-48 suggested that the molecule would not directly interfere with nucleotide binding. Indeed, there appeared to be a channel through the protein, with nucleotide on one end and JG-48 on the other (Figure 2.3A). To directly test this idea experimentally, we adapted a fluorescence polarization (FP) assay [43] in which competition with a tight binding (K_D ~ 400 nM) ATP probe, N^6-(6-Amino)hexyl-ATP-6-FAM (or ATP-FAM), is measured. We first confirmed that both unlabeled ATP and a known competitive inhibitor, VER-155008 (VER) [43], interrupted tracer binding with IC_{50} values of 200 ± 19 nM and 390 ± 28 nM, respectively (Figure 2.3B). In contrast, titration with JG-48 had no effect on ATP-FAM binding, confirming that it does not compete with ATP. Thus, its activities on Hsp70 appeared to be allosteric.

2.4.3 JG-48 weakly inhibits ATPase activity

We then turned to a series of biochemical assays, including those that measure ATP hydrolysis, client folding and co-chaperone interactions, to understand the

impact of JG-48 binding on Hsp70 functions *in vitro*. First, we tested the ability of JG-48 to inhibit Hsc70's steady state ATPase activity using a colorimetric assay [44]. In these studies, we used JG-273 as the negative control and two characterized inhibitors, VER [43] and myricetin [45] as positive controls. We tested each compound against human Hsc70 in the presence of its co-chaperones. By itself, Hsc70 is a weak ATPase; however, steady-state hydrolysis is known to be significantly increased in the presence of J-proteins and NEFs [44, 46]. Thus, the relevant ATPase activity in cells is thought to be a product of the three factors working together: the Hsc70, a J protein and a NEF [47]. There are typically multiple J proteins and NEFs expressed in mammalian cells [48] and the function of the chaperone is heavily influenced by which co-chaperones are bound [49-51]. To get a picture of how compounds might impact the whole range of possible complexes, we systematically tested them against some of the most abundant combinations composed of Hsc70, DnaJA1, DnaJA2, DnaJB1, DnaJB4, BAG1, BAG2 and BAG3 (Figure 2.4A). As expected, JG-273 combination (Appendix 2.2A), so it wasn't evaluated further. Both of the positive controls, myricetin and VER (50 μM), inhibited the activity of all the chaperone combinations tested (Figure 2.4B and Appendix 2.2A). We found that JG-48 also inhibited ATPase activity, stimulated by either J proteins or members of the BAG family of NEFs, but this effect was relatively modest (Figure 2.4B and Appendix 2.2A).

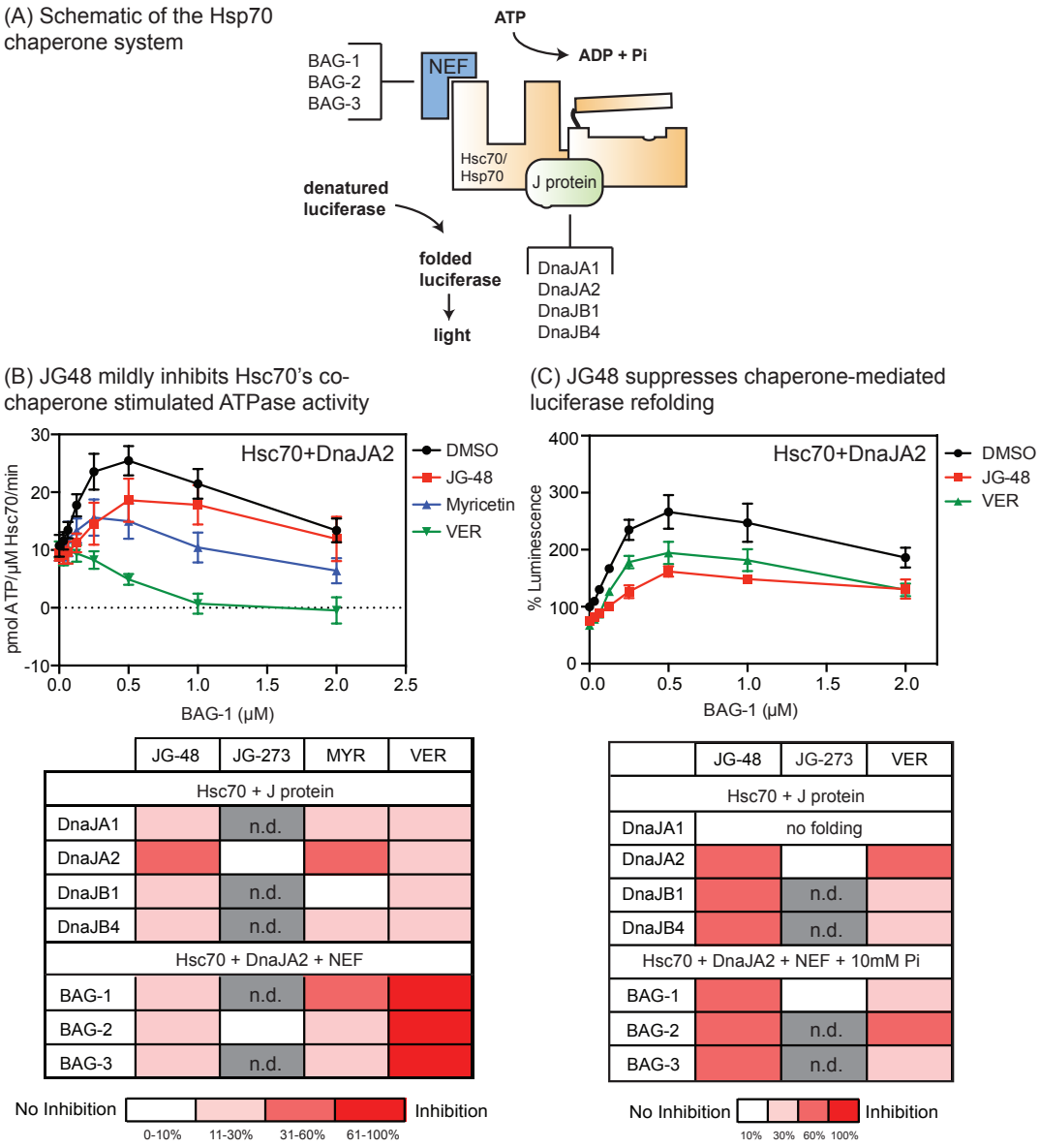

Figure 2.4 JG-48 is an inhibitor of chaperone functions. (A) Schematic of the Hsp70 system, highlighting the J protein and NEF family of co-chaperones. Hsp70 works with a J protein and NEF to hydrolyze ATP and refold denatured luciferase *in vitro*. In this study, we combined Hsc70 with the indicated co-chaperones. (B) Summary of the effects of JG-48 (and the negative control, JG-273) on steady state ATPase activity. MYR = myricetin VER = VER-155008. All compounds at 50 μM. Results are the average of at least three independent experiments performed in triplicate each. Table colors represent the percent reduction in ATPase rate at maximum stimulation. Representative curves are shown. (C) Summary of the effects of JG-48, JG-273 and VER on Hsc70-mediated luciferase refolding. All compounds at 50 μM. Results are the average of at least two independent experiments performed in triplicate each. DnaJA1 is not competent for luciferase folding. Table colors represent the percent reduction in luminescence signal at maximum stimulation.

2.4.4 JG-48 strongly inhibits substrate refolding by Hsc70

While informative, the ATPase assays do not report on Hsp70-client interactions. To explore this activity, we used a well-established assay in which Hsc70 and its co-chaperones cooperate to refold denatured firefly luciferase *in vitro*. This assay is known to require dynamic interactions between luciferase, J proteins and Hsp70s, providing a functional read-out of client cycling [52]. Similar to the design of the ATPase assays, we tested the inhibitory activity of JG-48, JG-273 and VER against Hsc70 and a panel of its co-chaperones. DnaJA1 does not support robust refolding of luciferase [49, 50], so it wasn't included. In control experiments, we found that none of the compounds directly interfered with luciferase activity (Appendix 2.2B), allowing us to test them in this platform without artifacts. We found that JG-48 and VER, but not JG-273, were dramatic inhibitors of chaperone-mediated luciferase refolding. Indeed, both JG-48 and VER reduced the amount of recovered luminescence by approximately 60% (Figure 2.4C and Appendix 2.2C). Compared to VER, JG-48 had even broader activity against all of the chaperone complexes.

2.4.5 JG-48 inhibits client release from Hsc70

The dramatic effects of JG-48 on luciferase refolding suggested that it might strongly impact client-chaperone interactions. To test this idea more directly, we turned to an FP assay in which binding to a labeled client peptide, HLA-FAM, is measured [53]. We found that Hsc70 binds the tracer with an apparent K_D of 5.1 ± 0.9 μM in the presence of 1 mM ADP, consistent with previous reports [49].

Titration of BAG1 into this mixture released the HLA-FAM tracer with an EC_{50} of 3.7 ± 0.8 μM (Figure 2.5A), consistent with previous reports [49]. For these experiments, BAG1 was used because it appears to be particularly important for tau [54, 55]. Then, we measured the ability of JG-48 to impact BAG1 activity. We found that JG-48, but not JG-273, stabilized the interaction with tracer by 7-fold (BAG1 EC_{50} 25 ± 8.6 μM) (Figure 2.5A).

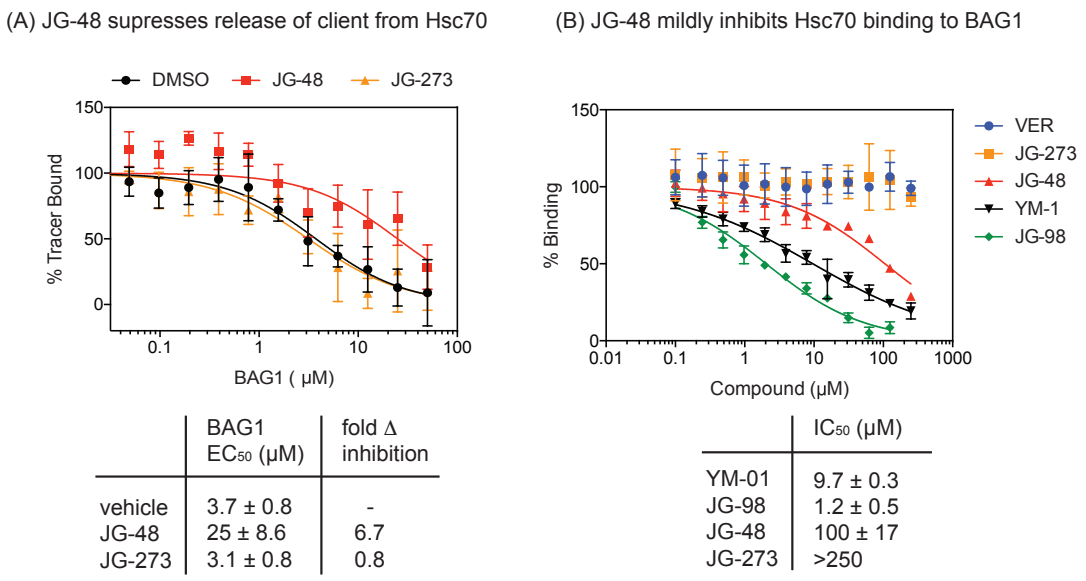

	BAG1 EC_{50} (μM)	fold Δ inhibition
vehicle	3.7 ± 0.8	-
JG-48	25 ± 8.6	6.7
JG-273	3.1 ± 0.8	0.8

	IC_{50} (μM)
YM-01	9.7 ± 0.3
JG-98	1.2 ± 0.5
JG-48	100 ± 17
JG-273	>250

Figure 2.5 JG-48 limits NEF binding and activity. (A) BAG1 accelerated release of a peptide tracer (HLA-FAM) from the SBD of Hsc70 was measured and the effects of 50μM compounds determined. The apparent EC50 values for BAG-1 are shown in the table. Results are the average of three independent experiments performed in triplicate each. Error bars represent the SD. (B) The interaction between Hsc70 and BA1 was measured by FCPIA. JG-98 and YM-01, but not the negative control JG-273, block the protein-protein interaction. JG-48 partially disrupted the interaction, but only at high concentrations. Results are the average of three independent experiments performed in triplicate each and the error bars represent SD.

NEFs promote release of clients from Hsc70 and Hsp70 by binding to the NBD [56-59]. To test if JG-48 could directly impact the protein-protein interaction between NEFs and Hsc70, biotinylated chaperone was immobilized on beads and incubated with fluorescently labeled BAG1 in a flow cytometry protein interaction assay (FCPIA) format. We found that JG-48, but not JG-273 or VER,

inhibited BAG1 binding, but with a relatively weak IC_{50} of 100 μM (Figure 2.5B). Thus, JG-48 had a much more dramatic effect on luciferase folding and HLA-FAM release than it did in this assay, suggesting that its major effects are to promote client binding through allosteric control.

2.4.6 Chemical and genetic manipulation of tau affinity reveals a correlation with tau turnover in cells

Next, we wanted to test if JG-48 would increase binding to tau, as it did for the model HLA-FAM client. To do this, we employed an ELISA [29] in which Hsc70 is immobilized and binding to 4R0N tau measured with a labeled antibody. In this format, Hsc70 had an affinity of ~5 μM for tau in the presence of ADP, while replacing ADP with ATP or non-hydrolyzable ATPγS weakened the apparent affinity of Hsc70 for tau by 101 and 177% (Table 2.1). DMSO alone had no effect on the strength of the complex in the presence of ADP, but JG-48 increased binding approximately 2-fold (K_D = 2.4 ± 0.3 μM) (Appendix 2.3A). This result suggests that, similar to what was observed in the FP assay with HLA-FAM, JG-48 also stabilizes chaperone-tau complexes.

Together, these results suggested a model in which stabilization of the tau complex might possibly be a signal for promoting its turnover. To test this idea, we wanted to systematically control the affinity of Hsc70 for tau and then measure the corresponding effects on tau levels in cells. Towards this goal, we assembled a collection of known inhibitors of Hsc70, including VER [43], MAL3-

Table 2.1 Summary of the results from ELISA and Western blot experiments

		ELISA		HeLaC3 cells
		tau K_D (app)	% change	% tau remaining
	ATP	12 ± 0.9	-101	---
	ADP	5.8 ± 0.7	---	---
	ATP-γS	16 ± 1.7	-177	---
controls	WT Hsc70	5.8 ± 0.7	---	93 ± 4
controls	WT Hsp72	5.3 ± 0.7	---	67 ± 14
controls	JG-273	7.9 ± 0.6	-36	102 ± 10
controls	R76A Hsc70	5.2 ± 0.7	+10	88 ± 11
controls	Y149A Hsc70	6.2 ± 0.9	-6	98 ± 14
promote binding	JG-48	2.4 ± 0.3	+58	55 ± 4
promote binding	YM-01	2.4 ± 0.2	+58	25 ± 10
promote binding	JG-98	2.9 ± 0.4	+50	28 ± 16
promote binding	Mal3-101	2.9 ± 0.5	+50	77 ± 12
promote release	VER	7.1 ± 1.3	-36	42 ± 19
promote release	H227A Hsc70	8.3 ± 0.6	-43	107 ± 5
promote release	L228A Hsc70	11 ± 1.2	-86	126 ± 10

101 [60], JG-98 [36] and YM-01 [31, 61]. Importantly, these compounds belong to three distinct chemical series and bind non-overlapping sites on Hsc70, so they provide a more rigorous test of the model than using only a single chemotype. In the ELISA, we found that MAL3-101, JG-98 and YM-01 enhanced binding of Hsc70 to tau by approximately 2-fold (Table 2.1 and Appendix 2.3B), similar to what we found for JG-48. However, VER was mildly destabilizing, decreasing the affinity of the Hsc70-tau complex by 36%. This result might be consistent with the design of VER, as it was intended to mimic the weakly-binding, ATP-bound state [43].

To complement these chemical perturbations, we also wanted to use point mutations in Hsc70 to alter the affinity for tau. We considered this experiment to be very important because the selectivity of small molecules in cells is often

uncertain, so combining them with genetics is a way to critically assess selectivity. Accordingly, we mutated residues in the proposed allosteric site in Hsc70 that is bound by JG-48 (see Fig. 2.3) to see if any of these residues, when mutated, might also allosterically disrupt affinity for tau. We found that mutations in R76A and Y149A had little impact on tau affinity in the ELISA platform (Table 2.1), so we used these variants as controls. However, H227A and L228A significantly weakened the affinity for tau by 40 to 80%, providing a genetic way to test the effects of affinity changes on tau homeostasis.

With this collection of genetic and chemical tools in-hand, we treated HeLa C3 cells or transiently over-expressed each of the Hsc70 point mutants. We found that strengthening the affinity for tau tended to reduce its levels (Table 2.1 and Figure 2.6A). For example, JG-98 enhanced Hsc70 binding by 2-fold *in vitro* and reduced tau levels by about 75% compared to the controls. Conversely, the H227A and L228A mutations weakened the interaction *in vitro* and their over-expression caused a reproducible increase in tau levels (Table 2.1). To determine if JG-48 can increase binding of Hsp70 to tau in a cell model, we performed immunoprecipitations of V5-tagged tau from HeLa C3 cells after treatment with JG-48. Consistent with the ELISA, JG-48 significantly enhanced binding of Hsp70 to tau (Figure 2.6B). Taken together, these results suggested a correlation between apparent affinity and tau turnover in cells (Figure 2.6A).

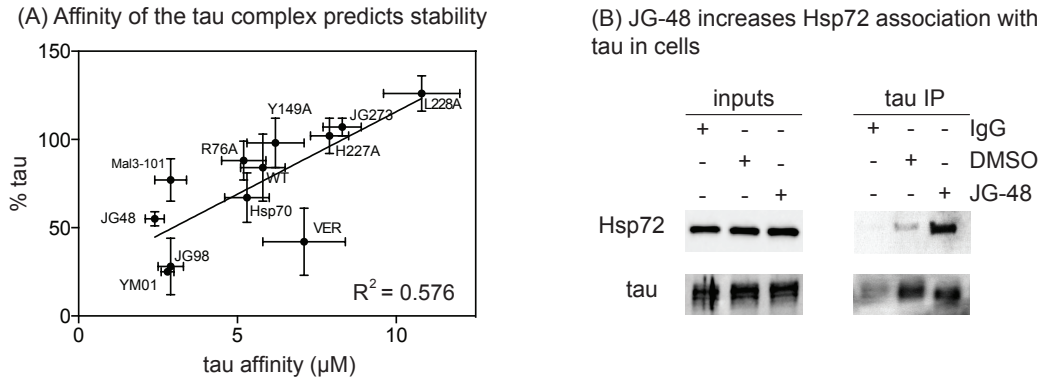

Figure 2.6 Affinity of the Hsc70-tau complex, measured *in vitro*, roughly correlates with the stability of tau in cells. (B) JG-48 increases co-immunoprecipitation of Hsp72 with tau. A representative blot of two independent experiments is shown. (C) Correlation between the relative affinity of the Hsc70-tau complex from the ELISA with the levels of tau in treated cells.

2.4.7 JG-48 preferentially stabilizes binding of Hsp70 to disease-associated tau variants

One of the unexplained aspects of JG-48 activity is its ability to preferentially enhance the turnover of disease-associated tau variants (see Figure 2.2). To better understand this selection process, we measured binding of Hsc70 to disease-associated tau variants in the ELISA format. A152T is a point mutation linked to PSP and other tauopathies, while K280Q mimics a lysine acetylation that is also associated with these disorders [21, 62, 63]. We found that, compared to wild type 4R0N tau, these variants had significantly worse affinity for Hsc70. Specifically, A152T had an affinity of 9.9 ± 1.0 μM and K280Q had an affinity of 16 ± 1.9 μM (Figure 2.7A), compared to the 5.8 μM of wild type. These results suggest that some disease-associated variants have a weakened affinity for chaperone, which might contribute to their aberrant accumulation in disease.

Because the point mutations are not located in known chaperone-binding sites [29, 30, 64], these effects likely occur through long-rage structural changes.

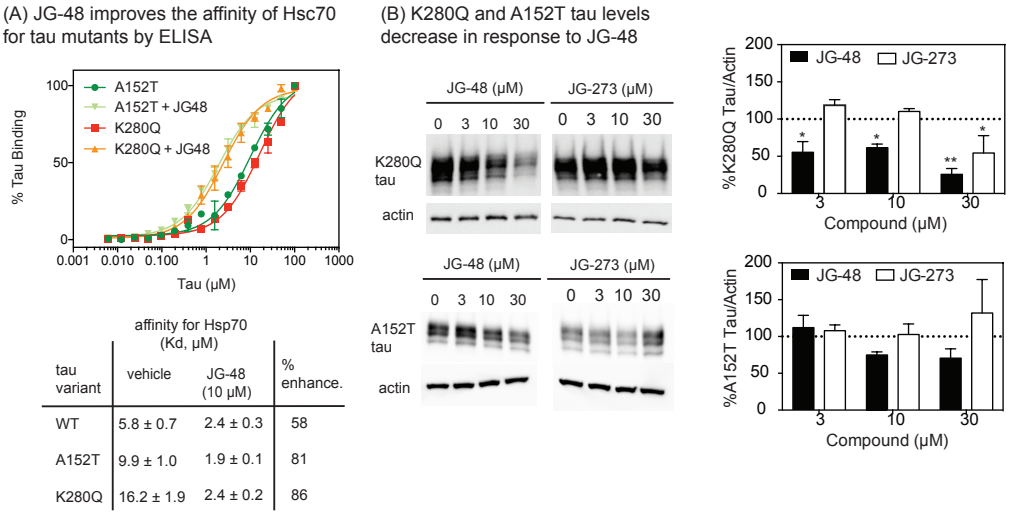

tau variant	affinity for Hsp70 (Kd, μM) vehicle	JG-48 (10 μM)	% enhance.
WT	5.8 ± 0.7	2.4 ± 0.3	58
A152T	9.9 ± 1.0	1.9 ± 0.1	81
K280Q	16.2 ± 1.9	2.4 ± 0.2	86

Figure 2.7 JG-48 improves the binding of Hsp70 to disease related mutants as well as their clearance. (A) ELISA results show that JG-48 increases the binding of Hsc70 to tau variants with point mutants related to tauopathy. Results are the average of two independent experiments performed in triplicate and error bars represent the SD. (B) JG-48, but not JG-273, reduces K280Q and A152T levels in transiently transfected HeLa cells. Results are the average of two independent experiments and error is SEM. Statistical analysis was performed using a 2-way ANOVA with Dunnett's test.*p<0.05, **p<0.005.

Next, we tested whether JG-48 might enhance the affinity of Hsc70 for the A152T and K280Q forms of tau. Indeed, JG-48 had a dramatic effect on the affinity of these complexes. JG-48 (10 μM) increased affinity for A152T tau by 5-fold and K280Q tau by nearly 7-fold (Figure 2.7A). In the presence of JG-48, these affinities were now comparable to, or better than, the affinity of the wild type complex. These results suggest the possibility that JG-48 normalizes tau interactions and thereby promotes clearance. Indeed, the levels of tau in cells expressing K280Q, A152T and 4R0N tau were highly sensitive to JG-48, but not JG-273 (Figure 2.7B).

2.4.8 Over-expression of Hsc70 interacting protein (HIP) mimics the effects of JG-48 on tau turnover

Based on these results, we considered a model in which chaperone uses affinity for its clients to guide quality control decisions (Figure 2.8). When tau is released from microtubules, it is known to encounter the chaperones [1]. The tau-bound chaperone would then be expected to cycle through nucleotide states, in collaboration with co-chaperones. In the proposed model, Hsc70 and Hsp70 might "choose" to release tau back to the microtubule for re-binding if the ADP-bound complex is sufficiently transient. However, if the tau complex is relatively long-lived, it might favor degradation, perhaps through recruitment of UPS or autophagy effectors. A key prediction of this model is that stabilizing the tau

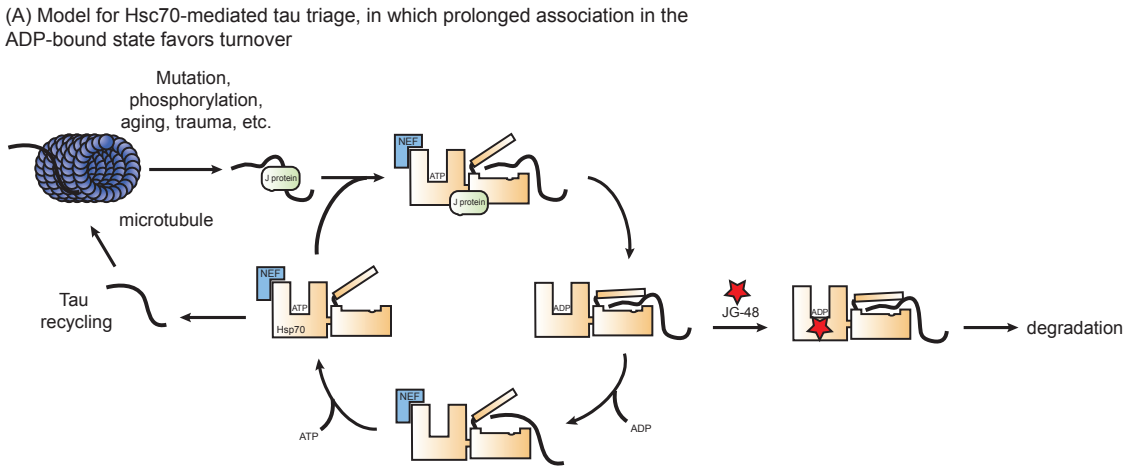

Figure 2.8 Model for Hsc70-mediated tau triage, in which prolonged association in the ADP-bound state favors turnover. JG-48 activates tau degradation by stabilizing the Hsc70 substrate-bound state.

complex should shift the balance towards turnover. This model might explain why over-expression of Hsc70 protects tau levels, while Hsp70 favors degradation, because Hsp70 is known to have a significantly tighter affinity for tau [30].

To test this model in a different way, we over-expressed the co-chaperone HIP in HeLa C3 cells. As mentioned above, HIP competes with NEFs for binding to Hsp70 and Hsc70 and, like JG-48, it stabilizes client binding [16]. Indeed, we found that over-expression of HIP in HeLa C3 cells decreased tau to a level comparable with that seen after JG-48 treatment (Figure 2.9). This result, obtained using a completely complimentary approach, supports the general model.

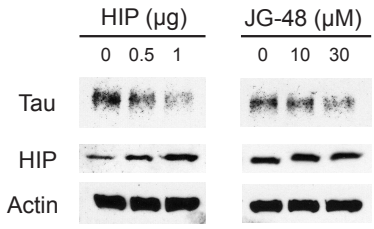

Figure 2.9 Hsc70 Interacting Protein (HIP) phenocopies compound effect on tau stability. HIP has the same effect on tau stability as JG-48 suggesting a similar mechanism of action. A representative blot of two independent experiments is shown.

2.5 Discussion

A network of chaperones, co-chaperones and stress response pathways is tasked with maintaining normal proteostasis [65]. In this network, Hsp70s are considered to be the “triage chaperones” that are involved with the folding or degradation of many clients [66, 67]. This system is emerging as a potential drug target in a number of diseases, including cancer and neurodegeneration [68-71]. Therefore, there is great interest in better understanding the molecular

mechanisms of Hsp70 with the ultimate goal of rebalancing these decisions to treat disease.

In this study, we have taken advantage of a new set of chemical probes, combined with new point mutants, to explore these mechanisms. As mentioned in Chapter 1, the key enabling observation was that Hsp70 inhibitors, such as YM-01, cause a robust loss of tau in disease models [31]. These findings suggested to us that YM-01 might be a powerful chemical probe for understanding Hsp70 mechanisms. Before embarking on such a study, we first had to resolve problematic features of YM-01, removing spectral properties that interfered with many biochemical measurements. This exercise yielded JG-48, which retained the ability to reduce abnormal tau in cultured cells and in other models of tauopathy (see Figure 2.1 and 2.2). By systematically examining many possible mechanisms (*e.g.* effects on ATPase activity, protein-protein interactions, *etc.*), we eventually found that the stability of the tau complex, as measured *in vitro*, seemed to best predict effects on tau turnover in cells. This prediction was then tested using an expanded collection of chemical and genetic perturbations, leading to a model in which one of the factors governing client triage (at least for tau) appeared to be its affinity for the chaperone.

This model, like many, leads to interesting, unanswered questions. What are the key factors that normally determine the affinity of Hsp70/Hsc70 for its clients? We found that some disease-associated tau mutants, such as K280Q, have a

weakened intrinsic affinity. This diminished binding might allow them to partially avoid the chaperone system, perhaps contributing to their accumulation and role in disease. Thus, it is tempting to speculate that Hsp70/Hsc70 might use affinity to enact similar quality control decisions for other clients too. These chaperones typically interact with extended, linear polypeptides containing hydrophobic residues, such as those commonly found in the interior of globular folded proteins [66, 72]. Thus, if a client is folded, it likely loses affinity for Hsp70s, whereas, if a client has trouble folding, it might be predicted to bind better. This feature might allow Hsp70 to preferentially remain bound to misfolded clients and, under conditions of sufficient dwell time, recruit effectors of degradation. This elegant model might explain why Hsp70 is able to operate on an entire proteome because relatively simple, physical metrics are used to enact fate decisions.

As mentioned above, over-expression of Hsp70 is known to lead to tau degradation, while over-expression of Hsc70 leads to its retention [30]. More recently, a dominant negative mutation of Hsc70 was found to induce tau degradation [2], suggesting that Hsc70, like Hsp72, is capable of linking tau to degradation if its ATPase activity is disrupted. Consistent with this idea, the binding site for JG-48 is invariant between Hsc70 and Hsp72; thus, our results suggest that interruption of either paralog's ATPase activity in cells may initiate tau turnover. Still Hsp70 is expected to play a prominent role because it has a tighter intrinsic affinity for tau and because it better couples with CHIP [30]. The expression of Hsp70 is strongly induced by stress, so a stress-associated

change in the Hsc70:Hsp70 ratio might favor turnover of tau by increasing the proportion that is stably bound by chaperone. Likewise, aging might dampen the stress response [73, 74] and make cells less able to defend themselves against tau accumulation.

The binding site of Hsc70 and Hsp70 on tau is overlapping with the regions required for microtubule binding [29]. Further, this same region is required for tau aggregation [75]. Thus, there are multiple protein-protein interactions that converge on this functionally important, but potentially dangerous region [75, 76]. As mentioned above, many disease-associated changes in tau, such as PTMs and point mutants, reduce binding of tau to microtubules, perhaps flooding the cytosol with aggregation-prone tau molecules. Hsp70s need to deal with this situation by either helping tau back onto the microtubule or by recruiting degradation effectors, such as CHIP. The results outlined here suggest that the logic of this system (*e.g.* whether this tau is ultimately retained or degraded) may be the result of a delicate balance of competing affinities. In disease or aging, this delicate balance may be tipped towards tau aggregation, whereas JG-48 or stress responses might counter-balance this disruption by removing excess tau.

It seems likely that the decision to retain or degrade tau should be impacted by additional factors, including the availability of co-chaperones. NEFs might be particularly important because they would be expected to help release tau from the Hsp70 complex. In other words, NEFs might be the key timing mechanism of

quality control. This general concept is supported by the findings that BAG1 overexpression increases total tau levels in an Hsp70 dependent manner [54]. Beyond tau, BAG2 and HspBP1 are known to prevent CHIP ubiquitination of the other Hsp70 clients, Raf-1 and cystic fibrosis transmembrane conductance regulator (CFTR) [77, 78], and BAG5 interferes with CHIP-assisted ubiquitination of α-synuclein [79] and the tumor suppressor PTEN [80]. These findings support the idea that the release of clients is associated with retention and that NEFs are important in “tuning” client dwell time. However, it is important to note that BAG1 coordinates with CHIP to target some Hsc70 clients for proteasomal degradation [55, 81]. Additionally, BAG2 is reported to increase ubiquitin-independent degradation of phosphorylated tau [82]. These findings illustrate the difficulty in identifying clear “rules” for protein quality control and, rather, point to a model that needs to take into account the specific properties of the individual clients, including its intrinsic affinity for chaperone. That being said, over-expression of HIP increases the clearance of not only tau, but other Hsp70 clients such as α-synuclein and polyQ-AR [83, 84], so client affinity may be a fundamental mechanism of quality control.

2.6 Methods

2.6.1 Cell culture and immunoblotting

HeLa C3 cells were stably transfected with V5-4R0N tau as previously described. Cells were cultured in supplemented Opti-MEM media. Cells were plated into 6-well plates (Corning) or 12-well plates (Corning) and treated with compound at

indicated concentrations for 24 hrs before lysis with RIPA buffer (150 mM sodium chloride, 1.0% Triton X-100, 0.5% sodium deoxycholate, 0.1% SDS, 50 mM Tris, pH 8.0) supplemented with protease inhibitor, PMSF and NaF. Following quantification, lysates were loaded to 10% gels (BioRad) and proteins identified via Western blot. For Hsc70 mutant transfections, HeLa C3 cells were plated into 12-well plates (Corning) and indicated amount of plasmid was added with Lipofectamine 3000 (Invitrogen). Transfection was allowed to proceed for 24 hrs before lysis with RIPA buffer. For HIP transfection, HeLa C3 cells were plated into 6-well plates (Corning) and indicated amounts of plasmid were added with Lipofectamine 2000 (Invitrogen). Transfection was allowed to proceed for 24 hrs before lysis with RIPA buffer. Cell or tissue lysates were separated and immonoblotted via Western blot. All quantification of Western blots was performed with NIH Image J or Biorad Image Lab analysis.

2.6.2 Brain aggregate cultures

Brain aggregates are prepared from E15 days rTg4510 mouse brains. Briefly, a pool of E15 day mouse brains are dissociated through two nylon meshes and plated in a 96-well plate. A sphere-shaped brain aggregate formed in each well is cultured in DMEM H21 supplemented with glucose (6 g/L), gentamicin (50 mg/L) and 10% FBS. At 15 days in culture, they are infected with 5 µL of 10% brain homogenates of rTg4510 mice for 10 days. They are treated with 10 µM of YM-01 or JG-48 for 24 hrs before harvesting at 35 days in culture. They are fixed with 4% paraformaldehyde for 3 days. Fixed brain aggregates are washed with PBS

for 1 hr (3X) and incubated with blocking buffer (0.3% Triton X-100, 0.1% Tween 20, 2% bovine serum albumin and 10% normal goat serum in PBS) overnight and stained with primary antibodies (PHF-tau (MN1020, Thermo Scientific) and anti-beta tubulin (H-235, Santa Cruz Biotech); 1:100) for 3 days. After incubation with primary antibodies, they are washed with PBS and incubated with secondary antibodies (goat anti-rabbit IgG conjugated with Alexa633 and goat anti-mouse conjugated with Alexa568, Jackson Immunoresearch Laboratory; 1:800) overnight. After washing with PBS for 1 hr (3X), they were coversliped with Vectashield mounting media containing DAPI (H-1500, Vector laboratories). Confocal images are taken with a Leica SP8 confocal microscope and 15-20 z-sectioned images are stacked together before measuring phospho-tau intensity with Image J.

2.6.3 Slice cultures

Hippocampal slices from 4 month old rTg4510 or wild type mice were perfused with JG-48 (30 μM) or 1% DMSO vehicle control for 6 hours. Baseline signal was recorded for 20 min, LTP was induced with TBS (5 bursts of 200 Hz separated by 200 ms, repeated 6 times with 10 s between the 6 trains), and LTP was recoded for 60 min as previously described [31]. Changes in fEPSP slope are expressed as a percentage of baselines.

2.6.4 Protein expression and purification

Hsc70, Hsp70 and their co-chaperones were expressed and purified using previously reported methods [49]. Apo chaperone was prepared from several days of dialysis in assay buffer (0.017% Triton X-100, 100 mM Tris-HCl, 20 mM KCl, and 6 mM $MgCl_2$, pH 7.4) at 4 °C to remove nucleotide.

2.6.5 NMR

Titration studies were carried out as previously described [36]. NMR samples of 160 μM ^{15}N labeled $Hsc70_{NBD}$ in 25 mM TrisHCl, 10 mM KCl, 8 mM $MgCl_2$, 10 mM PO_4^{2-}, 0.015% NaN_3, 5% D_2O and pH 7.0 was treated with either DMSO alone or JG-48 (200 μM). TROSY-HSQC data was processed in NMR PIPES and converted to SPARKY format. Spectra were manually analyzed in SPARKY.

2.6.6 Fluorescence Polarization

ATP-FAM. Fluorescence polarization experiments were performed in 384-well, black, low volume, round-bottom plates (Corning) using a SpectraMax plate reader. Increasing amounts of compound were incubated with nucleotide-free Hsc70 (400nM) and ATP-FAM (20 nM) (Jena Bioscience) for three hours at room temperature in assay buffer (0.017% Triton X-100, 100 mM Tris-HCl, 20 mM KCl, and 6 mM $MgCl_2$, pH 7.4) prior to measurement by plate reader (Ex. 485 nm, Em. 535nm, 530nm cutoff). The final DMSO concentration in each well was 4% and compounds were serially diluted two-fold in 100% DMSO. All data was subsequently analyzed by Prism (Graphpad Software).

HLA-FAM. Experiments were adapted from previously reported methods [49]. Briefly, 5 μM Hsc70 in the presence of 1 mM ADP was incubated with 25 nM HLA-FAM and treated with increasing concentrations of NEF proteins in 384-well, black, low volume, round-bottom plates (Corning) in the presence and absence of compound for 2 hrs at RT in assay buffer (0.017% Triton X-100, 100 mM Tris-HCl, 20 mM KCl, and 6 mM $MgCl_2$, pH 7.4). Following incubation, fluorescence polarization was measured using a SpectraMax plate reader (Ex. 485nm, Em. 535nm, 530nm cutoff). All data was subsequently analyzed by Prism (Graphpad Software).

2.6.7 ATPase Assay

Assay was adopted from previously reported methods [44]. Briefly, Hsc70 (1 μM), J-protein (0.2 μM), 1 mM ATP and increasing amounts of NEF were incubated for 1-2 hours in assay buffer (0.017% Triton X-100, 100 mM Tris-HCl, 20 mM KCl, and 6 mM $MgCl_2$, pH 7.4) in the presence and absence of compound. The final DMSO concentration was 4%. Afterwards, 80 μL of malachite green reagent was added for phosphate detection followed by the addition of sodium citrate to halt non-enzymatic ATP hydrolysis. Absorbance was measured by a SpectraMax plate reader (OD_{620}) to determine phosphate concentration.

2.6.8 Luciferase Refolding

Assay was adopted from previously reported methods [85]. Briefly, denatured luciferase (100 nM) was incubated with Hsc70 (1 μM), J-protein (0.2 μM), 1 mM

ATP and increasing amounts of NEF in assay buffer (23 mM HEPES, 120 mM KAc, 1.2 mM MgAc, 2.2 mM DTT, 1 mM ATP, 8.8 μM creatine phosphate, 35U/mL creatine kinase pH 7.4) for one hour in the presence and absence of compound. The final DMSO concentration was 4%. After the addition of the SteadyGlo reagent (Promega), luminescence was measured in a SpectraMax plate reader to determine the amount of refolded luciferase.

2.6.9 Flow Cytometry Protein Interaction Assay (FCPIA)

Procedure is adapted from previously reported methods [86]. Biotinylated Hsc70 was immobilized on polystyrene streptavidin coated beads (Spherotech), incubated with Alexa-Fluor 488 labeled NEF (50 nM) and increasing amounts of compound in buffer A (25 mM HEPES, 5 mM $MgCl_2$, 10 mM KCl, 0.03% Tween-20 pH 7.5). Protein complex inhibition was detected by measuring bead-associated fluorescence using an Accuri C6 Flow Cytometer. DMSO is used as a negative control and 1 μM excess unlabeled Hsc70 is used as a positive control.

2.6.10 Tau Binding ELISA

Method was adapted from a previous report [29]. Briefly, 1 μM human Hsc70 (30 μL) was immobilized overnight at 37 °C in clear, non-sterile 96-well plates (Thermo) in 50mM MES (pH 5.5) and 0.5 mM DTT with 1 mM ADP. Wells were washed with 100 μL of PSB-T (3 x 3 min., rocking) prior to the addition of 30 μL of 4RON tau solution in binding buffer (25 mM HEPES, 40 mM KCl, 8 mM $MgCl_2$, 100 mM NaCl, 0.01% Tween, pH 7.4) with 1 mM ADP and 1 μL of either DMSO

or compound for 3 hrs at RT. After blocking in 5% milk, quantification of tau binding was performed using rabbit anti-tau (H150) primary antibody (Santa Cruz, sc-5587, 1:2000 in TBS-T, 50 µL/well) and goat anti-rabbit HRP-conjugated secondary (Anaspec, 28177, 1:2000 in TBS-T, 50 µL/well). TMB substrate (Cell Signaling, 7400L) and 1N HCl were used to detect binding. Absorbance was measured using a SpectraMax plate reader (OD_{450}). Minimal, non-specific binding of 4R0N tau to empty wells was subtracted as background and curves were fit using non-zero intercept hyperbolic fits in Prism (GraphPad Software).

2.6.11 Immunoprecipitation of V5-Tau

The co-immunoprecipitation procedure was adopted from previously described methods [29]. Briefly, HeLa C3 cells were treated with bortezomib in a final concentration of 5 µM for 4 hours prior to lysis in mammalian protein extraction reagent (Thermo Scientific). Following protein quantification, 5 mg of lysate was incubated with 40 µL of anti-tau antibody (Santa Cruz, sc-166060) and 50 µM JG-48 or DMSO (5%) at 4 °C in the dark overnight. Lysate was incubated with normal goat IgG with DMSO (4%) as a negative control. Beads were then conjugated to Protein A/G agarose beads (Santa Cruz, sc-2003) for 4 hours at 4 °C and washed 3 times with 100 µL of PBS (Gibco) at 1000xg for 1 minute. Proteins were eluted by boiling at 96 °C in 40uL of SDS loading dye, and 10 µL of sample were separated on 4-15% Tris-trycine gels (Bio-rad) and transferred to nitrocellulose membrane. The membranes were blocked in nonfat milk (5% milk in TBS, 0.5% Tween) for 1 hour, incubated with primary antibodies for Tau

(Santa Cruz, sc-5587) and Hsp72 (Enzo, ADI-SPA-811) overnight at 4 °C in the dark, washed, and then incubated with a horseradish peroxidase-conjugated secondary antibody (Anaspec, 28177) for 1 hour. Finally, membranes were developed using chemiluminescence (Thermo Scientific, Supersignal® West Pico).

2.6.12 Protein Dynamics and Molecular Modeling

Computational modeling of JG-48 binding to $Hsc70_{NBD}$ (PDB: 3C7N) was obtained using similar methods as previously described [34, 35]. Briefly, AUTODOCK-4.2 was used for the docking of JG-48 to $Hsc70_{NBD}$ with the following parameters: GA runs = 100, initial population size = 1500, max number of evaluations = long, max number of surviving top individuals = 1, gene mutation rate = 0.02, rate of crossover = 0.8, GA crossover mode: two points, Caushy distribution mean for gene mutation = 0, Cauchy distribution variance for gene mutation = 1, number of generations for picking worst individuals = 10. The docked structures were clustered and then evaluated using PyMOL. All calculations were completed on an Apple MacBookPro computer equipped with a 64-bit 2.4 GHz Intel Core 2 Duo processor running MacOSX 10.6.8.

2.6.13 Synthesis of JG-48 and JG-273

First, functionalized anilines were cyclized by reaction with potassium ethyl xanthate, and the product was methylated by methyl iodide. The substituted 2-(methylthio)benzothiazole was reacted with *p*-TsOMe to afford its

methylthioiminium salt, which was subsequently condensed with various *N*-ethylrhodanine. The product was activated by *p*-TsOMe, followed by the condensation with 1-((1,3-dioxoisoindolin-2-yl)methyl)-2-methylpyridin-1-ium bromide. Finally, the protection group on the pyridine nitrogen was removed in the presence of catalytic amounts of aqueous ammonium hydroxide. Final products were collected in overall yield of approximately 40%.

JG-48: ^{1}H NMR (400 MHz, DMSO) δ 8.55 (d, *J* = 4.1 Hz, 1H), 8.12 (s, 1H), 7.67 (dd, *J* = 7.9, 5.2 Hz, 1H), 7.63 (dd, *J* = 7.4, 1.8 Hz, 1H), 7.46 (d, *J* = 8.7 Hz, 1H), 7.27 (d, *J* = 8.0 Hz, 1H), 6.97 (ddd, *J* = 7.3, 4.9, 1.1 Hz, 1H), 6.25 (s, 1H), 3.98 (s, 3H), 3.91 (q, *J* = 7.0 Hz, 2H), 1.21 (t, *J* = 7.1 Hz, 3H). ESI-MS: calculated for $C_{20}H_{17}F_3N_3OS_2^+$ 436.08, found 436.04.

JG-273: ^{1}H NMR (400 MHz, DMSO) δ 8.47 (d, *J* = 4.3 Hz, 1H), 7.59 (td, *J* = 7.8, 1.7 Hz, 1H), 7.19 (d, *J* = 8.0 Hz, 1H), 6.90 (dd, *J* = 6.7, 5.4 Hz, 1H), 6.08 (s, 1H), 3.81 (d, *J* = 7.1 Hz, 2H), 3.65 (t, *J* = 7.3 Hz, 2H), 3.32 (s, 3H), 3.08 (t, *J* = 7.2 Hz, 2H), 1.14 (t, *J* = 7.0 Hz, 3H). ESI-MS: calculated for $C_{15}H_{18}N_3OS_2^+$ 320.09, found 320.13.

Notes

This work was adapted from published material entitled “Stabilizing the Hsp70-Tau Complex Normalizes Proteostasis in a Model of Tauopathy” Young, ZT, Rauch, JN; Assimon, VA; Jinwal, UK; Ahn, M; Li, X; Dunyak, BM; Ahmad, A;

Carlson, GA; Srinivasan, SR; Zuiderweg, ERP; Dickey, CA; Gestwicki, JE. (2016) *Cell Chemical Biology* (in press).

Contributions

Zapporah T. Young performed all biochemical analyses including FP experiments, ATPase and luciferase refolding assays, FCPIAs and ELISAs. All Hsc70, mutant tau and HIP transfections were done by Zapporah T. Young along with all IP experiments and tau stability measurements in HeLa cells. Experiments were designed and interpreted by Zapporah T. Young and Jason E. Gestwicki. Measurements of tau reduction and LTP in SHSY cells and rTg4510 mice and rTg4510 brain slices were performed by Umesh K. Jinwal and Chad A. Dickey. Brain culture experiments were completed by Misol Ahn using material provided by George Carlson. Protein NMR studies were performed by Erik Zuiderwig and Atta Ahmad. Compound docking was conducted by Bryan M. Dunyak and Sharan R. Srinivasan. Victoria Assimon designed Hsc70 point mutations. Xiaokai Li and Hao Shao synthesized JG-48 and JG-273. Jennifer N. Rauch developed the FCPIA method.

2.7 Appendix

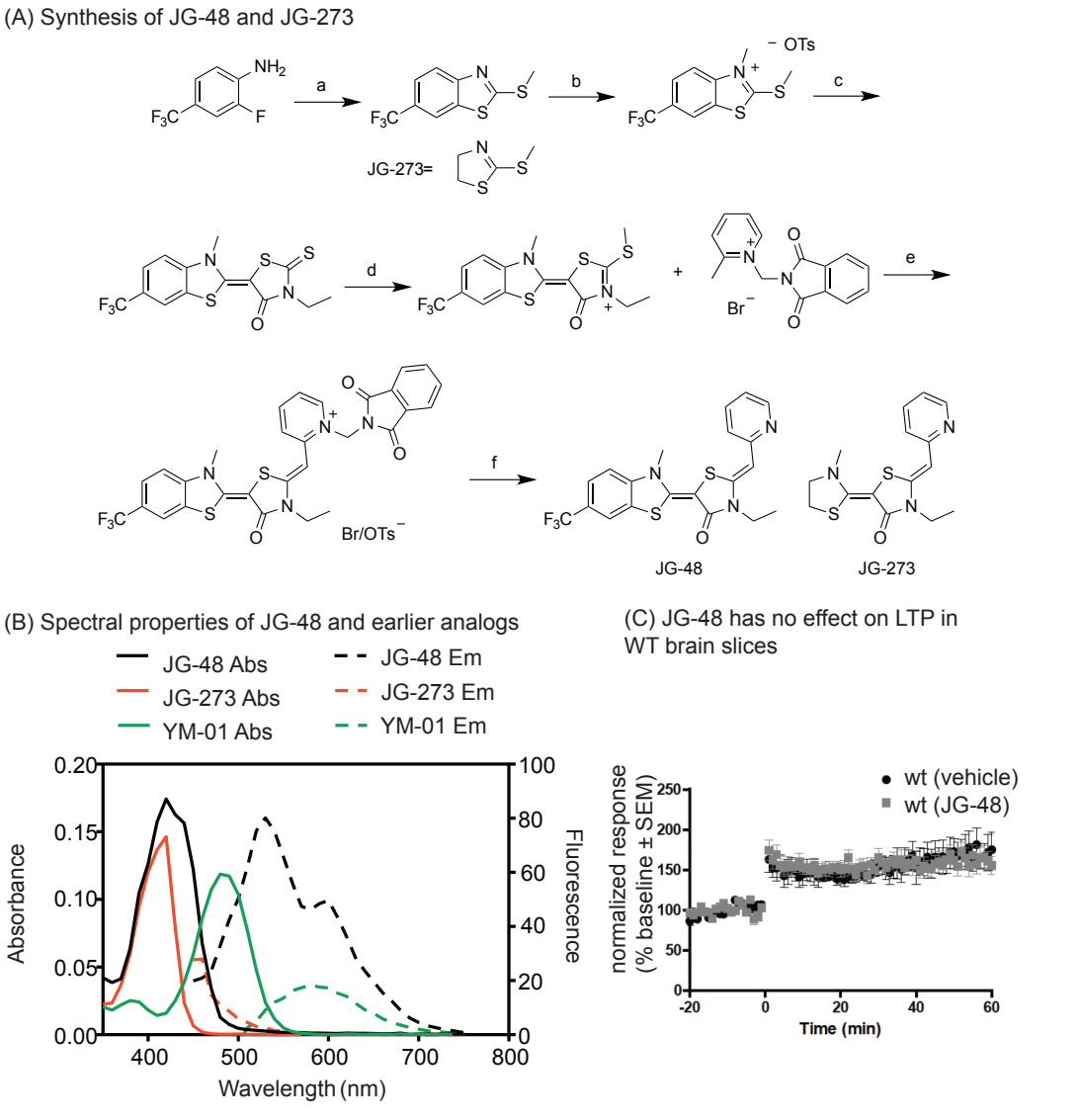

Appendix 2.1 Compound synthesis and characterization. (A) Synthetic route to JG-48 and JG-273. (a) Potassium ethyl xanthate, DMF, 4 h, 125 °C; 2. methyl iodide, triethyl-amine, ethanol, 1 h, 80 °C (b) methyl p-toluenesulfonate, anisole, 125 °C; for JG-273, was used as starting material. (c) 3-ethylrhodanine, triethylamine, acetonitrile, 4 h, 25 °C (d) methyl p-toluenesulfonate, DMF, 3 h, 135 °C (e) triethyl-amine, acetonitrile, 3 h, 70 °C (f) aqueous ammonia, DCM/methanol (1:3), 1 h, r.t. See the methods for NMR and MS characterization. (B) Spectral properties of JG-48, showing that it is less fluorescent at 535/620 nm, which is critical for its use in biochemical assays. (C) JG-48 (10 μM) has no effect on LTP in non-transgenic hippocampal slices from 3-4 month old WT mice. fEPSP traces are an average of JG-48 (n=9) or vehicle-treated (n=4).

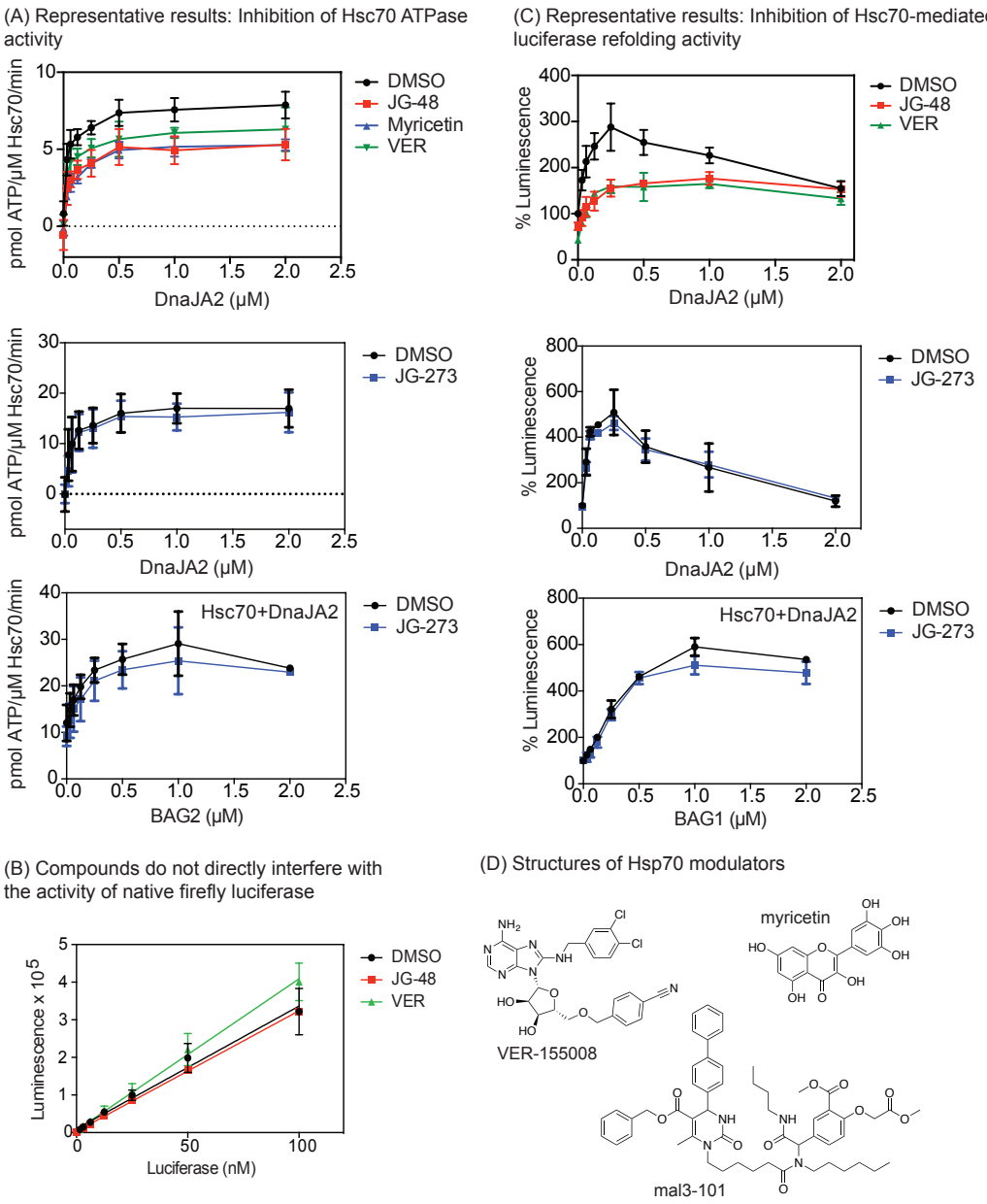

Appendix 2.2 Representative results from ATPase and luciferase refolding experiments. (A) Stimulation of ATPase activity by DnaJA2 is mildly inhibited. Similar results were seen for other DnaJ family members (se Figure 2.3.B). Likewise, inhibitors blocked stimulation of Hsc70 by BAG-1 and similar results were seen for other NEFs (see Figure 2.3.B). The control compound, JG-273, was inactive. Results are the average of three independent experiments performed in triplicate each. Error bars represent the standard deviations. Compounds were assayed at 50µM. Hsc70 = 1 µM. (B) None of the compounds (50µM) interfere with the enzyme activity of native firefly luciferase. (C) Luciferase refolding was measured by luminescence after treatment of denatured luciferase with chaperone systems. Representative results are shown for DnaJA2 and BAG-1, while similar results were seen for other J proteins and NEFs (see Figure 2.3.B). Results are the average of two independent experiments performed in triplicate each. Error bars represent the standard deviation. Compounds were assayed at 50µM. Hsc70 = 1 µM. (D) Chemical structures of Hsp70 modulators assayed.

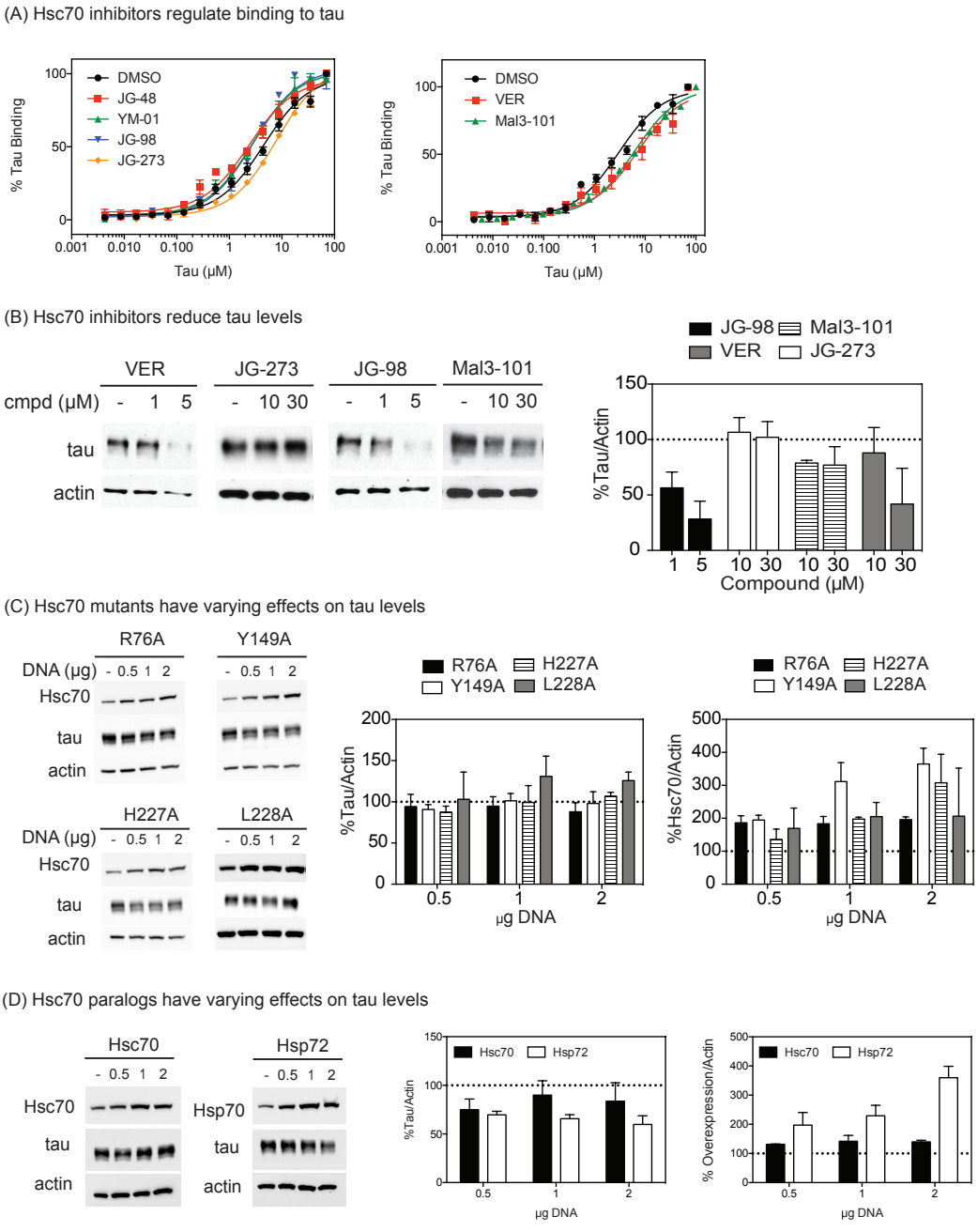

Appendix 2.3 Controls and raw data for the correlation studies in Table 2.1 and Figure 2.5. (A) ELISA study on the effects of Hsc70 inhibitors on tau affinity. (B) Sample of the raw data showing the effects of Hsc70 manipulations on tau levels in HeLaC3 cells. Results are representative of experiments performed in duplicate each and error bars represent the SEM. (C) Sample of the raw data showing the effects of Hsc70 mutations on tau levels in HeLaC3 cells. Results are representative of experiments performed in duplicate each and error bars represent the SEM. (D) Raw data showing the effects of Hsc70 paralogs on tau levels in HeLaC3 cells. Results are representative of experiments performed in triplicate each and error bars represent the SEM.

2.8 References

[1] Jinwal UK, O'Leary JC, 3rd, Borysov SI, Jones JR, Li Q, Koren J, 3rd, Abisambra JF, Vestal GD, Lawson LY, Johnson AG, Blair LJ, Jin Y, Miyata Y, Gestwicki JE, Dickey CA. Hsc70 rapidly engages tau after microtubule destabilization. J Biol Chem, 2010; 285: 16798-805.

[2] Fontaine SN, Rauch JN, Nordhues BA, Assimon VA, Stothert AR, Jinwal UK, Sabbagh JJ, Chang L, Stevens SM, Jr., Zuiderweg ER, Gestwicki JE, Dickey CA. Isoform-selective Genetic Inhibition of Constitutive Cytosolic Hsp70 Activity Promotes Client Tau Degradation Using an Altered Co-chaperone Complement. J Biol Chem, 2015; 290: 13115-27.

[3] Kettern N, Dreiseidler M, Tawo R, Hohfeld J. Chaperone-assisted degradation: multiple paths to destruction. Biol Chem, 2010; 391: 481-9.

[4] Pratt WB, Morishima Y, Gestwicki JE, Lieberman AP, Osawa Y. A model in which heat shock protein 90 targets protein-folding clefts: rationale for a new approach to neuroprotective treatment of protein folding diseases. Exp Biol Med (Maywood), 2014; 239: 1405-13.

[5] Jiang J, Prasad K, Lafer EM, Sousa R. Structural basis of interdomain communication in the Hsc70 chaperone. Mol Cell, 2005; 20: 513-24.

[6] Zhuravleva A, Clerico EM, Gierasch LM. An interdomain energetic tug-of-war creates the allosterically active state in Hsp70 molecular chaperones. Cell, 2012; 151: 1296-307.

[7] Bertelsen EB, Chang L, Gestwicki JE, Zuiderweg ER. Solution conformation of wild-type E. coli Hsp70 (DnaK) chaperone complexed with ADP and substrate. Proc Natl Acad Sci U S A, 2009; 106: 8471-6.

[8] Palleros DR, Reid KL, Shi L, Welch WJ, Fink AL. ATP-induced protein-Hsp70 complex dissociation requires K+ but not ATP hydrolysis. Nature, 1993; 365: 664-6.

[9] Sekhar A, Rosenzweig R, Bouvignies G, Kay LE. Mapping the conformation of a client protein through the Hsp70 functional cycle. Proc Natl Acad Sci U S A, 2015; 112: 10395-400.

[10] Bauer D, Merz DR, Pelz B, Theisen KE, Yacyshyn G, Mokranjac D, Dima RI, Rief M, Zoldak G. Nucleotides regulate the mechanical hierarchy between subdomains of the nucleotide binding domain of the Hsp70 chaperone DnaK. Proc Natl Acad Sci U S A, 2015; 112: 10389-94.

[11] Clerico EM, Tilitsky JM, Meng W, Gierasch LM. How hsp70 molecular machines interact with their substrates to mediate diverse physiological functions. J Mol Biol, 2015; 427: 1575-88.

[12] Zhuravleva A, Gierasch LM. Substrate-binding domain conformational dynamics mediate Hsp70 allostery. Proc Natl Acad Sci U S A, 2015; 112: E2865-73.

[13] Ha JH, McKay DB. Kinetics of nucleotide-induced changes in the tryptophan fluorescence of the molecular chaperone Hsc70 and its

subfragments suggest the ATP-induced conformational change follows initial ATP binding. Biochemistry, 1995; 34: 11635-44.
[14] Brehmer D, Rüdiger S, Gässler CS, Klostermeier D, Packschies L, Reinstein J, Mayer MP, Bukau B. Tuning of chaperone activity of Hsp70 proteins by modulation of nucleotide exchange. Nature structural biology, 2001; 8: 427-32.
[15] Jiang J, Maes EG, Taylor AB, Wang L, Hinck AP, Lafer EM, Sousa R. Structural basis of J cochaperone binding and regulation of Hsp70. Mol Cell, 2007; 28: 422-33.
[16] Li Z, Hartl FU, Bracher A. Structure and function of Hip, an attenuator of the Hsp70 chaperone cycle. Nat Struct Mol Biol, 2013; 20: 929-35.
[17] Dou F, Netzer WJ, Tanemura K, Li F, Hartl FU, Takashima A, Gouras GK, Greengard P, Xu H. Chaperones increase association of tau protein with microtubules. Proc Natl Acad Sci U S A, 2003; 100: 721-6.
[18] Petrucelli L, Dickson D, Kehoe K, Taylor J, Snyder H, Grover A, De Lucia M, McGowan E, Lewis J, Prihar G, Kim J, Dillmann WH, Browne SE, Hall A, Voellmy R, Tsuboi Y, Dawson TM, Wolozin B, Hardy J, Hutton M. CHIP and Hsp70 regulate tau ubiquitination, degradation and aggregation. Hum Mol Genet, 2004; 13: 703-14.
[19] Jinwal UK, Miyata Y, Koren J, 3rd, Jones JR, Trotter JH, Chang L, O'Leary J, Morgan D, Lee DC, Shults CL, Rousaki A, Weeber EJ, Zuiderweg ER, Gestwicki JE, Dickey CA. Chemical manipulation of hsp70 ATPase activity regulates tau stability. J Neurosci, 2009; 29: 12079-88.
[20] Narayanan RL, Durr UH, Bibow S, Biernat J, Mandelkow E, Zweckstetter M. Automatic assignment of the intrinsically disordered protein Tau with 441-residues. J Am Chem Soc, 2010; 132: 11906-7.
[21] Coppola G, Chinnathambi S, Lee JJ, Dombroski BA, Baker MC, Soto-Ortolaza AI, Lee SE, Klein E, Huang AY, Sears R, Lane JR, Karydas AM, Kenet RO, Biernat J, Wang LS, Cotman CW, Decarli CS, Levey AI, Ringman JM, Mendez MF, Chui HC, Le Ber I, Brice A, Lupton MK, Preza E, Lovestone S, Powell J, Graff-Radford N, Petersen RC, Boeve BF, Lippa CF, Bigio EH, Mackenzie I, Finger E, Kertesz A, Caselli RJ, Gearing M, Juncos JL, Ghetti B, Spina S, Bordelon YM, Tourtellotte WW, Frosch MP, Vonsattel JP, Zarow C, Beach TG, Albin RL, Lieberman AP, Lee VM, Trojanowski JQ, Van Deerlin VM, Bird TD, Galasko DR, Masliah E, White CL, Troncoso JC, Hannequin D, Boxer AL, Geschwind MD, Kumar S, Mandelkow EM, Wszolek ZK, Uitti RJ, Dickson DW, Haines JL, Mayeux R, Pericak-Vance MA, Farrer LA, Ross OA, Rademakers R, Schellenberg GD, Miller BL, Mandelkow E, Geschwind DH. Evidence for a role of the rare p.A152T variant in MAPT in increasing the risk for FTD-spectrum and Alzheimer's diseases. Human molecular genetics, 2012; 21: 3500-12.
[22] Vogelsberg-Ragaglia V, Bruce J, Richter-Landsberg C, Zhang B, Hong M, Trojanowski JQ, Lee VM. Distinct FTDP-17 missense mutations in tau produce tau aggregates and other pathological phenotypes in transfected CHO cells. Mol Biol Cell, 2000; 11: 4093-104.

[23] Kara E, Ling H, Pittman AM, Shaw K, de Silva R, Simone R, Holton JL, Warren JD, Rohrer JD, Xiromerisiou G, Lees A, Hardy J, Houlden H, Revesz T. The MAPT p.A152T variant is a risk factor associated with tauopathies with atypical clinical and neuropathological features. Neurobiol Aging, 2012; 33: 2231 e7-2231 e14.
[24] Hong M, Zhukareva V, Vogelsberg-Ragaglia V, Wszolek Z, Reed L, Miller BI, Geschwind DH, Bird TD, McKeel D, Goate A, Morris JC, Wilhelmsen KC, Schellenberg GD, Trojanowski JQ, Lee VM. Mutation-specific functional impairments in distinct tau isoforms of hereditary FTDP-17. Science, 1998; 282: 1914-7.
[25] Hanger DP, Anderton BH, Noble W. Tau phosphorylation: the therapeutic challenge for neurodegenerative disease. Trends Mol Med, 2009; 15: 112-9.
[26] Cook C, Carlomagno Y, Gendron TF, Dunmore J, Scheffel K, Stetler C, Davis M, Dickson D, Jarpe M, DeTure M, Petrucelli L. Acetylation of the KXGS motifs in tau is a critical determinant in modulation of tau aggregation and clearance. Hum Mol Genet, 2014; 23: 104-16.
[27] Morris M, Knudsen GM, Maeda S, Trinidad JC, Ioanoviciu A, Burlingame AL, Mucke L. Tau post-translational modifications in wild-type and human amyloid precursor protein transgenic mice. Nat Neurosci, 2015; 18: 1183-9.
[28] Voss K, Combs B, Patterson KR, Binder LI, Gamblin TC. Hsp70 alters tau function and aggregation in an isoform specific manner. Biochemistry, 2012; 51: 888-98.
[29] Thompson AD, Scaglione KM, Prensner J, Gillies AT, Chinnaiyan A, Paulson HL, Jinwal UK, Dickey CA, Gestwicki JE. Analysis of the tau-associated proteome reveals that exchange of hsp70 for hsp90 is involved in tau degradation. ACS chemical biology, 2012; 7: 1677-86.
[30] Jinwal UK, Akoury E, Abisambra JF, O'Leary JC, 3rd, Thompson AD, Blair LJ, Jin Y, Bacon J, Nordhues BA, Cockman M, Zhang J, Li P, Zhang B, Borysov S, Uversky VN, Biernat J, Mandelkow E, Gestwicki JE, Zweckstetter M, Dickey CA. Imbalance of Hsp70 family variants fosters tau accumulation. FASEB journal : official publication of the Federation of American Societies for Experimental Biology, 2013; 27: 1450-9.
[31] Abisambra J, Jinwal UK, Miyata Y, Rogers J, Blair L, Li X, Seguin SP, Wang L, Jin Y, Bacon J, Brady S, Cockman M, Guidi C, Zhang J, Koren J, Young ZT, Atkins CA, Zhang B, Lawson LY, Weeber EJ, Brodsky JL, Gestwicki JE, Dickey CA. Allosteric Heat Shock Protein 70 Inhibitors Rapidly Rescue Synaptic Plasticity Deficits by Reducing Aberrant Tau. Biological psychiatry, 2013.
[32] Lei Z, Brizzee C, Johnson GV. BAG3 facilitates the clearance of endogenous tau in primary neurons. Neurobiol Aging, 2015; 36: 241-8.
[33] Sahara N, Murayama M, Mizoroki T, Urushitani M, Imai Y, Takahashi R, Murata S, Tanaka K, Takashima A. In vivo evidence of CHIP up-regulation attenuating tau aggregation. J Neurochem, 2005; 94: 1254-63.

[34] Rousaki A, Miyata Y, Jinwal UK, Dickey CA, Gestwicki JE, Zuiderweg ER. Allosteric drugs: the interaction of antitumor compound MKT-077 with human Hsp70 chaperones. J Mol Biol, 2011; 411: 614-32.
[35] Miyata Y, Li X, Lee HF, Jinwal UK, Srinivasan SR, Seguin SP, Young ZT, Brodsky JL, Dickey CA, Sun D, Gestwicki JE. Synthesis and Initial Evaluation of YM-08, a Blood-Brain Barrier Permeable Derivative of the Heat Shock Protein 70 (Hsp70) Inhibitor MKT-077, Which Reduces Tau Levels. ACS chemical neuroscience, 2013.
[36] Li X, Srinivasan SR, Connarn J, Ahmad A, Young ZT, Kabza AM, Zuiderweg ER, Sun D, Gestwicki JE. Analogs of the Allosteric Heat Shock Protein 70 (Hsp70) Inhibitor, MKT-077, as Anti-Cancer Agents. ACS Med Chem Lett, 2013; 4.
[37] Otvos L, Jr., Feiner L, Lang E, Szendrei GI, Goedert M, Lee VM. Monoclonal antibody PHF-1 recognizes tau protein phosphorylated at serine residues 396 and 404. J Neurosci Res, 1994; 39: 669-73.
[38] Spires TL, Orne JD, SantaCruz K, Pitstick R, Carlson GA, Ashe KH, Hyman BT. Region-specific dissociation of neuronal loss and neurofibrillary pathology in a mouse model of tauopathy. Am J Pathol, 2006; 168: 1598-607.
[39] Ramsden M, Kotilinek L, Forster C, Paulson J, McGowan E, SantaCruz K, Guimaraes A, Yue M, Lewis J, Carlson G, Hutton M, Ashe KH. Age-dependent neurofibrillary tangle formation, neuron loss, and memory impairment in a mouse model of human tauopathy (P301L). J Neurosci, 2005; 25: 10637-47.
[40] Crimins JL, Rocher AB, Luebke JI. Electrophysiological changes precede morphological changes to frontal cortical pyramidal neurons in the rTg4510 mouse model of progressive tauopathy. Acta Neuropathol, 2012; 124: 777-95.
[41] Abisambra JF, Blair LJ, Hill SE, Jones JR, Kraft C, Rogers J, Koren J, 3rd, Jinwal UK, Lawson L, Johnson AG, Wilcock D, O'Leary JC, Jansen-West K, Muschol M, Golde TE, Weeber EJ, Banko J, Dickey CA. Phosphorylation dynamics regulate Hsp27-mediated rescue of neuronal plasticity deficits in tau transgenic mice. J Neurosci, 2010; 30: 15374-82.
[42] Amick J, Schlanger SE, Wachnowsky C, Moseng MA, Emerson CC, Dare M, Luo WI, Ithychanda SS, Nix JC, Cowan JA, Page RC, Misra S. Crystal structure of the nucleotide-binding domain of mortalin, the mitochondrial Hsp70 chaperone. Protein Sci, 2014; 23: 833-42.
[43] Williamson DS, Borgognoni J, Clay A, Daniels Z, Dokurno P, Drysdale MJ, Foloppe N, Francis GL, Graham CJ, Howes R, Macias AT, Murray JB, Parsons R, Shaw T, Surgenor AE, Terry L, Wang Y, Wood M, Massey AJ. Novel adenosine-derived inhibitors of 70 kDa heat shock protein, discovered through structure-based design. J Med Chem, 2009; 52: 1510-3.
[44] Chang L, Bertelsen EB, Wisén S, Larsen EM, Zuiderweg ER, Gestwicki JE. High-throughput screen for small molecules that modulate the ATPase

activity of the molecular chaperone DnaK. Anal Biochem, 2008; 372: 167-176.
[45] Chang L, Miyata Y, Ung PM, Bertelsen EB, McQuade TJ, Carlson HA, Zuiderweg ER, Gestwicki JE. Chemical screens against a reconstituted multiprotein complex: myricetin blocks DnaJ regulation of DnaK through an allosteric mechanism. Chem Biol, 2011; 18: 210-21.
[46] Packschies L, Theyssen H, Buchberger A, Bukau B, Goody RS, Reinstein J. GrpE accelerates nucleotide exchange of the molecular chaperone DnaK with an associative displacement mechanism. Biochemistry, 1997; 36: 3417-22.
[47] Assimon VA, Gillies AT, Rauch JN, Gestwicki JE. Hsp70 protein complexes as drug targets. Curr Pharm Des, 2013; 19: 404-17.
[48] Hageman J, van Waarde MA, Zylicz A, Walerych D, Kampinga HH. The diverse members of the mammalian HSP70 machine show distinct chaperone-like activities. Biochem J, 2011; 435: 127-42.
[49] Rauch JN, Gestwicki JE. Binding of human nucleotide exchange factors to heat shock protein 70 (Hsp70) generates functionally distinct complexes in vitro. J Biol Chem, 2014; 289: 1402-14.
[50] Tzankov S, Wong MJ, Shi K, Nassif C, Young JC. Functional divergence between co-chaperones of Hsc70. J Biol Chem, 2008; 283: 27100-9.
[51] Gao X, Carroni M, Nussbaum-Krammer C, Mogk A, Nillegoda NB, Szlachcic A, Guilbride DL, Saibil HR, Mayer MP, Bukau B. Human Hsp70 Disaggregase Reverses Parkinson's-Linked alpha-Synuclein Amyloid Fibrils. Mol Cell, 2015; 59: 781-93.
[52] Sharma SK, De Los Rios P, Goloubinoff P. Probing the different chaperone activities of the bacterial HSP70-HSP40 system using a thermolabile luciferase substrate. Proteins, 2011; 79: 1991-8.
[53] Ricci L, Williams KP. Development of fluorescence polarization assays for the molecular chaperone Hsp70 family members: Hsp72 and DnaK. Current chemical genomics, 2008; 2: 90-5.
[54] Elliott E, Tsvetkov P, Ginzburg I. BAG-1 associates with Hsc70.Tau complex and regulates the proteasomal degradation of Tau protein. J Biol Chem, 2007; 282: 37276-84.
[55] Luders J, Demand J, Hohfeld J. The ubiquitin-related BAG-1 provides a link between the molecular chaperones Hsc70/Hsp70 and the proteasome. J Biol Chem, 2000; 275: 4613-7.
[56] Liu Y, Gierasch LM, Bahar I. Role of Hsp70 ATPase Domain Intrinsic Dynamics and Sequence Evolution in Enabling its Functional Interactions with NEFs. PLoS Comput Biol, 2010; 6.
[57] Xu Z, Page RC, Gomes MM, Kohli E, Nix JC, Herr AB, Patterson C, Misra S. Structural basis of nucleotide exchange and client binding by the Hsp70 cochaperone Bag2. Nat Struct Mol Biol, 2008; 15: 1309-17.
[58] Sondermann H, Scheufler C, Schneider C, Hohfeld J, Hartl FU, Moarefi I. Structure of a Bag/Hsc70 complex: convergent functional evolution of Hsp70 nucleotide exchange factors. Science, 2001; 291: 1553-7.

[59] Briknarova K, Takayama S, Brive L, Havert ML, Knee DA, Velasco J, Homma S, Cabezas E, Stuart J, Hoyt DW, Satterthwait AC, Llinas M, Reed JC, Ely KR. Structural analysis of BAG1 cochaperone and its interactions with Hsc70 heat shock protein. Nat Struct Biol, 2001; 8: 349-52.
[60] Fewell SW, Smith CM, Lyon MA, Dumitrescu TP, Wipf P, Day BW, Brodsky JL. Small molecule modulators of endogenous and co-chaperone-stimulated Hsp70 ATPase activity. J Biol Chem, 2004; 279: 51131-40.
[61] Wang AM, Miyata Y, Klinedinst S, Peng HM, Chua JP, Komiyama T, Li X, Morishima Y, Merry DE, Pratt WB, Osawa Y, Collins CA, Gestwicki JE, Lieberman AP. Activation of Hsp70 reduces neurotoxicity by promoting polyglutamine protein degradation. Nature chemical biology, 2013; 9: 112-8.
[62] Martin L, Latypova X, Terro F. Post-translational modifications of tau protein: implications for Alzheimer's disease. Neurochem Int, 2011; 58: 458-71.
[63] Cohen TJ, Guo JL, Hurtado DE, Kwong LK, Mills IP, Trojanowski JQ, Lee VM. The acetylation of tau inhibits its function and promotes pathological tau aggregation. Nat Commun, 2011; 2: 252.
[64] Sarkar M, Kuret J, Lee G. Two motifs within the tau microtubule-binding domain mediate its association with the hsc70 molecular chaperone. J Neurosci Res, 2008; 86: 2763-73.
[65] Powers ET, Morimoto RI, Dillin A, Kelly JW, Balch WE. Biological and chemical approaches to diseases of proteostasis deficiency. Annu Rev Biochem, 2009; 78: 959-91.
[66] Mayer MP, Bukau B. Hsp70 chaperones: cellular functions and molecular mechanism. Cell Mol Life Sci, 2005; 62: 670-84.
[67] Hohfeld J, Cyr DM, Patterson C. From the cradle to the grave: molecular chaperones that may choose between folding and degradation. EMBO Rep, 2001; 2: 885-90.
[68] Miyata Y, Koren J, Kiray J, Dickey CA, Gestwicki JE. Molecular chaperones and regulation of tau quality control: strategies for drug discovery in tauopathies. Future Med Chem, 2011; 3: 1523-37.
[69] Powers MV, Clarke PA, Workman P. Death by chaperone: HSP90, HSP70 or both? Cell Cycle, 2009; 8: 518-26.
[70] Pratt WB, Gestwicki JE, Osawa Y, Lieberman AP. Targeting hsp90/hsp70-based protein quality control for treatment of adult onset neurodegenerative diseases. Annu Rev Pharmacol Toxicol, 2015; 55: 353-71.
[71] Evans CG, Chang L, Gestwicki JE. Heat shock protein 70 (hsp70) as an emerging drug target. J Med Chem, 2010; 53: 4585-602.
[72] Rudiger S, Buchberger A, Bukau B. Interaction of Hsp70 chaperones with substrates. Nature structural biology, 1997; 4: 342-9.

[73] Kern A, Ackermann B, Clement AM, Duerk H, Behl C. HSF1-controlled and age-associated chaperone capacity in neurons and muscle cells of C. elegans. PLoS One, 2010; 5: e8568.
[74] Labbadia J, Morimoto RI. The biology of proteostasis in aging and disease. Annu Rev Biochem, 2015; 84: 435-64.
[75] Mandelkow EM, Mandelkow E. Biochemistry and cell biology of tau protein in neurofibrillary degeneration. Cold Spring Harbor perspectives in medicine, 2012; 2: a006247.
[76] Morris M, Maeda S, Vossel K, Mucke L. The many faces of tau. Neuron, 2011; 70: 410-26.
[77] Arndt V, Daniel C, Nastainczyk W, Alberti S, Hohfeld J. BAG-2 acts as an inhibitor of the chaperone-associated ubiquitin ligase CHIP. Mol Biol Cell, 2005; 16: 5891-900.
[78] Alberti S, Bohse K, Arndt V, Schmitz A, Hohfeld J. The cochaperone HspBP1 inhibits the CHIP ubiquitin ligase and stimulates the maturation of the cystic fibrosis transmembrane conductance regulator. Mol Biol Cell, 2004; 15: 4003-10.
[79] Kalia LV, Kalia SK, Chau H, Lozano AM, Hyman BT, McLean PJ. Ubiquitinylation of alpha-synuclein by carboxyl terminus Hsp70-interacting protein (CHIP) is regulated by Bcl-2-associated athanogene 5 (BAG5). PLoS One, 2011; 6: e14695.
[80] Ying Z, Haiyan G, Haidong G. BAG5 regulates PTEN stability in MCF-7 cell line. BMB Rep, 2013; 46: 490-4.
[81] Demand J, Alberti S, Patterson C, Hohfeld J. Cooperation of a ubiquitin domain protein and an E3 ubiquitin ligase during chaperone/proteasome coupling. Curr Biol, 2001; 11: 1569-77.
[82] Carrettiero DC, Hernandez I, Neveu P, Papagiannakopoulos T, Kosik KS. The cochaperone BAG2 sweeps paired helical filament- insoluble tau from the microtubule. J Neurosci, 2009; 29: 2151-61.
[83] Howarth JL, Glover CP, Uney JB. HSP70 interacting protein prevents the accumulation of inclusions in polyglutamine disease. J Neurochem, 2009; 108: 945-951.
[84] Roodveldt C, Bertoncini CW, Andersson A, van der Goot AT, Hsu ST, Fernandez-Montesinos R, de Jong J, van Ham TJ, Nollen EA, Pozo D, Christodoulou J, Dobson CM. Chaperone proteostasis in Parkinson's disease: stabilization of the Hsp70/alpha-synuclein complex by Hip. Embo j, 2009; 28: 3758-70.
[85] Chang L, Thompson AD, Ung P, Carlson HA, Gestwicki JE. Mutagenesis reveals the complex relationships between ATPase rate and the chaperone activities of Escherichia coli heat shock protein 70 (Hsp70/DnaK). The Journal of biological chemistry, 2010; 285: 21282-91.
[86] Rauch JN, Nie J, Buchholz TJ, Gestwicki JE, Kennedy RT. Development of a capillary electrophoresis platform for identifying inhibitors of protein-protein interactions. Anal Chem, 2013; 85: 9824-31.

Chapter 3

Functional Genomics Guides Hsp70 Target Validation in a Phenotype Driven Medicinal Chemistry Campaign

3.1 Introduction

In Chapter 2, I described the use of rhodacyanine analogs, such as JG-48, as inhibitors of the molecular chaperone Hsp70. In addition to its roles in tau homeostasis, Hsp70 is also predicted to be a promising target in cancer because of its high expression in transformed cells and its key roles in anti-apoptotic signaling. Therefore, there was interest in developing JG-48 and its analogs as possible anti-cancer agents. Accordingly, hit-to-lead studies on JG-48 produced ~450 analogs and led to improvements in both potency (EC_{50} ~ 30 nM) and safety (therapeutic index ~100) in cell-based viability assays. Like most successful hit-to-lead studies, we noticed “jumps” in safety and efficacy as the campaign progressed, ultimately improving activity by approximately two orders of magnitude. In phenotypic assays, these improvements are often ascribed to better on-target binding, reduced off-target binding, better membrane permeability or some combination of these factors. However, the “black box” nature of phenotypic assays often prevents deeper insight into the mechanistic origins of the improvements, precluding the purposeful exploitation of the driving

feature. We envisioned that this model system and our experience in Hsp70 biology (see Chapter 1 and 2) might provide an opportunity to reveal the mechanistic reasons of improved activity throughout the medicinal chemistry campaign in “real time”. Specifically, we reasoned that full-genome CRISPR knockdown technology (termed CRISPRi) might be deployed to profile the on- and off-target activity of benchmark molecules through the chemical series, with a special focus on molecules near the activity “leaps”. Using this approach, we confirmed that the rhodacyanines require Hsp70 for their activity in cells, but, unexpectedly, we found that greater selectivity was associated with a switch from inhibition of mitochondrial and cytoplasmic Hsp70 to preferential inhibition of endoplasmic reticulum Hsp70. Using microscopy and genetics, we confirmed that compounds partitioned into distinct sub-cellular compartments and that this localization was important for their relative safety in normal fibroblasts. These findings provide unprecedented insight into the mechanistic reasons for improved activity during phenotype-driven medicinal chemistry campaigns. In addition, they illustrate that specific Hsp70 paralogs are better targets than others for cancer.

3.2 Current methods for target validation

Treating disease requires the careful selection of relevant protein targets that can be modulated to produce a desired phenotype. Often, the suitability of the target is first confirmed using genetics, such as knockdowns or the results of genome-wide association studies (GWAS). Then, the initial inhibitor scaffold is uncovered through a screening approach and iteratively improved through a medicinal

chemistry campaign to advance affinity, selectivity, pharmacokinetics and other parameters. At the conclusion of the campaign, confirmation of target engagement in cells and animals and phenotype evaluation in a given disease model are performed to help guide the selection of candidates for further clinical and pre-clinical development. The initial goal of a clinical trial, especially for novel targets, is often to confirm (or deny) that engaging the target is indeed safe and effective.

While drug discovery can bottleneck at the pharmacokinetic and pharmacodynamics stage [1], rigorous assessment of target engagement remains a major challenge to overcoming costly failures of potential drugs in Phase I and Phase II clinical trials [2-5]. Retrospective analyses of failed trials performed by major pharmaceutical companies suggest that target engagement is sometimes not satisfyingly confirmed, raising questions as to whether the initial hypothesis of the target's possible role in disease was addressed.

How does one know that a phenotypic change occurs through the action of a small molecule on a specific protein target? One approach is to use computational protein modeling to predict compound binding sites and interactions; however, this practice works best when a target is known and a protein structure is available. Furthermore, this approach, along with biochemical characterization of rationally designed compounds binding to known targets, does not account for off-target or non-specific binding to proteins which can lead

to complications early in clinical development. Another method is chemoproteomics, in which immobilized small molecules are used to identify binding partners. Eluted proteins can be separated and analyzed by mass spectroscopy to identify or confirm binding of compounds to a protein targets, a method which was recently applied to find chemical probes for the chaperones Hsp70 [6] and Hsp90 [7]. Another form of chemoproteomics, competitive activity based protein profiling (ABPP), utilizes affinity probes based on natural protein ligands. Competitive ABPP can be used to characterize compounds by revealing proteins that are blocked from binding the probes in the presence of test compounds [8]. Chemoproteomics is valuable in its ability to evaluate compound selectivity in that small molecules with multiple binding partners can be easily distinguished. Nevertheless, this approach is currently limited to application with protein classes such as kinases, cysteine proteases and ATP binding proteins which have ligands that are easily modifiable into affinity probes [2, 8]. A variant of this approach is theranostics, in which the molecule is appended to an imaging agent suitable for PET, such that target engagement and retention can be directly correlated with outcomes [9].

Because of the time and cost involved in probe development, these approaches rarely allow careful analysis of target engagement throughout the medicinal chemistry campaign. Rather, these methods are often deployed at the conclusion of the process, only on the “best” molecules. We wondered if emerging methods in whole-genome CRISPR screens might be used to over-come this limitation

and provide detailed insight into target validation at each incremental step in a medicinal chemistry campaign, with the goal of providing “real time” guidance into on- and off-target binding.

3.3 CRISPR genetic screens as a new tool for target identification

Functional genetic screening modalities like RNA interference (RNAi), have been applied to cancer and neurodegenerative disease models in order to identify targets of small molecules [10, 11] or identify genes with the potential to become drug targets. Recently, clustered regularly interspaced short palindromic repeats (CRISPR) has emerged as a complementary method, with superior selectivity and the ability to be adopted for either gene deletion, modification or amplification. The CRISPR interference (CRISPRi) technology utilizes an adapted Cas9 nuclease system with a designed short hairpin guide RNA (sgRNA) that both activates Cas9 and recognizes a specific DNA sequence leading to gene silencing through inhibition of translation [12]. With a designed library of sgRNAs to target specific genes, CRISPRi can be used for profiling genome wide repression of protein expression [13]. When applied to drug discovery, benefits of CRISPRi include a comprehensive exploration of small molecule mechanism through definition of on-target and off-target pathway activation. Functional genomic screens also provide insights into mechanisms of compound trafficking, such as which ABC transporters might be used to gain entry. CRISPRi screens can even be performed in parallel with CRISPR activation (CRISPRa), in which the dCas9 is appended to transcriptional

activation proteins, such that the sgRNA drives over-expression of the target protein. For some targets, especially those with some redundancy or multiple paralogs, CRISPRa might be expected to provide highly complementary information about which target is most important for the phenotype.

Here we report that genome wide CRISPRi/a screens can be used to confirm the molecular chaperone Hsp70 as the target of the rhodacyanine compound series described in Chapter 2. Additionally, comprehensive sgRNA library coverage of Hsp70 paralogs revealed un-expected, preferential to organelle-specific Hsp70s that is tightly linked to the relative safety of the molecules. Fluorescence microscopy confirmed the proposed compound localization in the mitochondria, cytoplasm and ER. Using this knowledge, we used the compounds as chemical probes to reveal which distinct Hsp70 paralogs are superior targets for cancer, and tauopathy.

3.4 Results

3.4.1 Improvement of Hsp70 inhibitors through a structure-guided medicinal chemistry campaign.

As discussed in Chapters 1 and 2, rhodacyanines, such as MKT-077, JG-48 and JG-98, bind to Hsp70 in a highly conserved allosteric pocket [14, 15]. HSPA8/Hsc70 is the constitutively expressed form of Hsp70 and is primarily located in the cytosol along with HSPA1A/Hsp72, which is highly expressed during cell stress. HSPA5 is the gene encoding binding immunoglobulin protein

(BiP), the endoplasmic reticulum (ER) localized form of Hsp70. Another major form is HSPA9 or mortalin which regulates protein homeostasis in the mitochondria. Sequence alignment shows that while these proteins have different localization in cells, the hydrophobic cleft where MKT-077 analogs bind has little variability (Appendix 3.1A).

Other members of the Gestwicki group have been interested in developing MKT-077 and its analogs as potential treatments for cancer. Based on the binding site of MKT-077 and JG-98 in Hsc70, Dr. Xiaokai Li synthesized a library of ~450 analogs and, in collaboration with Dr. Hao Shao, tested each of them for anti-proliferative activity in two breast cancer cell lines, MDA-MB-231 and MCF7, as well as two lines of normal fibroblasts, MEFs and IMR90s. Using MTT assays performed in quadruplicate, they calculated a growth inhibition value (GI50) and then calculated a relative therapeutic index (TI) by comparing the activity against the transformed and normal cells. In addition, each compound was tested for solubility by HPLC, projected membrane permeability in PAMPA assays and for metabolic stability in mouse liver microsome experiments. Compounds were synthesized and tested in groups of approximately 20 to 30 molecules and the holistic results of the assays were examined to help guide the next round of synthesis, with the goal of optimizing safety, solubility, potency and stability. Binding of a subset of the molecules to Hsc70 was tested *in vitro*, using biotinylated compounds in an ELISA format [16]. In addition, the binding site of a subset of molecules, including JG-98 and JG-48, were confirmed using HSQC

NMR [16]. Finally, a subset of molecules was tested for anti-tumor activity in xenograft models. After calculation of pharmacokinetic and pharmacodynamic parameters, Dr. Hao Shao developed a dosing scheme and found that JG-98 and JG-231 were active in preventing tumor growth in mice (unpublished) [16, 17]. Together, these results tentatively confirmed that Hsp70 is a potential drug target for breast cancer. Similar studies with other collaborators have shown that Hsp70 is also a good target for castration-resistant prostate cancer and multiple myeloma (data not shown), suggesting that this target might play relatively broad roles. Two former graduate students in the Gestwicki laboratory. Drs. Sharan Srinivasan and Laura Cesa, led studies to suggest that Hsp70 stabilizes anti-apoptotic proteins, including IAP1/2 (data not shown). I contributed to many of these efforts, through the synthesis of a subset of analogs and the testing of others in assays described in Chapter 2. However, my primary interest was to leverage the ongoing medicinal chemistry campaign to understand target engagement and target selectivity. In turn, my goal was to use this knowledge to more deeply probe the roles of Hsp70 in tau homeostasis, as discussed in Chapter 1. More specifically, the relatively rapid pace of the anti-cancer projects provided a convenient platform for using CRISPRi/a, as described above. Importantly, the challenges facing this project were similar to many oncology drug discovery projects, in that the assays are primarily phenotypic (*e.g.* cell viability) so it isn't always clear why improvements in potency or safety arise.

When we plotted compound number versus the anti-cancer GI_{50} values, the improvement in potency is clear (Figure 3.1A). Similarly, the relative safety of the molecules also improved, from about TI ~ 3 to TI >30 (Fig 3.1A; Appendix 3.7). Benchmark molecules through the campaign were then selected for closer inspection, including molecules from the early part of the series (i.e. MKT-077 and JG-98; Figure 3.1B) and those points throughout the campaign (i.e. JG-194, JG-231, JG-294 and JG-345; Figure 3.1B). These particular compounds were selected because they represented points in the campaign associated with marked improvements in either potency or safety. We wondered if these transitions might be ascribed to specific changes in target engagement.

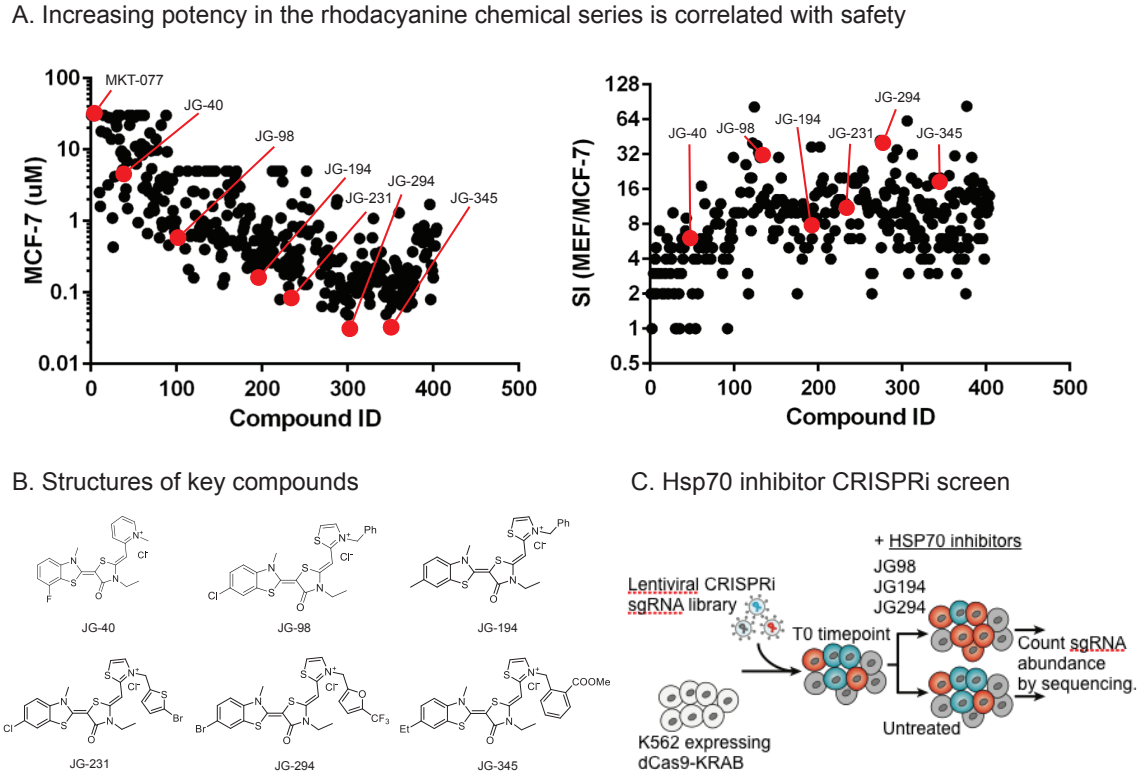

Figure 3.1 Summary of the rhodacyanine chemical series. (A) Chronological compound number versus MCF-7 EC_{50} shows a strong increase in potency throughout the chemical series. (B) Diversity in the modifications to the rhodacyanine scaffold drive potency. (C) CRISPRi screens identify rhodacyanines which show preferential binding to Hsp70 paralogs

Using the benchmark compounds, we conducted comprehensive CRISPRi screening in collaboration with Luke Gilbert and Jonathan Weissman (UCSF). For these experiments, K562 cells with a stable and inducible dCas9 expression system are infected by lentiviral methods with a well-designed sgRNA library for broad gene silencing. Infected cells are treated with compounds JG-98, JG-194 and JG294 and passaged for about 10 doublings. Treated cells are harvested and subjected to deep sequencing for sgRNA quantification (Figure 3.1C). Statistical comparison of sgRNA guide abundance in treated and untreated populations identifies genes that are significantly enriched or depleted by compound treatment. We expect guides for genes that are sensitive to compound treatment to deplete in the treated population when compared to untreated control cells. Guides for genes that confer resistance will enrich in the treated population when compared to control cells. We use rho (ρ) to represent compound phenotypes based on fold change in cell count compared to unselected cells. Plotting significant changes in frequency of sgRNA against rho reveals genes that are sensitive to compound (negative ρ) and resistant to compound (positive ρ) (Appendix 3.2, 3.3 and 3.4).

Thanks to the use of a well-designed CRISPRi guide library with excellent coverage of the Hsp70 family of genes, we find varying degrees of preference for Hsp70 paralogs among the compounds. All three compounds show sensitivity to the Hsp70 paralogs HSPA9 (mitochondria) and HSPA5 (ER); however, both JG-98 and JG-194 are most sensitive to HSPA9 while JG-294 shows a preference

for HSPA5 (Appendix 3.2, 3.3 and 3.4). Compounds JG-98 and JG-194 have very similar CRISPRi profiles in cells; however, comparison of JG-194 to JG-294 highlights the differences in sensitive genes (Figure 3.2A, Appendix 3.7). In line with these results, GO term enrichment analysis of JG-194 hits reveals disruption of mitochondrial protein networks while JG-294 appears to mostly affect protein synthesis gene sets (Figure 3.2B). These findings point to potentially significant differences in compound mechanisms in cells, which might explain variabilities in potency and safety index. This is an important result because it shows, for the first time, that improvements in a medicinal chemistry campaign can arise from changes in on- and off-target binding. We are currently validating addition genes from the CRISPR screens, especially those that are not Hsp70 paralogs. One interest set is the ABC transporters because preliminary evidence suggests that the rhodacyanines might use these proteins to enter cells. Other possible off-target proteins are included in Tables 3.2 and 3.3. We are also completing CRISPRa screens on each benchmark molecule. Recent results on JG-294 seem to confirm the suspected role of BiP (data not shown). Unlike ABPP, this approach cannot be used to discern if a target is directly bound, only that altering its levels impacts the phenotype. Thus, some of the genes identified by CRISPR may be indirectly involved. Biochemical binding studies will be needed to explore this issue. Regardless, we were excited to see that Hsp70s (the desired target) were predominant in the datasets. The CRISPR screens take approximately 1 month to complete and four molecules can be routinely tested at one time, so the speed of whole-genome interrogation is favorable.

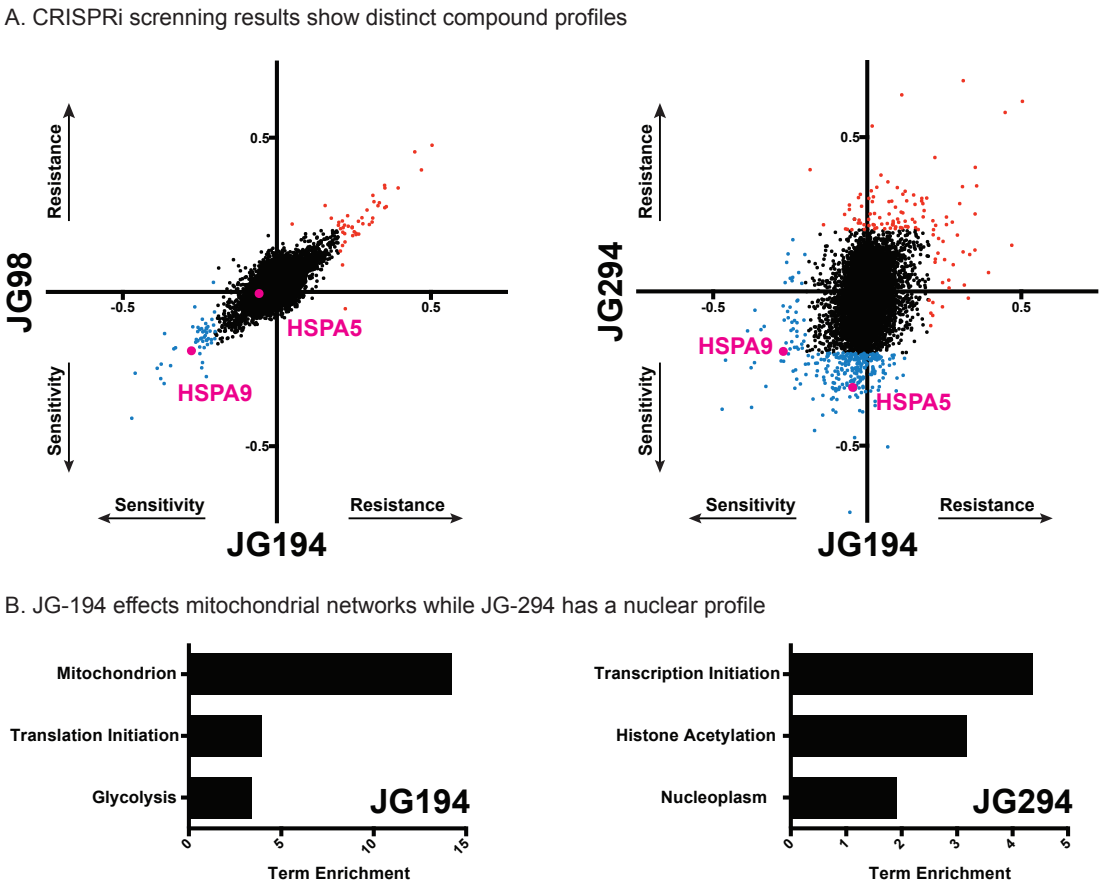

Figure 3.2 Summary of CRISPRi screening data. (A) JG-98 and JG-194 have highly similar sensitive and resistant genes in cells suggesting these compounds have overlapping mechanisms. In contrast, JG-294 has only a moderately similar CRISPRi profile to JG-98 and JG194, which underscores the differences in efficacy and safety for these compounds. (B) Identification of GO terms for compounds JG-194 and JG-294 reveals a significant number of mitochondrial targets for JG-194 and several early protein synthesis targets for JG-294.

3.4.2 Rhodacyanines partition distinctly in cells by fluorescence microscopy

The CRISPR screens suggested that there was a “switch” from cytoplasmic/mitochondrial Hsp70s to ER Hsp70 during the course of the medicinal chemistry campaign. Specifically, JG-98 and JG-194 seemed to require mortalin for activity, while JG-294 and JG-345 required BiP. In order to test this theory, we first needed to confirm that compounds do in fact localize differently in cells by microscopy. We utilized the intrinsic fluorescence of the

rhodacyanine scaffold along with HeLa cells stably expressing fluorescent organelle markers to observe and quantify compound localization in live cells. Because of the broad excitation and emission spectrum of the compounds (Appendix 3.8), we used a far red monomeric infrared fluorescent protein (mIFP) to label the mitochondria and ER while preventing signal overlap with compounds [18]. After treatment with 1μM compound for 30 minutes, live cells were washed and imaged. Using a Manders calculation [19, 20], colocalization was quantified for each compound in both ER and mitochondrial labeled cells. Specifically, I found that both JG-98 and JG-194 show just over %70 signal colocalization with the mitochondria while the fraction of signal colocalization with the ER (~50%) is similar to that which is seen with a commercially available mitochondrial probe (Mito Tracker® Green) (Figure 3.4). These results confirm the HSPA9 sensitivity observed for JG-98 and JG-194 in the CRISPR screen. Interestingly, JG-231, a close analog of JG-294, shows the most ER localization in cells with 80% signal overlap. Preliminary results from a collaboration with Jeffrey Brodsky's lab show that JG-231 induces mRNA levels and expression of HSPA5 and proteins involved in the regulation of the unfolded protein response (UPR) including CHOP (data not shown). We expect future CRISPRi/a screening of JG-231 to reveal important protein targets related to its subcellular localization.

Although the CRISPRi results comparing JG-98 to JG-294 indicate a difference in cellular targets and mechanism, JG-294 has a cellular distribution profile similar to that off JG-98. It is possible that a longer incubation is required to

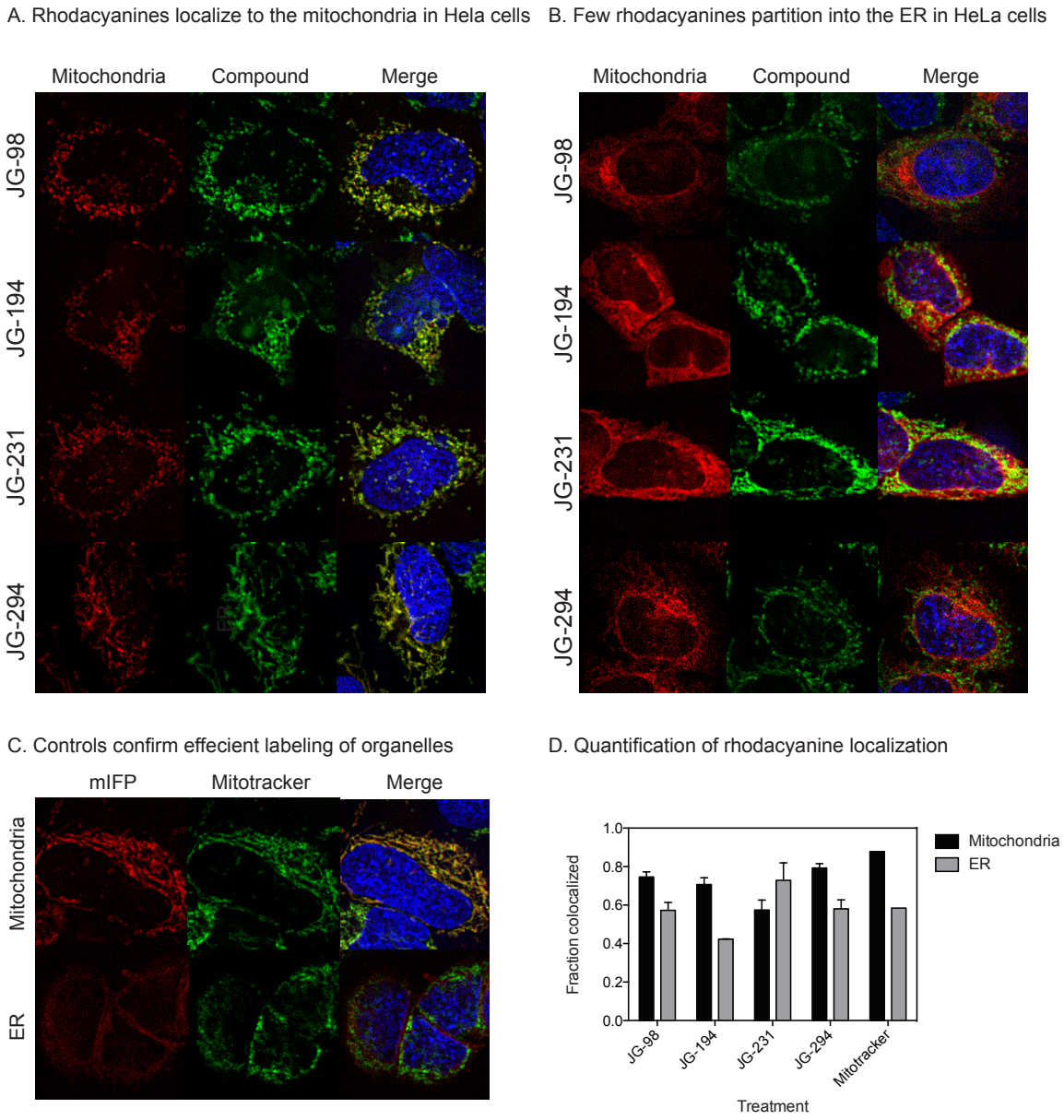

Figure 3.3 Measurement of compound localization in HeLa cells by fluorescence microscopy. (A) Rhodacyanines localize with mitochondria in cells. Images are representative of experiments performed in duplicate. (B) Only JG-231 localizes with the ER in cells. Images are representative of experiments performed in duplicate. (C) Control experiments show that the mitochondrial probe MitoTracker® colocalizes with mIFP labeled mitochondria but not ER. (D) Quantification of compound localization using Mander's coefficients. Results are averages of at least two independent calculations and error bars represent SEM.

observe distinct localization of JG-294 in cells; however, for these initial experiments, we monitored fluorescence after a 30-minute incubation in order to distinguish results from confounding factors such as cell death and potential degradation of signal. Now that we have validated fluorescence microscopy as a

platform for probing compound localization in cells, future experiments will utilize Z-stacks for 3D reconstruction of cellular organelles and robust colocalization quantification.

3.4.3 Paralog specific rhodacyanines reduce tau levels with varying efficiency

As discussed in chapters 1 and 2, Hsp70 is a strong target for normalizing tau homeostasis in instances of tau mislocalization or accumulation. While the effects of modulating Hsc70 and Hsp72 on tau stability are well-characterized, the roles of Hsp70 paralogs like BiP and mortalin have only been somewhat explored. The accumulation of tau in transgenic mice induces the unfolded protein response (UPR) in the ER in response to impairment of normal endoplasmic reticulum associated degradation (ERAD) [21]. A similar result was observed in HEK cells with inducible tau expression. In these cells, upregulation of tau simultaneously induced UPR as measured by increases in levels of BiP, ubiquitin and a pathway associated kinase [21]. Furthermore, activation of the UPR increases tau phosphorylation prior to tau aggregation signifying therapeutic potential in modulating ER degradation and stress pathways as a means of preventing tau pathogenesis [22, 23].

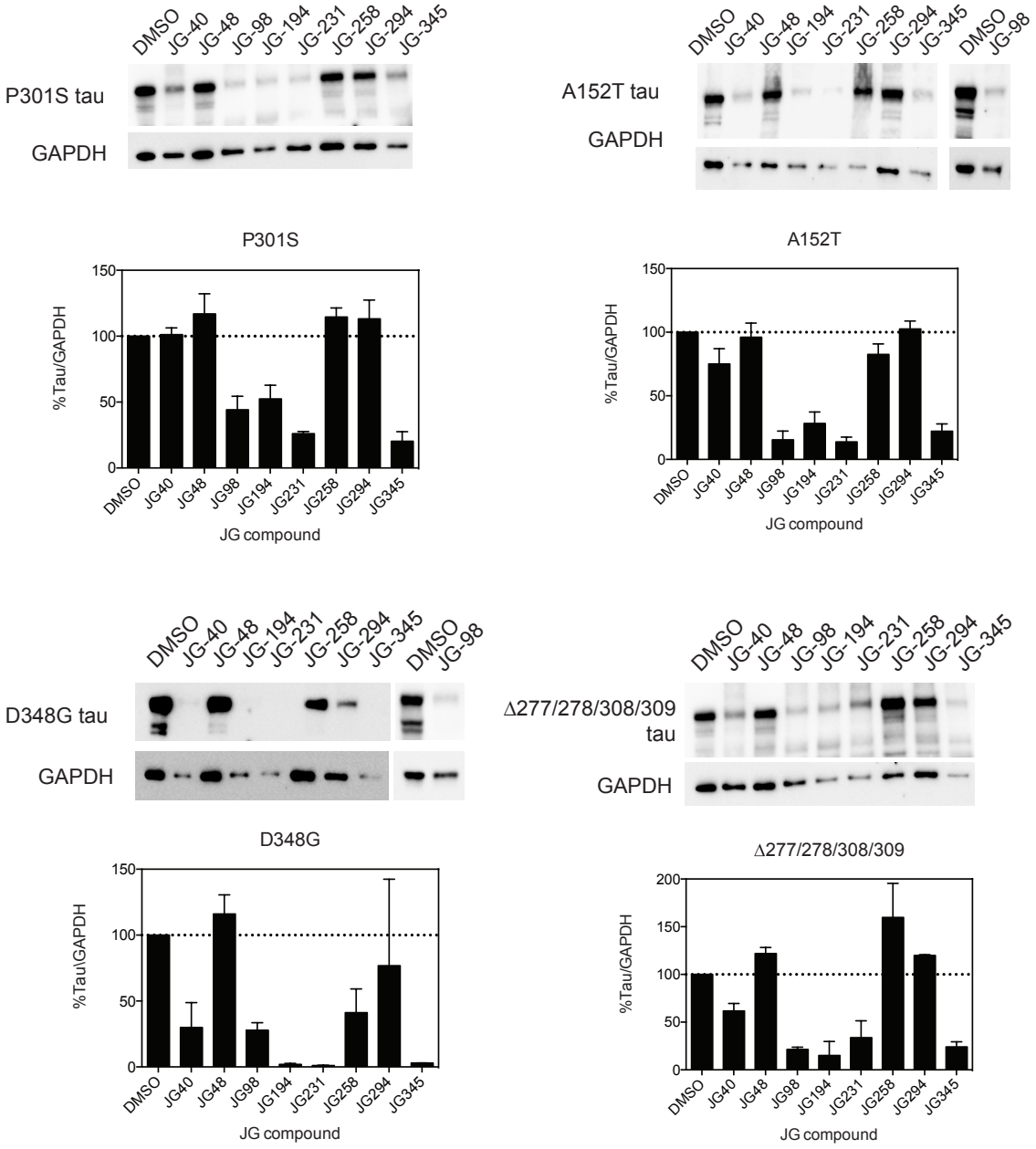

Figure 3.4 Rhodacyanines increase degradation of tau variants in HEK cells. Cells were treated with 5μM compound with the exception of JG-40 and JG-48 which were used at 10μM. Compounds were tested in duplicate and representative western blots are shown. Error bars represent the SEM.

Given precedence for the role of the ER and BiP in tau quality control, we probed the ability of rhodacyanines to modulate tau levels in cells. HEK cells stably

expressing doxycycline (DOX) inducible tau variants were treated with compounds to measure degradation of disease-related tau mutants P301S, A152T and D348G. Each of these mutations cause aberrations in tau homeostasis which induce tau accumulation or aggregation and eventual cell death [24-28]. We also treated HEK cells expressing a tau variant with deletions of residues important for microtubule binding referred to as Δ277/278/308/309 tau. Immunostaining of cell lysates shows that active compounds totally reduce tau levels after 24 hours for all of the tau variants tested (Figure 3.4). The strongest phenotype is observed with compounds JG-98, JG-194, JG-231 and JG-345, while the negative control JG-258 has no effect. Interestingly, all of these active compounds show preference for mitochondrial or ER Hsp70 paralogs over the cytosolic versions which points to chaperone networks in these two organelles playing a significant role in tau degradation. Overexpression of BiP in the tau inducible cells leads to a dramatic reduction in tau levels, further pointing to BiP as an underexplored yet promising target for regulating tau homeostasis (Figure 3.5).

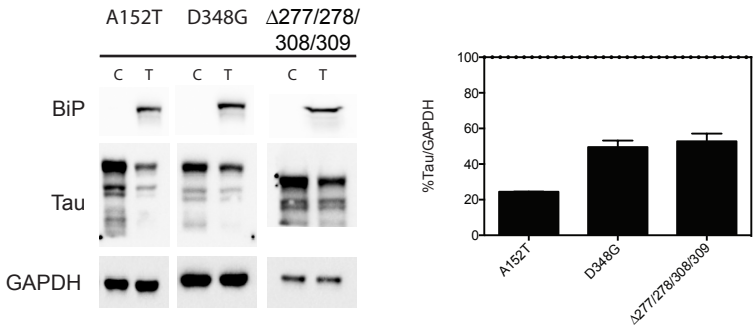

Figure 3.5 BiP overexpression reduces levels of tau variants in HEK293 cells. Experiment was performed in duplicate and a representative blot is shown. C=control T=transfected. Error bars represent SEM.

As discussed in Chapter 2, we used Hsp70 mutants to illustrate that Hsp70 affinity for substrates like tau is roughly correlated with client degradation in cells. Future work will utilize Hsp70 mutants to elucidate the role and function of Hsp70 paralogs in models for diseases like tauopathy. Using docking models and previously reported protein NMR results [14, 16], Victoria Assimon, a former student in the lab, and I have designed and characterized Hsc70 point mutants with modified resides within the rhodacyanine binding site (Appendix 3.9A). Through analysis of co-chaperone mediated ATPase activity and luciferase refolding activity, I found that some mutants exhibit WT-like activity while others are either hyperactive or hypoactive (Appendix 3.9B and 3.9C). We expect the variability in enzymatic behavior of the Hsp70 mutants to manifest *in vivo* as mutants that stabilize substrate binding are likely to present phenotypes very different from mutants that destabilize Hsp70-tau complexes. Therefore, application of these point mutants to Hsp70 paralogs like BiP and mortalin are likely to result in varying phenotypes that will aid in understanding the role of subcellular Hsp70 networks in the initiation and transmission of pathology.

3.5 Discussion

CRISPR screening strategies have emerged for the identification of drug targets, resistance mechanisms and functional genomics. Here, we applied this technology to better understand how medicinal chemistry campaigns evolve during a phenotype-driven optimization. In the past, such optimization steps might have been “black box” efforts in which potency is improved without insight

into on- or off-target interactions. As discussed above, our novel implementation of CRISPRi technology revealed distinct compound targets and we envision that this approach might represent a way to explain efficacy and/or safety “jumps” in a medicinal chemistry series. For example, we found that rhodacyanines exhibit preferential binding to individual Hsp70 paralogs (or sets of paralogs) and that less toxic/more effective molecules tended to bind BIP. JG-294 may be a particularly good lead candidate for developing BIP/HSPA5 selective inhibitors and future work in the Gestwicki laboratory will exploit these observations to further improve selectivity. In addition, we plan to complete additional CRISPRi screens to further aid in the design of more potent, selective and safe compounds. This effort will need to include a CRISPR-based method for simultaneously removing both cytoplasmic paralogs (Hsc70 and Hsp72) because these forms seem to be partly redundant. Because of the central role of Hsp70 in protein homeostasis, these CRISPR tools, as well as paralog specific Hsp70-binding compounds will be particularly helpful in understanding which forms can be safely targeted for an individual disease.

In addition to revealing Hsp70 paralog selectivity, the CRISPR screens also revealed other interesting mechanisms related to these compounds. For example, some of the genes that displayed strong resistance phenotypes following JG-294 treatment were members of the ER membrane protein complex (EMC) (Appendix 3.6 and 3.7). Because the role of the EMC is not well understood [29, 30], there is great opportunity to use JG-294 as a chemical

biology tool to understand functions of this protein complex and its implication in disease. Another important observation was that ABC transporters appeared to be broadly required for compound efficacy. For example, ABCC1 is a member of the multi drug resistant protein family, which is responsible for transporting biomolecules across cellular membranes. Knockdown limited compound activity, suggesting that it might serve a role in drug uptake. Additionally, we found that ATP1A1 and ATP1B3, which encode sodium and potassium ATPases, were strong hits in the CRISPRi screens. Because these proteins regulate osmolarity and the compounds contain a cationic pyridinium, these ion channels may also be involved in compound transport into the cell. Knowledge of compound trafficking mechanisms is likely to improve chances for success at the drug development and pre-clinical stages where an understanding drug pharmacokinetics is critical. Among the other genes identified in the CRISPR screens, there are likely off-target interaction partners. Although we have not yet validated any of these off-target partners, this approach may provide new opportunities to further guide safety and selectivity.

Previous work has identified cytosolic Hsc70 networks and the compound JG-40 as regulators of Dengue virulence [31]. However, JG-40 and JG-48 have weak activity in reducing tau levels in inducible tau models, whereas the compounds later in the chemical series, such as JG-294, exhibit strong anti-tau activity (Figure 3.5). These results suggest that certain Hsp70 paralogs are better targets for some diseases (*e.g.* cytosolic Hsp70 for Dengue viral infection and BIP for

tauopathies). Thus, molecules in this series might prove to be powerful chemical probes for understanding which Hsp70 paralogs are linked to individual diseases. We envision that it will be important to supplement these chemical tools with genetic ones, such as the point mutants developed above, because of the potential for off-target binding.

The comprehensive and unbiased nature of CRISPRi screen makes application of this technology invaluable to drug discovery efforts. In this Chapter, I used whole genome CRISPR screen to understand compound selectivity and trafficking. Each screen required approximately 1 month to complete and four compounds can be explored simultaneously in the most recent set-up at UCSF. The throughput of this method permits testing of key molecules throughout a medicinal chemistry campaign – not just the lead candidates. I found that this approach could rather quickly characterize the targets of small molecules and help elucidate their mechanism of action. This method has the potential to remove the single largest barrier to phenotypic screens – which is the target identification step [32]. In addition, this approach can simultaneously identify biomarkers or sets of biomarkers. Our results illustrate that functional genomics offers many benefits, especially when used to in conjunction with phenotypic assays and medicinal chemistry campaigns.

3.6 Methods

3.6.1 Synthesis

JG-98: ^{1}H-NMR (400 MHz, DMSO-d_6): δ 8.26 (d, J = 4.0 Hz, 1H), 8.04 (d, J = 4.0 Hz, 1H), 7.89 (d, J = 4.0 Hz, 1H), 7.65 (d, J = 8.0 Hz, 1H), 7.51 (dd, J = 8.0, 4.0 Hz, 1H), 7.43-7.30 (m, 5H), 6.50 (s, 1H), 5.75 (s, 2H), 4.09-4.01 (m, 5H), 0.94 (t, J = 8.0 Hz, 3H). ESI-MS: calculated for $C_{24}H_{21}ClN_3OS_3^+$ 498.05; found 498.05.

JG-194: ^{1}H-NMR (400 MHz, DMSO-d_6): δ 8.26 (d, J = 4.0 Hz, 1H), 7.89 (d, J = 4.0 Hz, 1H), 7.75 (s, 1H), 7.60 (d, J = 8.0 Hz, 1H), 7.43 (t, J = 8.0 Hz, 2H), 7.39-7.33 (m, 4H), 6.52 (s, 1H), 5.76 (s, 2H), 4.14-4.05 (m, 5H), 2.40 (s, 3H), 0.98 (t, J = 8.0 Hz, 3H). ESI-MS: calculated for $C_{25}H_{24}N_3OS_3^+$ 478.11; found 478.07.

JG-231: ^{1}H-NMR (400 MHz, DMSO-d_6): δ 8.24 (d, J = 4.0 Hz, 1H), 8.07 (d, J = 2.0 Hz, 1H), 7.88 (d, J = 4.0 Hz, 1H), 7.70 (d, J = 12.0 Hz, 1H), 7.55 (dd, J = 8.0, 4.0 Hz, 1H), 7.24 - 7.20 (m, 2H), 6.76 (s, 1H), 5.97 (s, 2H), 4.21 (q, J = 8.0 Hz, 2H), 4.10 (s, 3H), 1.18 (t, J = 8.0 Hz, 3H). ESI-MS: calculated for $C_{22}H_{18}BrClN_3OS_4^+$ 581.92; found 581.89.

JG-258: ^{1}H-NMR (400 MHz, DMSO-d_6): δ 8.22 (d, J = 4.0 Hz, 1H), 7.83 (d, J = 4.0 Hz, 1H), 7.38 (d, J = 8.0 Hz, 2H), 7.35 - 7.29 (m, 3H), 6.43 (s, 1H), 5.71 (s, 2H), 4.00 – 3.85 (m, 4H), 3.45 (s, 3H), 3.22 (t, J = 8.0 Hz, 2H), 0.88 (t, J = 8.0 Hz, 3H). ESI-MS: calculated for $C_{20}H_{22}N_3OS_3^+$ 416.09; found 416.02.

JG-294: ^{1}H-NMR (400 MHz, DMSO-d_6): δ 8.21 (d, J = 2.0 Hz, 1H), 8.20 (d, J = 4.0 Hz, 1H), 7.88 (d, J = 4.0 Hz, 1H), 7.69 (dd, J = 8.0, 2.0 Hz, 1H), 7.64 (d, J = 12.0 Hz, 1H), 7.29 (d, J = 4.0 Hz, 1H), 6.93 (d, J = 4.0 Hz, 1H), 6.79 (s, 1H), 5.95

(s, 2H), 4.21 (q, J = 8.0 Hz, 2H), 4.11 (s, 3H), 1.19 (t, J = 8.0 Hz, 3H). ESI-MS: calculated for $C_{23}H_{18}BrF_3N_3O_2S_3^+$ 599.97; found 599.99.

JG-345: ^{1}H-NMR (400 MHz, DMSO-d_6): δ 8.06-7.99 (m, 2H), 7.87 (d, J = 4.0 Hz, 1H), 7.80 (s, 1H), 7.62 (t, J = 8.0 Hz, 2H), 7.52 (t, J = 8.0 Hz, 1H), 7.40 (t, J = 12.0 Hz, 1H), 6.91 (d, J = 8.0 Hz, 1H), 6.41 (s, 1H), 6.02 (s, 2H), 4.14 (s, 3H), 3.99 (q, J = 4.0 Hz, 2H), 3.90 (s, 3H), 2.70 (q, J = 8.0 Hz, 2H), 1.22 (t, J = 8.0 Hz, 3H), 0.87 (t, J = 8.0 Hz, 3H). ESI-MS: calculated for $C_{28}H_{28}N_3O_3S_3^+$ 550.13; found 550.05.

3.6.2 CRISPRi screening methods and data analysis

Cell culture, DNA transfections, viral production, and construction of CRISPRi/a cell lines. HEK293T cells were maintained in Dulbecco's modified eagle medium (DMEM) in 10 % FBS, 100 units/mL streptomycin and 100 µg/mL penicillin with or without 2mM glutamine. K562 cells were grown in RPMI-1640 with 25mM HEPES and 2.0 g/L NaHCo3 in 10 % FBS, 2 mM glutamine, 100 units/mL streptomycin and 100 µg/mL penicillin. Lentivirus was produced by transfecting HEK293T with standard packaging vectors using *Trans*IT®-LTI Transfection Reagent (Mirus, MIR 2306). Viral supernatant was harvested 72 hours following transfection and filtered through a 0.45 µm PVDF syringe filter.

To construct the CRISPRi K562 cell line, K562 cells were lentivirally transduced to express our previously described dCas9-BFP-KRAB fusion protein from the SFFV promoter. Pure polyclonal populations of CRISPRi K562 cells were sorted by flow cytometry using a BD FACS Aria2 for stable BFP expression.

High throughput pooled CRISPRi/a screening. CRISPRi K562 cell lines were infected with sgRNA libraries as previously described [33]. The infection was scaled to achieve an effective multiplicity of infection of less than one sgRNA per cell. Two days after infection, cells were selected with 0.75-1 μg / mL puromycin (Tocris) for 2 days, and then allowed to recover for 2 or 3 days before starting the screens. For the CRISPRi genome-scale growth and HSP70 inhibitor screens, cells were passaged or treated with two pulses of 400nM and then 520nM JG98, 200nM and then 270nM JG194 or one pulse of 250nM JG294 over 17 days to achieve between 8.5 and 14 population doublings difference between untreated and drug treated treated cell. The untreated, JG98 and JG194 were performed as biological replicate screens while only one JG294 screen was performed. Cells were maintained at a density of between 250,000 and 1,000,000 cells / mL continually maintaining a library coverage of at least 500-1000 cells per sgRNA. Populations of cells expressing this library of sgRNAs were either harvested at the outset of the experiment (the t0 time point), grown under standard conditions (untreated), or treated with HSP70 inhibitors. Genomic DNA was harvested from all samples; the sgRNA-encoding regions were then amplified by PCR and sequenced on an Illumina HiSeq-2500 using custom primers at high coverage with previously described protocols (http://weissmanlab.ucsf.edu/links/links.html). From this data, we quantified the frequencies of cells expressing different sgRNAs in each sample. The data from replicate screens was averaged. From this data we quantified the phenotype of each sgRNA, which have previously

defined for growth (γ) or resistance to treatment (ρ) [34]. A python script for processing our CRISPRi library sequencing data is available at https://github.com/mhorlbeck/ScreenProcessing.

Bioinformatic analysis of hit genes. Hit genes were ranked based on average phenotype of the 3 most extreme sgRNAs targeting them or by a Mann-Whitney test. Pathways and gene sets enriched among hit genes were identified using GSEA and DAVID software.

Individual re-test of sgRNA phenotypes and CRISPRi/a transcript repression and activation. Individual phenotype re-test experiments for sgRNAs from the HSP70 inhibitor screens were performed as competitive growth experiments on partially-transduced populations of CRISPRi K562 cells. Briefly, cells were partially transduced ~25-60%. Three or four days following infection, cells were counted and seeded in 24 well plates at 0.25-0.5 million cells / mL. Triplicate samples for each sgRNA were grown under standard conditions or, were treated with 325nM or 350nM JG294. Each population of cells was allowed to grow or recover for 5 or 6 days. The absolute cell number and percentage of cells that express BFP (indicating sgRNA expression) was measured for each sample at the beginning and end of the experiment. Rho scores were calculated as described previously [13].

3.6.3 Fluorescence Microscopy

Plasmids containing N-terminally labeled mIFP-Calenexin and a mIFP labeled mitochondrial targeting sequence were transfected into HeLa cells using a nucleofection protocol. Polyclonal selection for stable expression was performed with Geneticin. Cells expressing mIFP-Calnexin were sorted by flow cytometry using a BD FACS Aria II. Cells were maintained in Minimum Essential Medium supplemented with penicillin/streptomycin and FBS. For microscopy, cells were plated into 96 well µclear plates (Greiner 655090) and incubated 48hrs with 25µM billiverdin prior to compound treatments. Cells were then treated with 1µM compound at 2% DMSO and Hoescht for 30 min. Cells were washed and imaged in Fluorobrite Dulbecco's Modified Eagle Medium. Images were captured using a Nikon spinning disk confocal microscope with a 40X objective. Image deconvolution and colocalization analysis was performed with IamgeJ.

3.6.4 Cell culture and immunoblotting

Stably expressing tau cells were harvested using the T-Rex™ HEK 293 system. Transfection of tau PCDNA3 tau plasmids was performed using a nucleofection protocol followed by hygromycin selection. Cells were maintained in Dulbecco's Modified Eagle Medium supplemented with penicillin/streptomycin and FBS. Immunostaining for tau levels was performed in either 12 well or 6 well plates in which tau expression was induced with 3ng/mL of DOX along with compound treatment at either 10µM (JG-40 and JG-48) or 5µM (all others) for 24 hours (0.2% DMSO). Cells were lysed with MPer buffer supplemented with protease

inhibitor and 10µg of proteins were separated by gel electrophoresis. Immunoblotting was performed with D8 mouse tau (sc-166060) and rabbit GAPDH (cell signaling, 2118) and mouse (cell signaling, 7076) and rabbit (cell signaling, 7074) HRP-conjugated secondaries. Quantification and image analysis was performed using Biorad Image Lab.

Contributions

Zapporah T. Young performed all fluorescence microscopy imaging and quantification, transfections of Hsp70 paralogs and compound characterization in tauopathy models. Luke Gilbert and Jonathon Weissman performed CRISPRi screening, data analysis and validation. Victoria Assimon and Zapporah Young designed, produced and characterized the Hsp70 mutants. Xiaokai Li and Hao Shao synthesized and characterized compounds referenced in this study. Experiments were designed by Zapporah T. Young and Jason E. Gestwicki.

3.7 Appendix

A. Alignment of the NBD ofHsp70 paralogs shows highly reseved rhodacyanine binding site

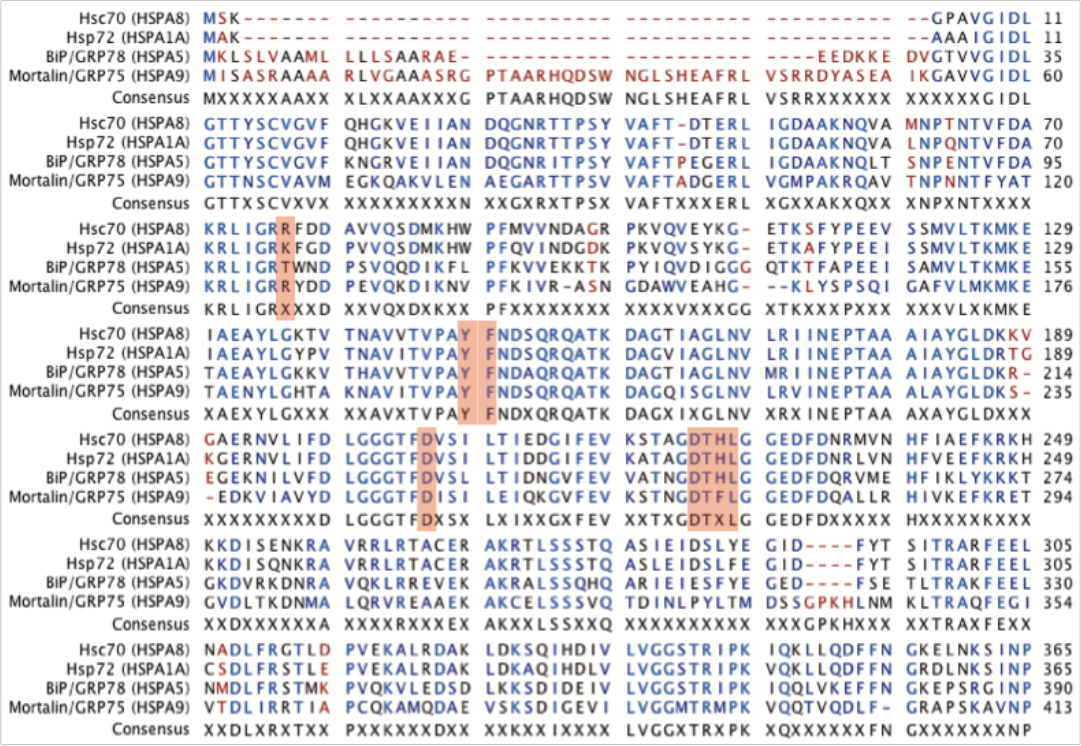

B. Sythesis of rhodacyanine analogs

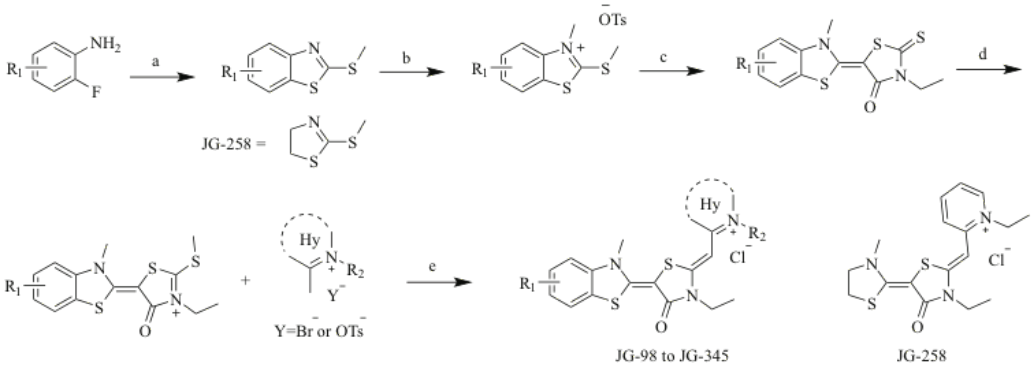

Appendix 3.1 Hsp70 alignment and rhodacyanine synthesis. A. Alignment of Hsp70 paralogs shows a highly conserved NBD. Residues with significant shifts by protein NMR in the presence of compound are highlighted in red. B. Synthetic route for JG compound. (a) 1. Potassium ethyl xanthate, DMF, 4 h, 125 °C; 2. methyl iodide, triethyl- amine, ethanol, 1 h, 80 °C; (b) methyl p-toluenesulfonate, anisole, 125 °C; (c) N-substituted rhodanine, triethylamine, acetonitrile, 4 h, 25 °C; (d) methyl p-toluenesulfonate, DMF, 3 h, 135 °C; (e) 1. triethylamine, acetonitrile, 3 h, 80 °C, 2. Cl-ion exchange column.

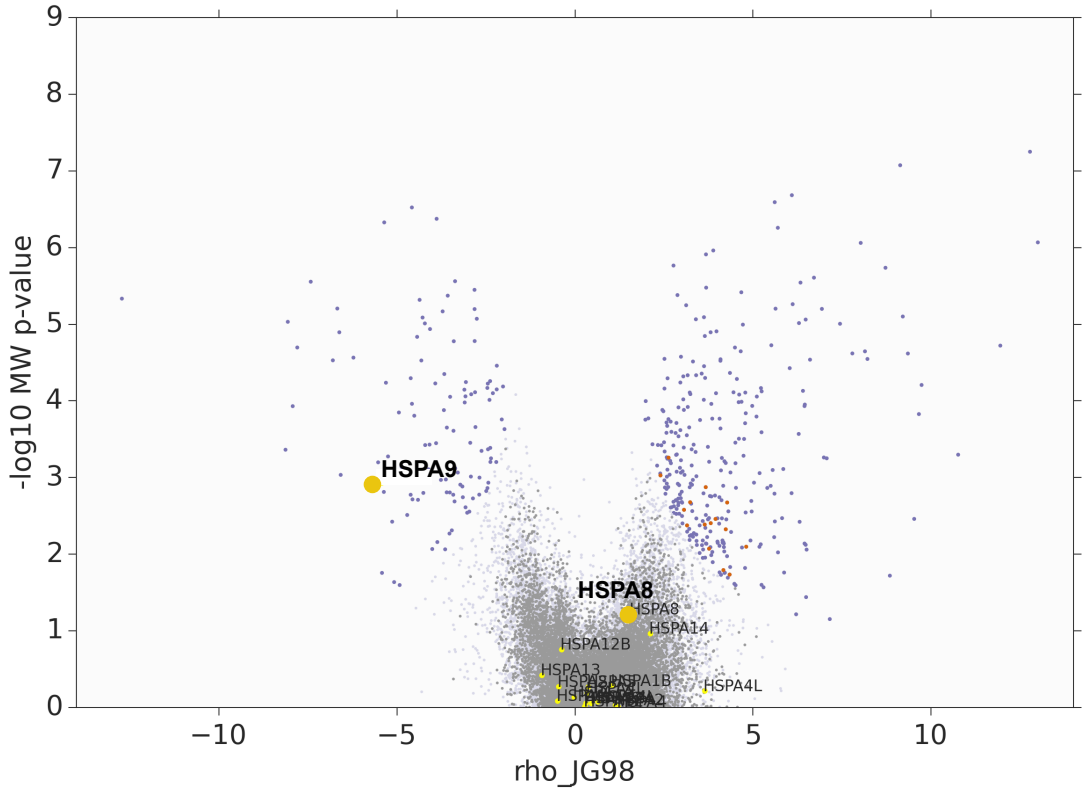

Appendix 3.2 CRISPRi reveals JG-98 treated cells are sensitive to HSPA9 (mortalin).

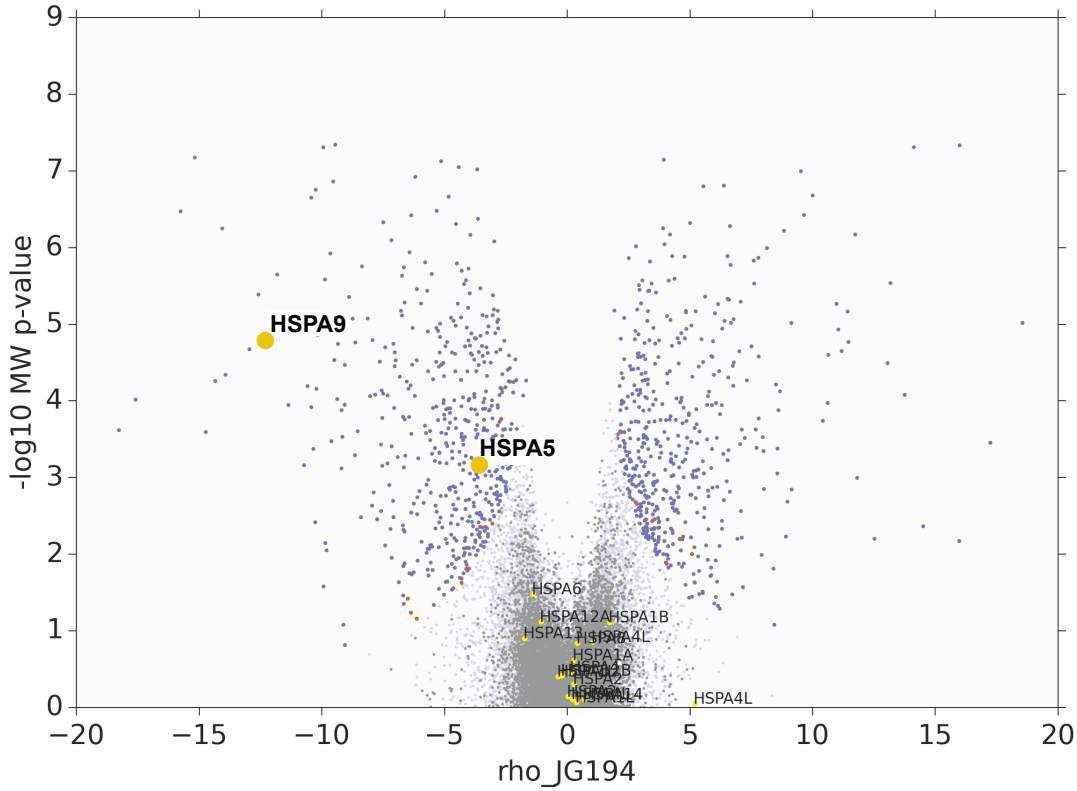

Appendix 3.3 CRISPRi reveals JG-194 treated cells are more sensitive to HSPA9 (mortalin) than HSPA5 (BiP).

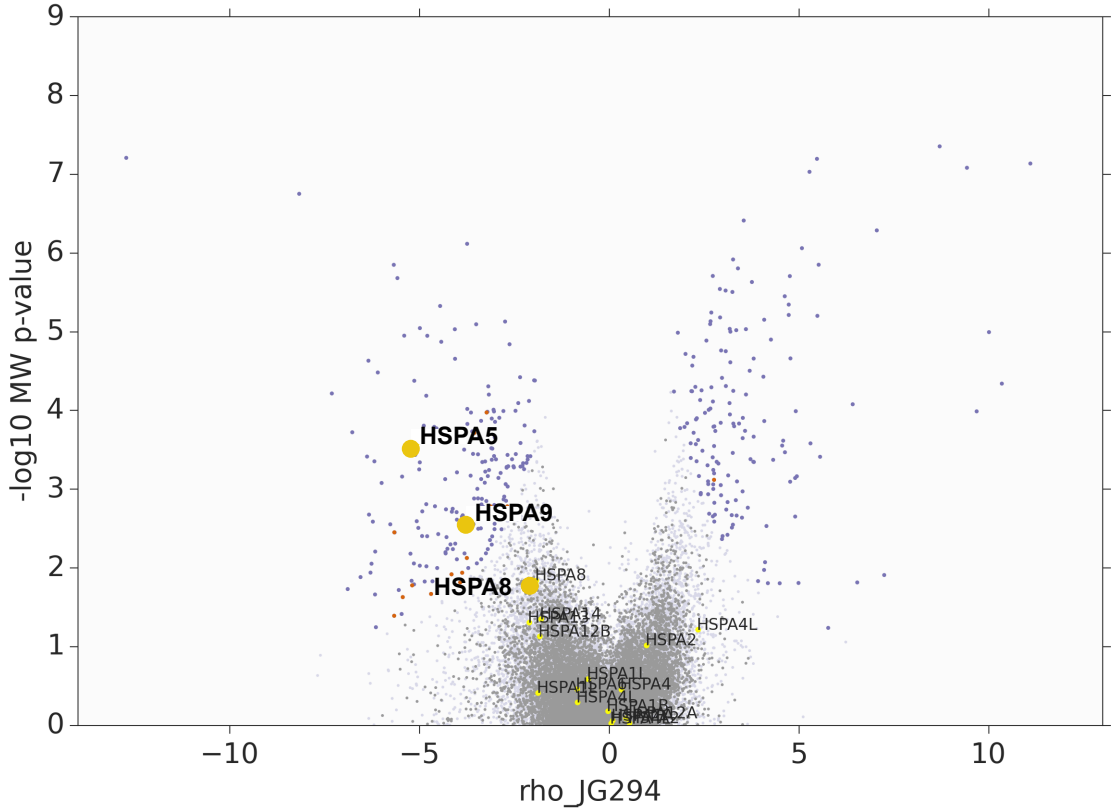

Appendix 3.4 CRISPRi reveals JG-294 treated cells are most sensitive to HSPA5 (BiP) over HSPA9 (mortalin) and HSPA8 (Hsc70).

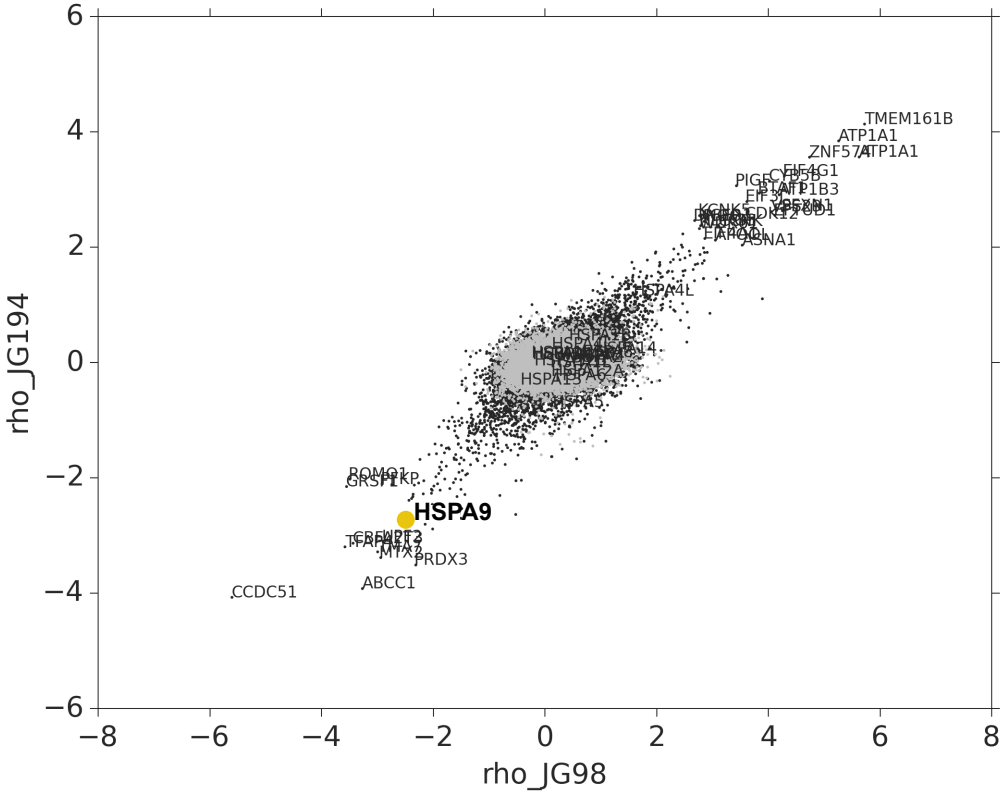

Appendix 3.5 CRISPRi reveals JG-98 and JG-194 have similar profiles in cells. HSPA9 (mortalin) is highlighted in yellow.

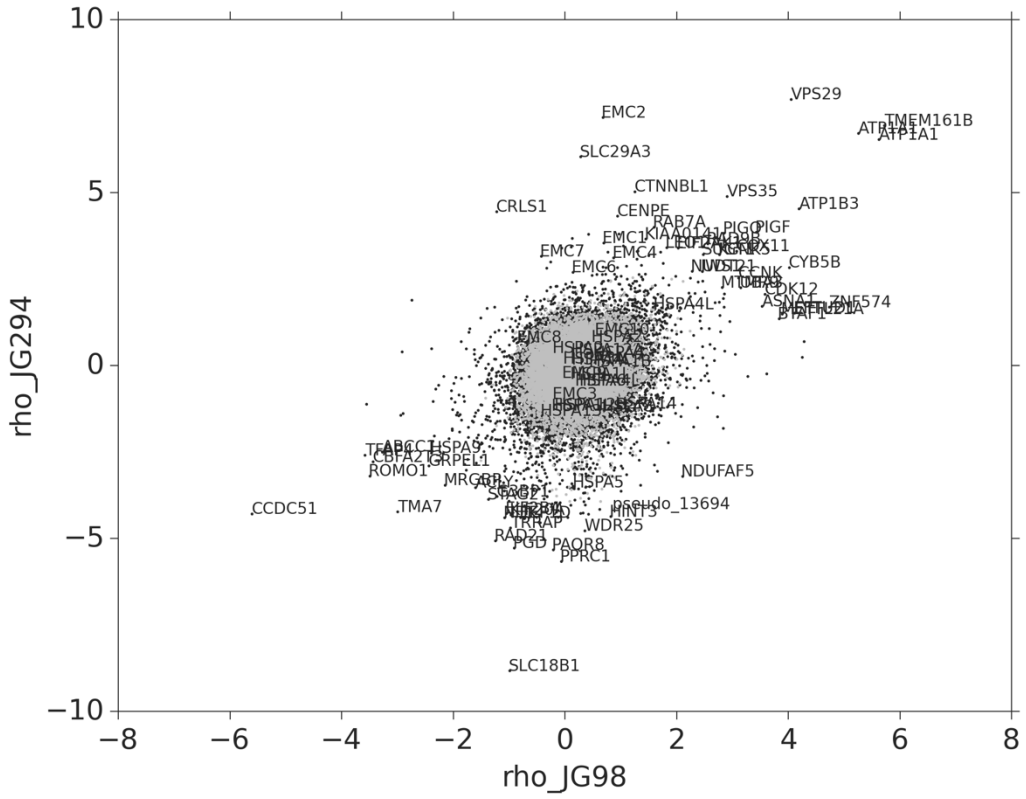

Appendix 3.6 CRISPRi reveals JG-98 and JG-294 have distinct profiles in cells.

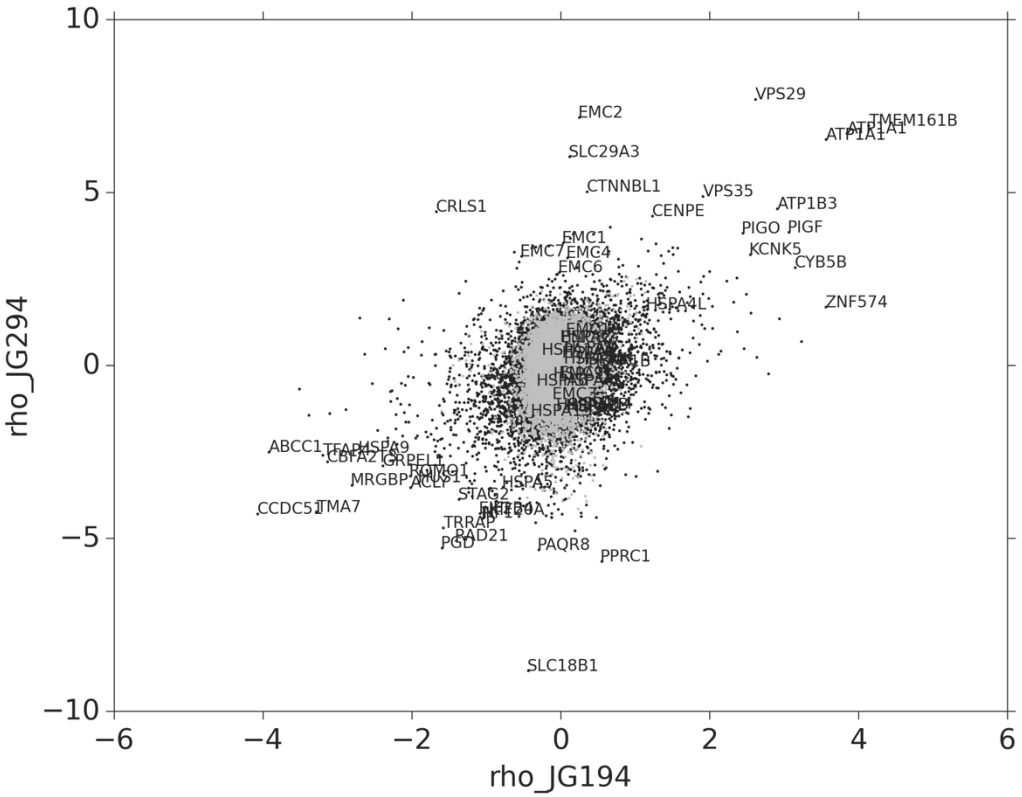

Appendix 3.7 CRISPRi reveals JG-194 and JG-294 have distinct profiles in cells.

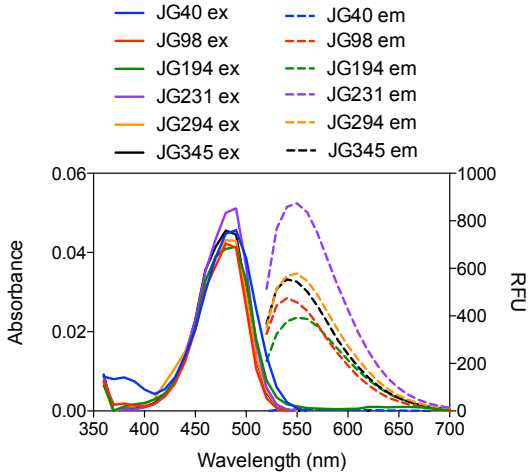

Appendix 3.8 Intrinsic fluorescence of rhodacyanine analogs.

A. Hsc70 NBD with residues important for rhodacyanine binding shown in blue

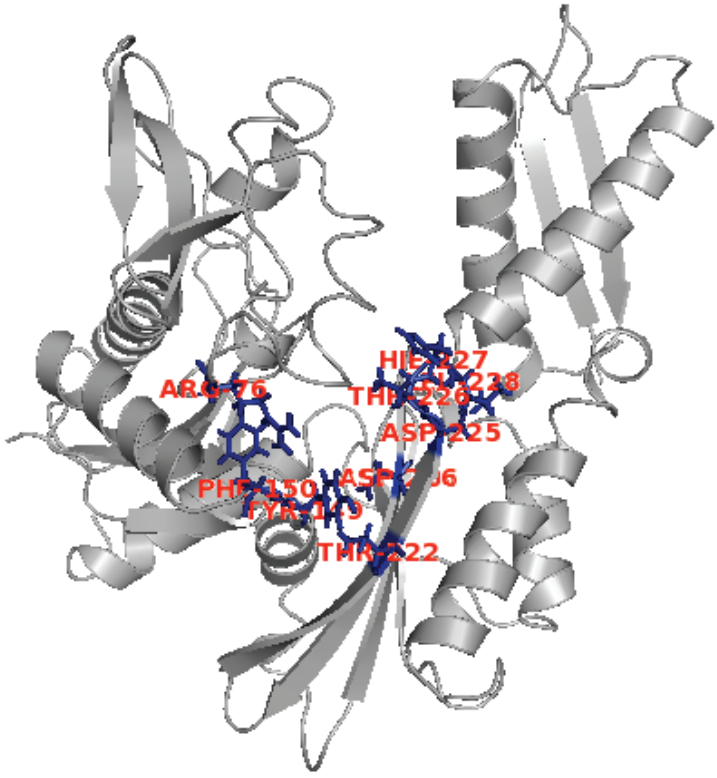

B. Hsc70 mutants have variable ATPase activity

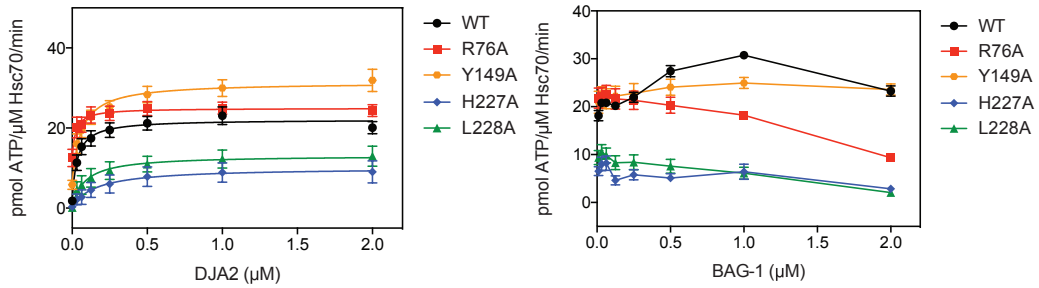

C. Hsc70 mutants have variable luciferase refolding activity

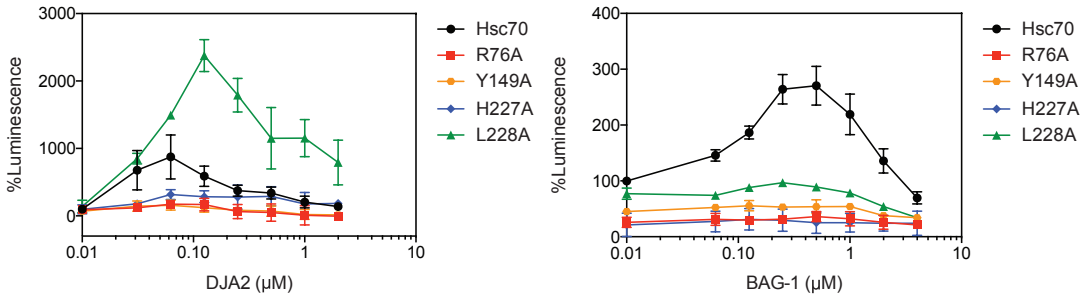

Appendix 3.9 Development and characterization of Hsc70 NBD point mutants. (A) Point mutantions withing the rhodacyanien binding site as tools for probing effecs of Hsc70 perturbations (B) and (C) Results are average of two independent experiments performed in triplicate. Error bars represent the SEM.

Table 3.1 Summary of rhodacyanine characterization

Compound	MW	MDA-MB-231 EC_{50} (μM)	MCF-7 EC_{50} (μM)	MEF EC_{50} (μM)	IMR90 EC_{50} (μM)	Solubility (μM)	Microsome Stability $t_{1/2}$ (min)
JG40	435.96	6.2 ± 1.0	8.5 ± 3.0	>50	NT	NT	NT
JG98	534.54	0.53 ± 0.05	0.7 ± 0.2	24 ± 1.3	1.4 ± 0.2	31	68
JG194	514.12	0.082 ± .009	0.20 ± 0.02	1.9 ± 0.1	1.8 ± 0.3	16	40
JG231	619.45	0.27 ± 0.03	0.12 ± 0.01	2.5 ± 0.1	4.6 ± 0.3	16	NT
JG294	636.94	0.12 ± 0.01	0.062 ± .006	3.5 ± 0.4	9.5 ± 1.9	31	60
JG345	586.18	0.031 ± .008	0.067 ± .007	1.0 ± 0.1	3.1 ± 0.7	32	25

Table 3.2 Top 50 CRISPRi hits for JG-98 and JG-194

JG-98				JG-194			
Hit	**Gene**	**p value**	**rho**	**Hit**	**Gene**	**p value**	**rho**
1	ATP1A1	5.68E-08	0.4544	1	PFKP	4.47E-08	-0.2438
2	CYB5B	9.08E-08	0.2734	2	ATP1A1	4.51E-08	0.4478
3	DICER1	1.53E-07	0.2399	3	CYB5B	4.76E-08	0.3504
4	PGAM1	2.35E-07	-0.1493	4	KIAA1191	4.98E-08	-0.2447
5	PEX5	2.49E-07	0.1902	5	ZNF281	5.97E-08	0.1083
6	KIAA1191	4.34E-07	-0.1497	6	GOT1	6.19E-08	-0.1140
7	ABCC4	5.15E-07	-0.1891	7	MTX2	6.65E-08	-0.3884
8	ASNA1	5.75E-07	0.2472	8	HUWE1	8.59E-08	-0.1044
9	IGF2BP1	6.82E-07	0.0892	9	PYROXD1	9.29E-08	0.1312
10	BTAF1	7.37E-07	0.2892	10	PNP	9.53E-08	-0.1333
11	UFM1	8.21E-07	0.1784	11	FAM136A	9.58E-08	-0.2357
12	NAA50	9.53E-07	0.1098	12	APOOL	1.26E-07	0.2447
13	MCUR1	1.10E-06	-0.1599	13	NAA50	1.67E-07	0.1133
14	TSC22D1	1.20E-06	0.1327	14	PEX5	2.08E-07	0.2573
15	PFKP	1.37E-06	-0.2457	15	SLC5A6	2.08E-07	0.0676
16	TMEM161B	1.66E-06	0.4756	16	ERAL1	2.28E-07	-0.2504
17	PSMA1	1.82E-06	0.1888	17	ABCC4	2.32E-07	-0.2691
18	RNF149	1.86E-06	-0.1051	18	LIN7C	2.34E-07	-0.1336
19	G3BP1	1.90E-06	-0.1074	19	NONO	2.94E-07	-0.1672
20	ERAL1	2.05E-06	-0.1220	20	PGAM1	4.43E-07	-0.1585
21	EIF4E	2.22E-06	0.1464	21	MINOS1-NBL1	4.77E-07	0.2658

22	MTX2	2.67E-06	-0.2474	22	CDK6	4.90E-07	0.0952
23	IFITM1	2.78E-06	0.1090	23	PRPS1	5.09E-07	0.1734
24	RAD21	3.19E-06	-0.1005	24	HSCB	5.37E-07	-0.1706
25	POLG2	3.90E-06	0.1261	25	TRAP1	6.34E-07	-0.0986
26	PYROXD1	4.26E-06	0.1158	26	RBM6	6.39E-07	-0.1028
27	ABCC1	4.59E-06	-0.2632	27	MED23	6.63E-07	-0.2059
28	CCDC51	4.64E-06	-0.4094	28	PSMA7	6.65E-07	0.0864
29	HSCB	4.81E-06	-0.0694	29	TOMM5	6.69E-07	0.0968
30	PRPS1	5.44E-06	0.1439	30	GRAMD1A	6.83E-07	0.0941
31	NDRG3	5.73E-06	0.2215	31	NPC2	7.24E-07	-0.1530
32	SUGT1	5.76E-06	0.1822	32	UBL7	7.39E-07	0.0665
33	ATP5J2-PTCD1	6.27E-06	-0.1542	33	CLPP	7.67E-07	-0.1835
34	DENND1A	6.49E-06	-0.1084	34	ZCCHC6	8.06E-07	0.1014
35	PIGO	6.51E-06	0.2268	35	DSTYK	8.40E-07	-0.1092
36	SPI1	8.11E-06	0.1561	36	STEAP3	8.56E-07	-0.0904
37	DPH6	8.64E-06	0.2259	37	DAZAP1	8.61E-07	0.1618
38	VPS29	9.29E-06	0.3132	38	BTAF1	8.70E-07	0.3325
39	PSMD1	9.42E-06	0.1146	39	CBFA2T3	8.79E-07	-0.3766
40	APOOL	9.50E-06	0.2110	40	EIF4E	8.80E-07	0.1882
41	HSP90AB1	9.68E-06	-0.0741	41	SLC38A5	9.20E-07	0.1212
42	KCNK5	9.69E-06	0.2185	42	WDHD1	9.97E-07	-0.1526
43	RPRD2	1.02E-05	0.1936	43	SLC7A1	1.00E-06	0.1533
44	TMEM185B	1.12E-05	-0.0677	44	MAX	1.01E-06	-0.0831
45	RHOBTB1	1.17E-05	-0.1415	45	DICER1	1.04E-06	0.3115
46	TFAM	1.27E-05	-0.1307	46	YIPF5	1.06E-06	0.0726
47	IMP3	1.30E-05	0.1357	47	COPS7B	1.07E-06	-0.1223
48	HK2	1.40E-05	-0.2286	48	GRSF1	1.10E-06	-0.2444
49	MTA1	1.40E-05	0.1137	49	MMD	1.10E-06	0.1679
50	FAM210A	1.41E-05	-0.1566	50	PGK1	1.15E-06	-0.2557
368	HSPA9	1.67E-03	-0.1909	365	HSPA9	1.31E-04	-0.2795
3844	HSPA8	7.53E-02	0.0521	1715	HSPA5	1.15E-02	-0.0740

Table 3.3 Top 50 CRISPRi hits for JG-294

JG-294			
Hit	**Gene**	**p value**	**rho**
1	SLC29A3	4.42E-08	0.5362

2	SLC18B1	6.16E-08	-0.7157
3	PQLC2	6.37E-08	0.3370
4	VPS29	7.30E-08	0.6834
5	ATP1A1	8.27E-08	0.5805
6	KIAA0141	9.31E-08	0.3249
7	PPRC1	1.77E-07	-0.5036
8	SQLE	3.87E-07	0.2181
9	VPS35	5.16E-07	0.4341
10	HPS5	7.64E-07	-0.2310
11	RAD9B	8.68E-07	0.3126
12	NFYC	1.21E-06	0.2008
13	PIGO	1.41E-06	0.3397
14	ZIC2	1.41E-06	-0.3500
15	RNF214	1.57E-06	0.2087
16	C7orf26	1.96E-06	0.1679
17	WDR91	1.96E-06	0.2929
18	STAG2	2.08E-06	-0.3442
19	SHOC2	2.34E-06	0.2314
20	ANKRD17	2.86E-06	0.1794
21	PWWP2A	3.00E-06	0.1886
22	GLCE	3.12E-06	0.1997
23	KCNK5	3.54E-06	0.2847
24	SOS1	4.52E-06	0.2911
25	KLF1	4.71E-06	-0.2748
26	PLEKHH3	5.70E-06	0.1655
27	TMEM147	6.12E-06	0.2911
28	XPO1	6.28E-06	0.3377
29	CCND3	6.58E-06	0.1797
30	CYB5B	7.03E-06	0.2513
31	ZMAT5	7.35E-06	0.1642
32	COPS7B	7.42E-06	-0.1694
33	SLC38A5	7.99E-06	0.1636
34	CSDE1	8.04E-06	-0.2163
35	WDR11	8.99E-06	-0.3077
36	TMED10	9.20E-06	0.1954
37	TFDP1	9.27E-06	0.2216
38	TAL1	9.29E-06	-0.2509
39	NAA50	9.55E-06	0.2060
40	CNBP	9.97E-06	0.1964

41	TMEM161B	1.01E-05	0.6163
42	COX7C	1.03E-05	0.1111
43	COPS4	1.12E-05	-0.2957
44	MCM3AP	1.26E-05	0.2623
45	PLEKHA1	1.29E-05	0.1575
46	EIF2B2	1.34E-05	-0.2730
47	PTPN7	1.44E-05	-0.1621
48	DBR1	1.73E-05	0.1814
49	STOML2	1.77E-05	0.1889
50	NAA60	1.91E-05	0.1235
144	HSPA5	2.62E-04	-0.3129
386	HSPA9	2.46E-03	-0.2250

3.8 References

[1] Lipinski CA, Lombardo F, Dominy BW, Feeney PJ. Experimental and computational approaches to estimate solubility and permeability in drug discovery and development settings. Adv Drug Deliv Rev, 2001; 46: 3-26.

[2] Moellering RE, Cravatt BF. How chemoproteomics can enable drug discovery and development. Chem Biol, 2012; 19: 11-22.

[3] Smith C. Drug target validation: Hitting the target. Nature, 2003; 422: 341-347.

[4] Plenge RM, Scolnick EM, Altshuler D. Validating therapeutic targets through human genetics. Nature Reviews Drug Discovery, 2013; 12: 581-594.

[5] Plenge RM. Disciplined approach to drug discovery and early development. Sci Transl Med, 2016; 8: 349ps15.

[6] Howe MK, Bodoor K, Carlson DA, Hughes PF, Alwarawrah Y, Loiselle DR, Jaeger AM, Darr DB, Jordan JL, Hunter LM, Molzberger ET, Gobillot TA, Thiele DJ, Brodsky JL, Spector NL, Haystead TA. Identification of an allosteric small-molecule inhibitor selective for the inducible form of heat shock protein 70. Chem Biol, 2014; 21: 1648-59.

[7] Fadden P, Huang KH, Veal JM, Steed PM, Barabasz AF, Foley B, Hu M, Partridge JM, Rice J, Scott A, Dubois LG, Freed TA, Silinski MA, Barta TE, Hughes PF, Ommen A, Ma W, Smith ED, Spangenberg AW, Eaves J, Hanson GJ, Hinkley L, Jenks M, Lewis M, Otto J, Pronk GJ, Verleysen K, Haystead TA, Hall SE. Application of chemoproteomics to drug discovery: identification of a clinical candidate targeting hsp90. Chem Biol, 2010; 17: 686-94.

[8] Cravatt BF, Wright AT, Kozarich JW. Activity-based protein profiling: from enzyme chemistry to proteomic chemistry. Annu Rev Biochem, 2008; 77: 383-414.
[9] Matthews PM, Rabiner I, Gunn R. Non-invasive imaging in experimental medicine for drug development. Curr Opin Pharmacol, 2011; 11: 501-7.
[10] Kampmann M, Horlbeck MA, Chen Y, Tsai JC, Bassik MC, Gilbert LA, Villalta JE, Kwon SC, Chang H, Kim VN, Weissman JS. Next-generation libraries for robust RNA interference-based genome-wide screens. Proc Natl Acad Sci U S A, 2015; 112: E3384-91.
[11] Deans RM, Morgens DW, Ökesli A, Pillay S, Horlbeck MA, Kampmann M, Gilbert LA, Li A, Mateo R, Smith M, Glenn JS, Carette JE, Khosla C, Bassik MC. Parallel shRNA and CRISPR-Cas9 screens enable antiviral drug target identification. Nature Chemical Biology, 2016; 12: 361-366.
[12] Qi LS, Larson MH, Gilbert LA, Doudna JA, Weissman JS, Arkin AP, Lim WA. Repurposing CRISPR as an RNA-guided platform for sequence-specific control of gene expression. Cell, 2013; 152: 1173-83.
[13] Gilbert LA, Horlbeck MA, Adamson B, Villalta JE, Chen Y, Whitehead EH, Guimaraes C, Panning B, Ploegh HL, Bassik MC, Qi LS, Kampmann M, Weissman JS. Genome-Scale CRISPR-Mediated Control of Gene Repression and Activation. Cell, 2014; 159: 647-61.
[14] Rousaki A, Miyata Y, Jinwal UK, Dickey Ca, Gestwicki JE, Zuiderweg ERP. Allosteric drugs: the interaction of antitumor compound MKT-077 with human Hsp70 chaperones. Journal of molecular biology, 2011; 411: 614-32.
[15] Li X, Srinivasan SR, Connarn J, Ahmad A, Young ZT, Kabza AM, Zuiderweg ERP, Sun D, Gestwicki JE. Analogues of the Allosteric Heat Shock Protein 70 (Hsp70) Inhibitor, MKT-077, As Anti-Cancer Agents. ACS Medicinal Chemistry Letters, 2013; 4: 1042-1047.
[16] Li X, Srinivasan SR, Connarn J, Ahmad A, Young ZT, Kabza AM, Zuiderweg ER, Sun D, Gestwicki JE. Analogs of the Allosteric Heat Shock Protein 70 (Hsp70) Inhibitor, MKT-077, as Anti-Cancer Agents. ACS Med Chem Lett, 2013; 4.
[17] Li X, Colvin T, Rauch JN, Acosta-Alvear D, Kampmann M, Dunyak B, Hann B, Aftab BT, Murnane M, Cho M, Walter P, Weissman JS, Sherman MY, Gestwicki JE. Validation of the Hsp70-Bag3 protein-protein interaction as a potential therapeutic target in cancer. Mol Cancer Ther, 2015; 14: 642-8.
[18] Yu D, Baird MA, Allen JR, Howe ES, Klassen MP, Reade A, Makhijani K, Song Y, Liu S, Murthy Z, Zhang SQ, Weiner OD, Kornberg TB, Jan YN, Davidson MW, Shu X. A naturally monomeric infrared fluorescent protein for protein labeling in vivo. Nat Methods, 2015; 12: 763-5.
[19] Manders EMM, Verbeek FJ, Aten JA. Measurement of co-localization of objects in dual-colour confocal images. Journal of Microscopy, 1993; 169: 375-382.

[20] Dunn KW, Kamocka MM, McDonald JH. A practical guide to evaluating colocalization in biological microscopy. In: ed.^eds., Am J Physiol Cell Physiol, 2011; pp. C723-42.
[21] Abisambra JF, Jinwal UK, Blair LJ, O'Leary JC, 3rd, Li Q, Brady S, Wang L, Guidi CE, Zhang B, Nordhues BA, Cockman M, Suntharalingham A, Li P, Jin Y, Atkins CA, Dickey CA. Tau accumulation activates the unfolded protein response by impairing endoplasmic reticulum-associated degradation. J Neurosci, 2013; 33: 9498-507.
[22] van der Harg JM, Nolle A, Zwart R, Boerema AS, van Haastert ES, Strijkstra AM, Hoozemans JJ, Scheper W. The unfolded protein response mediates reversible tau phosphorylation induced by metabolic stress. Cell Death Dis, 2014; 5: e1393.
[23] Liu ZC, Chu J, Lin L, Song J, Ning LN, Luo HB, Yang SS, Shi Y, Wang Q, Qu N, Zhang Q, Wang JZ, Tian Q. SIL1 Rescued Bip Elevation-Related Tau Hyperphosphorylation in ER Stress. Mol Neurobiol, 2016; 53: 983-94.
[24] Bugiani O, Murrell JR, Giaccone G, Hasegawa M, Ghigo G, Tabaton M, Morbin M, Primavera A, Carella F, Solaro C, Grisoli M, Savoiardo M, Spillantini MG, Tagliavini F, Goedert M, Ghetti B. Frontotemporal dementia and corticobasal degeneration in a family with a P301S mutation in tau. J Neuropathol Exp Neurol, 1999; 58: 667-77.
[25] Ozcelik S, Fraser G, Castets P, Schaeffer V, Skachokova Z, Breu K, Clavaguera F, Sinnreich M, Kappos L, Goedert M, Tolnay M, Winkler DT. Rapamycin Attenuates the Progression of Tau Pathology in P301S Tau Transgenic Mice. PLoS ONE, 2013; 8: e62459.
[26] Coppola G, Chinnathambi S, Lee JJ, Dombroski BA, Baker MC, Soto-Ortolaza AI, Lee SE, Klein E, Huang AY, Sears R, Lane JR, Karydas AM, Kenet RO, Biernat J, Wang LS, Cotman CW, Decarli CS, Levey AI, Ringman JM, Mendez MF, Chui HC, Le Ber I, Brice A, Lupton MK, Preza E, Lovestone S, Powell J, Graff-Radford N, Petersen RC, Boeve BF, Lippa CF, Bigio EH, Mackenzie I, Finger E, Kertesz A, Caselli RJ, Gearing M, Juncos JL, Ghetti B, Spina S, Bordelon YM, Tourtellotte WW, Frosch MP, Vonsattel JP, Zarow C, Beach TG, Albin RL, Lieberman AP, Lee VM, Trojanowski JQ, Van Deerlin VM, Bird TD, Galasko DR, Masliah E, White CL, Troncoso JC, Hannequin D, Boxer AL, Geschwind MD, Kumar S, Mandelkow EM, Wszolek ZK, Uitti RJ, Dickson DW, Haines JL, Mayeux R, Pericak-Vance MA, Farrer LA, Alzheimer's Disease Genetics C, Ross OA, Rademakers R, Schellenberg GD, Miller BL, Mandelkow E, Geschwind DH. Evidence for a role of the rare p.A152T variant in MAPT in increasing the risk for FTD-spectrum and Alzheimer's diseases. Hum Mol Genet, 2012; 21: 3500-12.
[27] Kara E, Ling H, Pittman AM, Shaw K, de Silva R, Simone R, Holton JL, Warren JD, Rohrer JD, Xiromerisiou G, Lees A, Hardy J, Houlden H, Revesz T. The MAPT p.A152T variant is a risk factor associated with tauopathies with atypical clinical and neuropathological features. Neurobiology of Aging, 2012; 33: 2231.e7-2231.e14.

[28] Di Fonzo A, Ronchi D, Gallia F, Cribiu FM, Trezzi I, Vetro A, Della Mina E, Limongelli I, Bellazzi R, Ricca I, Micieli G, Fassone E, Rizzuti M, Bordoni A, Fortunato F, Salani S, Mora G, Corti S, Ceroni M, Bosari S, Zuffardi O, Bresolin N, Nobile-Orazio E, Comi GP. Lower motor neuron disease with respiratory failure caused by a novel MAPT mutation. Neurology, 2014; 82: 1990-8.

[29] Lahiri S, Chao JT, Tavassoli S, Wong AK, Choudhary V, Young BP, Loewen CJ, Prinz WA. A conserved endoplasmic reticulum membrane protein complex (EMC) facilitates phospholipid transfer from the ER to mitochondria. PLoS Biol, 2014; 12: e1001969.

[30] Christianson JC, Olzmann JA, Shaler TA, Sowa ME, Bennett EJ, Richter CM, Tyler RE, Greenblatt EJ, Harper JW, Kopito RR. Defining human ERAD networks through an integrative mapping strategy. Nat Cell Biol, 2012; 14: 93-105.

[31] Taguwa S, Maringer K, Li X, Bernal-Rubio D, Rauch JN, Gestwicki JE, Andino R, Fernandez-Sesma A, Frydman J. Defining Hsp70 Subnetworks in Dengue Virus Replication Reveals Key Vulnerability in Flavivirus Infection. Cell, 2015; 163: 1108-23.

[32] Townsend MJ, Arron JR. Reducing the risk of failure: biomarker-guided trial design. Nature Reviews Drug Discovery, 2016; 15: 517-518.

[33] Bassik MC, Kampmann M, Lebbink RJ, Wang S, Hein MY, Poser I, Weibezahn J, Horlbeck MA, Chen S, Mann M, Hyman AA, Leproust EM, McManus MT, Weissman JS. A systematic mammalian genetic interaction map reveals pathways underlying ricin susceptibility. Cell, 2013; 152: 909-22.

[34] Kampmann M, Bassik MC, Weissman JS. Integrated platform for genome-wide screening and construction of high-density genetic interaction maps in mammalian cells. Proc Natl Acad Sci U S A, 2013; 110: E2317-26.

Chapter 4

Conclusions and Future Directions

4.1 Conclusions

Dysfunctions in protein quality control underlie the initiation of disease in the cell. Molecular chaperones are major regulators of protein homeostasis; thus, improving chaperone function is a promising therapeutic avenue. However, the best routes for achieving this remain unclear. As discussed in Chapter 1, the intrinsically disordered protein tau is prone to regulation by molecular chaperones. This makes it a perfect model substrate for improving our basic understanding of the mechanisms of chaperone-mediated proteostasis in order to effectively target chaperone function for the treatment of disease. Specifically, this thesis work is focused on using tauopathy models to explore the ways in which the molecular chaperone Heat shock protein 70 (Hsp70) normalizes proteostasis.

One goal of my thesis was to determine how manipulation of Hsp70 by rhodacyanines directs tau fate. We identified a brain penetrant analog, JG-48, and in Chapter 2, I used biochemical assays to measure JG-48 effects on Hsp70 enzymatic activity and interactions with co-chaperones. We hypothesized that

stalling Hsp70 in the ADP bound state was a result of inhibition of Hsp70 interactions with a class of co-chaperones called nucleotide exchange factors (NEFs). With the help of a former student Jennifer Rauch, I verified that rhodacyanine analogs allosterically inhibit NEF binding, and as a result, compounds prevent substrate release from Hsp70. These findings expanded our understanding of the Hsp70-co-chaperone system and contributed to our work characterizing compounds in cancer [1, 2]. With no previous reports of small molecule inhibitors of Hsp70-NEF interactions in the literature, rhodacyanines represent first in class NEF inhibitors.

In Chapter 3, we initiated a strategic collaboration with Luke Gilbert and Jonathan Weissman to characterize rhodacyanines with strong anti-cancer activity using CRISPRi technology. We were interested in using functional genomics to understand shifts in potency and safety observed in the later stages of the medicinal chemistry campaign. From these genetic screens we learned that rhodacyanines exhibit preferential binding to organelle specific Hsp70 paralogs. We felt that fluorescence microscopy would be the best way to confirm these result *in vivo* since we could utilize the intrinsic fluorescence of the rhodacyanine scaffold. Therefore, I developed stable cells lines expressing mitochondria and endoplasmic reticulum (ER) targeting sequences and proteins labeled with monomeric infrared protein (mIFP). Analysis of colocalization by microscopy combined with results from compound characterization in tauopathy models revealed that organelle partitioning by rhodacyanines might explain variability in

potency. The results from this study will guide our future efforts to optimize the rhodacyanine scaffold as a precision medicine tool for targeting paralogs of Hsp70 in various proteostasis disorders.

The work described in this thesis has advanced our understanding of Hsp70-mediated protein quality control. We developed a “dwell time” model for directing the fate of bound Hsp70 substrates by stalling the ATPase cycle in the ADP-bound state. Now that we know how to manipulate Hsp70 for client degradation, we can apply this model to diseases in which aberrations in protein quality control have overburdened the cell. Additionally, we discovered targeting specific Hsp70 paralogs may provide a new and safer alternative to global Hsp70 modulation. Overall this work represents the first steps in developing Hsp70-targeting small molecule therapeutics for tauopathies, cancer and diseases related to collapses in protein homeostasis.

4.2 Future Directions

4.2.1 Development of tauopathy models for studying proteostasis networks

In Chapter 1, we summarized the mechanisms of normal and abnormal tau homeostasis, and the many points of therapeutic intervention tau misregulation pathways. To begin exploring targets for normalizing tau homeostasis, we need to first develop useful and robust models of tauopathy. Previously, the Gestwicki lab used HeLa C3 cells overexpressing full length tau to characterize

rhodacyanine activity in cells. While this model was useful for monitoring changes in tau levels following compound treatment, I found that overexpression of tau in these cells resulted in primarily soluble and mislocalized tau or free tau as illustrated by immunofluorescene staining. As reviewed in Chapter 1, tau is normally localized to the microtubule network where it aids in polymerization and provides cytoskeletal stability. Therefore, for our future studies we wanted to develop a more biologically relevant model for studying tau homeostasis. To do this, I made HEK293 cell lines with inducible expression of wild type tau as well as disease relevant point mutants and deletions (Chapter 1). A commercially available targeted integration system was used to produce stable cell lines with homogenous expression of tau. We chose HEK293 cells, because they lack endogenous tau; therefore, we can be confident that our experiments are well-controlled. In these cells, tau was labeled with an N-terminal GFP tag, making protein levels easily quantifiable by microscopy and flow cytometry. Initially I created cells lines with inducible expression of the following tau mutants: A152T, P301S and D348G (Figure 4.1A). Each of these mutations are associated with disease and provide tools for assessing differences in homeostasis when compared to wild-type tau. I have also prepared a cell line expressing tau with deletions of residues reported to be important for microtubule binding referred to as ∆277/278/308/309 tau (Figure 4.1A).

To characterize these cell lines, I first observed tau localization by fluorescence microscopy. After induction of wild-type tau expression with doxycycline (DOX),

immunofluorescence staining of tubulin shows that GFP-tau localizes well to the microtubule (data not shown). Imaging of the GFP-tau mutants yields a similar cytoskeletal profile and morphology (Figure 4.1B). This is in agreement with previous reports of a similar inducible tau cell model whereby expression of tau promoted microtubule stabilization [3]. A DOX incubation time-course illustrated that nearly 100% of cells exhibit tau induction after 20 hours by flow cytometry and western blot (Figure 4.1C). These preliminary results confirm successful development of a biologically relevant system with normal tau localization and controllable expression.

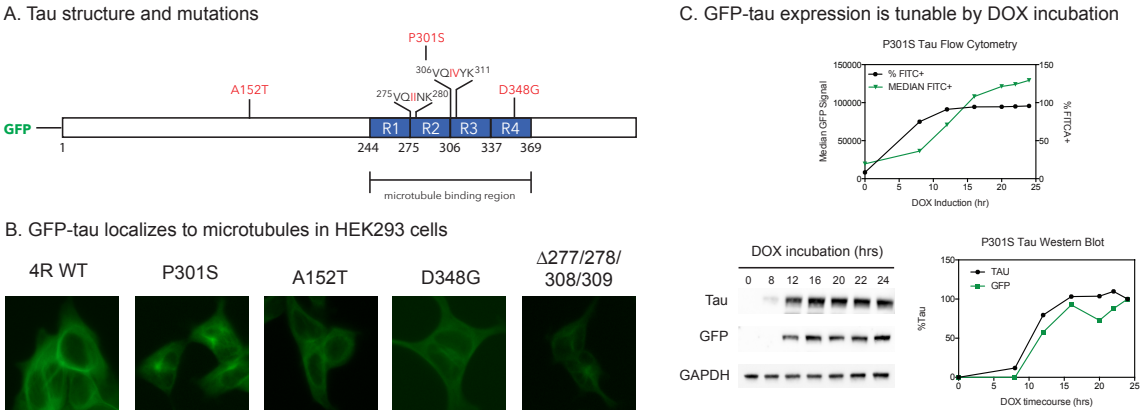

Figure 4.1 HEK293 cells with inducible tau expression as new models of tauopathy. A. Diagram of GFP-tau construct, mutations and deletions shown in red. (B) After 24hr induction of tau expression with DOX, tau imaging suggests localization to microtubule networks. (C) Tau expression is sensitive to length of DOX incubation. Flow cytometry analysis shows maximum expression after 20hrs of DOX treatment. Similar results are observed by western blot.

To demonstrate the utility of these tauopathy models in assessing mechanisms of tau quality control, the half-life of each tau variant was measured. After induction of tau with DOX for 24 hours, time points were taken every 24 hours for up to 7 days. For P301S tau, levels reached half-maximal expression at approximately 40 hours by western blot (Figure 4.2A) and flow cytometry (Figure 4.2B). Tau variants have shorter half-lives compared to wild-type, suggesting an

increase in rates of clearance for tau mutants (Figure 4.2B). As discussed in Chapter 1, mutations decrease tau binding to microtubules resulting in an increased population of soluble or free tau. This may explain the differences in stability of the tau variants as the abnormal or free tau is more susceptible to entry into degradation pathways.

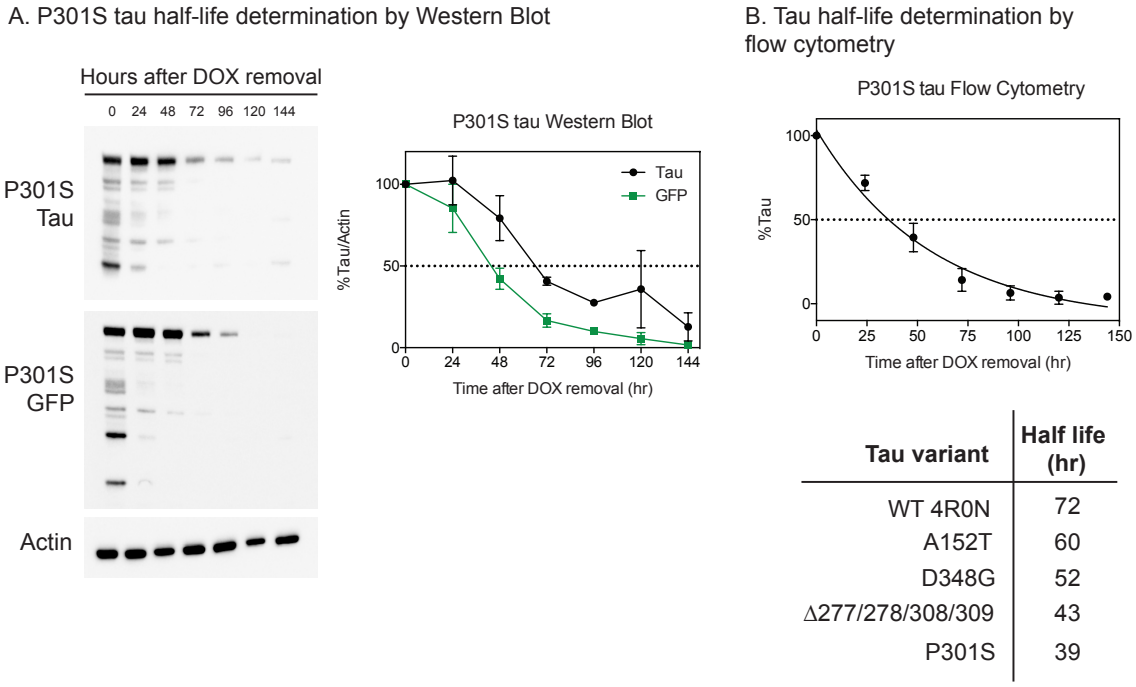

Tau variant	Half life (hr)
WT 4R0N	72
A152T	60
D348G	52
Δ277/278/308/309	43
P301S	39

Figure 4.2 Determination of tau stability in HEK293 cells. (A) Western blot shows tau levels decline steadily following termination of induction. (B) Half-life determination by flow cytometry reveals that tau variants are less stable compared to wild-type tau. All results are averages of experiments performed in duplicate. Error bars represent SEM.

4.2.2 Tauopathy models for drug discovery

With robust and meaningful models of tauopathy, we are now prepared to evaluate mechanisms of tau proteostasis using rhodacyanines, Hsp70 paralogs, Hsp70 mutants, and functional genomics. The Gestwicki lab has synthesized over 400 rhodacyanine analogs. Evaluating these compounds in the tau models

described above would provide valuable SAR and guide the development of new and more potent analogs. As a first step, I have measured the activity of biochemically interesting rhodacyanines including JG-48 using a high-throughput flow cytometry platform. In these experiments, the expression of GFP-P301S tau was induced with DOX and increasing amounts of compound were added simultaneously for 24 hours. Following treatment cells were analyzed by flow cytometry to quantify the amount of GFP-tau expressing cells. Results indicated a reduction in tau levels at high concentrations of JG-48 (Figure 4.3A). Preliminary experiments suggest this will be a valuable platform for analyzing compounds. VER-155008, an ATP-competitive inhibitor of Hsp70, greatly reduced tau levels and may be used for future studies as a positive control. Additionally, these experiments can be conducted in a 96 well plate format making this method suitable for assaying compounds in high volume.

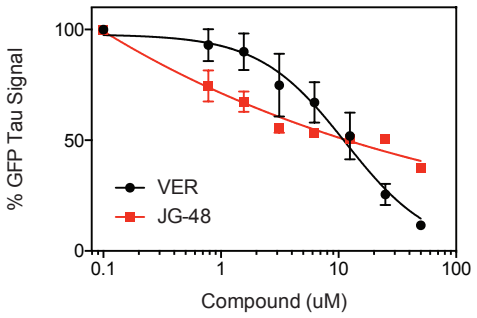

	IC_{50} (μM)
VER	11
JG-48	>25

Figure 4.3 Development of a high-throughput flow cytometry tau degradation assay. Cells were treated in 96 well cell culture plates before resuspension for quantification of GFP signal by FACS. Data shown represents average of two independent experiments performed in duplicate each. Error bars represent SEM.

Because the positively charged rhodacyanines have a strong and broad intrinsic fluorescence (Chapter 3), they cannot be assayed in the current GFP-tau models due to signal overlap. However, the development of tau models with expression

of far red labeled tau should overcome these challenges. The potential for success in identifying compounds with potent anti-tau activity is highlighted in Chapter 3, where immunoblotting of rhodacyanine treated cells showed significant reduction in tau levels. We also plan to use the tau models to evaluate activators of the ubiquitin proteasome degradation pathway, developed from an ongoing project guided by Kojo Opoku-Nsiah, a current student in the lab. Phenotypic screens using high-content imaging and a UCSF library of brain penetrant compounds is yet another future application of these cell models. Meredith Kuo, a current postdoc in the lab is directing this effort.

4.2.3 Tauopathy models for target identification

In Chapter 3, I detailed the benefits of using functional genomics for target validation, specifically gene regulation. In collaboration with the Weissman lab, we utilized CRISPRi technology to identify sensitive and resistant rhodacyanine phenotypes based on gene knockdown. A more traditional method of genome wide knockdown uses short hairpin RNA (shRNA) libraries to control gene expression. This method yields results similar to those of CRISPRi/a [4]. Application of shRNA screening to tauopathy models could identify novel therapeutic targets and reveal important protein networks specific for a given tau variant. For example, we hypothesize that D348G will have impaired degradation via the lysosome-autophagy pathway given that the mutated residue is within an autophagy degradation targeting sequence. Therefore, we might expect shRNA screens in D348G cells to reveal sensitivity and resistance phenotypes for

autophagic pathways. The development of reliable controls and methods is required for genome wide studies, and Sue Ann Mok, a postdoc in the lab, is pursuing the design and optimization of shRNA screens.

4.3 Optimization of the rhodacyanine scaffold

Currently we are screening more rhodacyanine compounds using CRISPRi in collaboration with Jonathan Weissman's lab. With knowledge gained from the CRISPRi screens described in Chapter 3, combined with fluorescence microscopy we will design and synthesize more rhodacyanines with selectivity for Hsp70 paralogs. One approach is to increase modifications to ring D (Figure 5.4) based on previous work [5], substitutions of ring D appear to be driving the shifts in potency and selectivity, despite the fact that docking models place this ring outside of the binding pocket. Efforts to make potent anti-cancer compounds like JG-98 more drug-like and suitable for development as tauopathy therapeutics are ongoing. We reported that removing the cationic nitrogen from ring C increases brain uptake in mice [6]. However, in modifying the charged nitrogen, ring D was also removed. Thus, future synthesis will focus on reintroducing the important ring D to the neutral scaffold. A current postdoc in the lab, Hao Shao, is developing synthetic methods to add the fourth ring to the neutral scaffold.

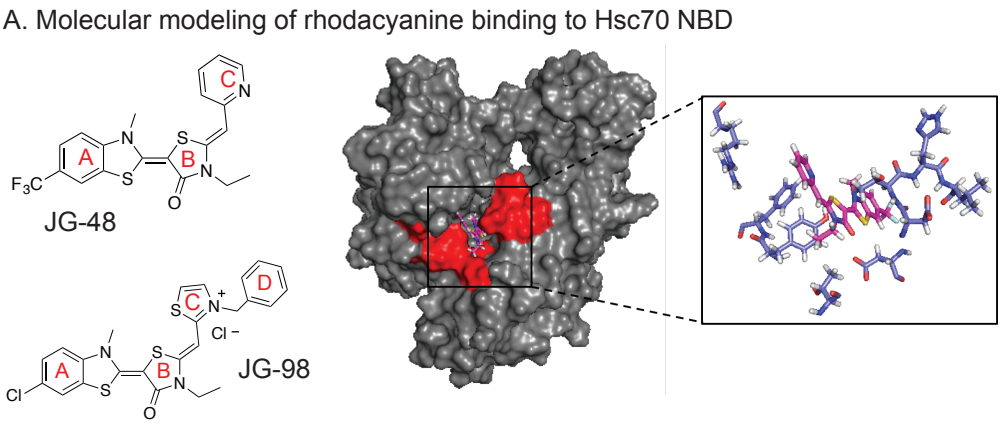

Figure 4.4 Molecular docking of JG-48 in the NBD of Hsc70 directs synthesis of future analogs.

4.4 Probing Hsp70 kinetics

In Chapter 2, we describe a model for Hsp70 “triage” of substrates like tau in which trapping Hsp70-substrate complexes leads to increased degradation of substrates *in vivo*. Future studies should use optimized rhodacyanines as probes for measuring Hsp70 protein-protein interaction kinetics. Knowledge of on/off rates for Hsp70 clients in the presence and absence of compound will further validate our dwell time theory and advance our understanding of chaperone biology. Furthermore, methods to quantify rates of substrate release by stopped flow, surface plasmon resonance (SPR) or some other means could be used to rank order compounds in the rhodacyanine chemical series and determine structure activity relationships (SAR) for identifying strong candidates.

4.5 References

[1] Colvin TA, Gabai VL, Gong J, Calderwood SK, Li H, Gummuluru S, Matchuk ON, Smirnova SG, Orlova NV, Zamulaeva IA, Garcia-Marcos M, Li X, Young ZT, Rauch JN, Gestwicki JE, Takayama S, Sherman MY.

Hsp70–Bag3 Interactions Regulate Cancer-Related Signaling Networks. Cancer Research, 2014; 74: 4731-4740.

[2] Li X, Colvin T, Rauch JN, Acosta-Alvear D, Kampmann M, Dunyak B, Hann B, Aftab BT, Murnane M, Cho M, Walter P, Weissman JS, Sherman MY, Gestwicki JE. Validation of the Hsp70-Bag3 protein-protein interaction as a potential therapeutic target in cancer. Mol Cancer Ther, 2015; 14: 642-8.

[3] Fontaine SN, Martin MD, Akoury E, Assimon VA, Borysov S, Nordhues BA, Sabbagh JJ, Cockman M, Gestwicki JE, Zweckstetter M, Dickey CA. The active Hsc70/tau complex can be exploited to enhance tau turnover without damaging microtubule dynamics. Human Molecular Genetics, 2015; 24: 3971-3981.

[4] Deans RM, Morgens DW, Ökesli A, Pillay S, Horlbeck MA, Kampmann M, Gilbert LA, Li A, Mateo R, Smith M, Glenn JS, Carette JE, Khosla C, Bassik MC. Parallel shRNA and CRISPR-Cas9 screens enable antiviral drug target identification. Nature Chemical Biology, 2016; 12: 361-366.

[5] Li X, Srinivasan SR, Connarn J, Ahmad A, Young ZT, Kabza AM, Zuiderweg ER, Sun D, Gestwicki JE. Analogs of the Allosteric Heat Shock Protein 70 (Hsp70) Inhibitor, MKT-077, as Anti-Cancer Agents. ACS Med Chem Lett, 2013; 4.

[6] Miyata Y, Li X, Lee HF, Jinwal UK, Srinivasan SR, Seguin SP, Young ZT, Brodsky JL, Dickey CA, Sun D, Gestwicki JE. Synthesis and initial evaluation of YM-08, a blood-brain barrier permeable derivative of the heat shock protein 70 (Hsp70) inhibitor MKT-077, which reduces tau levels. ACS Chem Neurosci, 2013; 4: 930-9.